Julius-Maximilians-Universität Würzburg

Fakultät für Biologie

Immunotherapy with Vaccinia virus co-expressing tumor-associated antigens and mouse IL-2 cytokine in mice with mammary cancer

Dissertation zur Erlangung des

naturwissenschaftlichen Doktorgrades

der Julius-Maximilians-Universität Würzburg

vorgelegt von

Mingyu Ye

aus

Zhejiang, China

Würzburg, November 2021

Muster der Rückseite des Titelblatts

Eingereicht am: ……..……..

<u>Mitglieder der Promotionskommission:</u>

Vorsitzender: ……Prof. Dr. Aladar A. Szalay ……..

Gutachter: ……Prof. Dr. Thomas Dandekar ……

Gutachter: ……Prof. Dr. Utz Fischer……

Tag des Promotionskolloquiums: ……..…

Doktorurkunde ausgehändigt am: …….…….

TABLE OF CONTENTS

Zusammenfassung

Interleukin 2 (IL-2) war das erste Zytokin in der Geschichte des Menschen, das zur Krebsbehandlung eingesetzt wurde. Es ist von der FDA als Monotherapie für Nierenzellkarzinome und Melanome zugelassen und kann bei Patienten die Rückbildung von Tumorerkrankungen fördern. Einer der möglichen Mechanismen ist, dass die Verabreichung von IL-2 zu einer T-Zell-Expansion führte. Darüber hinaus zeigte eine aktuelle Studie, dass auch antigenspezifische T-Zellen vermehrt werden können, was eine entscheidende Rolle bei der Vermittlung der Tumorregression spielt. Trotz des langjährigen und umfangreichen Einsatzes von IL-2 in der Klinik war der Anteil der Patienten, die eine komplette Antwort Zeigten, jedoch immer noch gering, und nur etwa ein Fünftel der Patienten weist eine objektive Tumorregression auf. Daher sollte die Funktion von IL-2 in der Krebsbehandlung weiter optimiert und untersucht werden. Eine Studie von Franz O. Smith et al. hat gezeigt, dass die Kombinationsbehandlung von IL-2 und tumorassoziiertem Antigenimpfstoff im Vergleich zu Melanomapatienten, die IL-2 allein erhalten, einen starken Trend zu verstärkten objektiven Reaktionen aufweist. Peptidimpfstoff ist ein Anti-Krebs-Impfstoff, der in der Lage ist, eine starke tumorantigenspezifische Immunantwort zu induzieren, die die Tumore ausrotten kann. Je nach Art der Antigene kann es in zwei verschiedene Kategorien eingeteilt werden: Impfstoff gegen tumorassoziierte Antigene (TAA) und Impfstoff gegen tumorspezifische Neoantigene (TSA). Derzeit werden Peptidimpfstoffe hauptsächlich in klinischen Studien in Phasen I und II an Patienten mit verschiedenen fortgeschrittenen Krebsarten wie Lungenkrebs, Magen-Darm-Tumoren und Brustkrebs untersucht.

Das Vacciniavirus (VACV) ist einer der sichersten Vektoren, der in der Krebsbehandlung und Krankheitsprävention weit verbreitet eingesetzt wird. Als onkolytischer Vektor kann VACV mehrere große Fremdgene tragen, die es dem Virus ermöglichen, diagnostische und therapeutische Mittel einzuführen, ohne die Virusreplikation dramatisch zu verändern. Inzwischen kann das rekombinante Vacciniavirus (rVACV) leicht durch die Technik der homologen Rekombination erzeugt werden. Hier haben wir das Vacciniavirus als therapeutischen Krebsvektor verwendet, das

Maus-Interleukin 2 (IL-2) und tumorassoziierte Antigene gleichzeitig exprimiert, um die Kombinationswirkung der Anti-Tumor-Immunantwort im 4T1-Mausmodell zu untersuchen.

Wie erwartet, erhöhte das VACV-exprimierte mIL-2 bemerkenswert sowohl die CD4+- als auch die CD8+-Population in vivo und die virusexprimierten, tumorassoziierten Peptide lösten erfolgreich die antigenspezifische T-Zell-Antwort auf, um das Wachstum des Tumors hemmen zu können. Darüber hinaus zeigten die Ergebnisse des Tierversuchs, dass der mIL-2 plus Tumorantigene exprimierende VACV-Vektor eine bessere Anti-Krebs-Antwort zeigt, als der mIL2 allein exprimierende Vektor, wobei das Erste das Tumorwachstum im Vergleich zu dem Letzteren signifikant hemmen konnte. Darüber hinaus bestätigten die Ergebnisse auch unsere früheren unveröffentlichten Daten, dass die mIL-2-Expression, die durch den synthetischen frühen/späten Promotor im Lister-Stamm rVACV angetrieben wird, die Tumorregression im 4T1-Mausmodell verstärkte.

Summary

Interleukin 2 (IL-2) was the first cytokine applied for cancer treatment in human history. It has been approved as monotherapy for renal cell carcinoma and melanoma by the FDA and does mediate the regression of the tumors in patients. One of the possible mechanisms is that the administration of IL-2 led to T lymphocytes expansion, including CD4+ and CD8+ T cells. In addition, a recent study demonstrated that antigen-specific T cells could also be expanded through the induction of IL-2, which plays a crucial role in mediating tumor regression. However, despite the long-term and extensive use of IL-2 in the clinic, the ratio of patients who get a complete response was still low, and only about one-fifth of patients showed objective tumor regression. Therefore, the function of IL-2 in cancer treatment should continue to be optimized and investigated. A study by Franz O. Smith et al. has shown that the combination treatment of IL-2 and tumor-associated antigen vaccine has a strong trend to increased objective responses compared to patients with melanoma receiving IL-2 alone. Peptide vaccines are anti-cancer vaccines able to induce a powerful tumor antigen-specific immune response capable of eradicating the tumors. According to the type of antigens, peptide vaccines can be classified into two distinct categories: Tumor-associated antigens (TAA) vaccine and tumor-specific neoantigens (TSA) vaccine. Currently, Peptide vaccines are mainly investigated in phase I and phase II clinical trials of human cancer patients with various advanced cancers such as lung cancer, gastrointestinal tumors, and breast cancers.

Vaccinia virus (VACV) is one of the safest viral vectors, which has been wildly used in cancer treatment and pathogen prevention. As an oncolytic vector, VACV can carry multiple large foreign genes, which enable the virus to introduce diagnostic and therapeutic agents without dramatically reducing the viral replication. Meanwhile, the recombinant vaccinia virus (rVACV) can be easily generated by homologous recombination. Here, we used the vaccinia virus as the therapeutic cancer vector, expressing mouse Interleukin 2 (IL-2) and tumor-associated antigens simultaneously to investigate the combined effect of anti-tumor immune response in the 4T1 mouse tumor model. As expected, the VACV driven mIL-2 expression remarkably increased both CD4+ and CD8+ populations in vivo, and the virus-expressed tumor-associated peptides successfully elicited the

antigen-specific T cell response to inhibit the growth of tumors. Furthermore, the experiments with tumor-bearing animals showed that the mIL-2 plus tumor antigens expressing VACV vector gave a better anti-cancer response than the mIL-2 alone expressing vector. The combinations did significantly more inhibit tumor growth than mIL-2 treatment alone. Moreover, the results confirmed our previous unpublished data that the mIL-2 expression driven by synthetic early/late promoter in the Lister strain VACV could enhance the tumor regression in the 4T1 mouse model.

1. Introduction

1.1 Breast Cancer

1.1.1 Overview of breast cancer and standard treatment

Breast cancer (BC) is cancer that forms in the breast tissue and is the most common cancer occurring among women worldwide (Figure.1) [1, 2]. At least 7.8 million people have been diagnosed with BC from 2016 to 2020, making it the most prevalent cancer in females globally. Only in 2020, there were 2.3 million women diagnosed with breast cancer resulting in 685 000 cases of deaths globally (Figure.2) [2]. It can develop in women at any age, especially at the age over 45 years old. BC is the leading cause of cancer-related deaths worldwide [3]. However, breast cancer in men is rare, only about 1% diagnosed is found in a man [4]. Based on histomorphology, 50%-75% of BC patients have invasive ductal carcinoma, which is the most common category in BC. 5%-15% of patients have invasive lobular carcinoma. The mixed ductal/lobular carcinomas and other rare histologies are comparatively less [5].

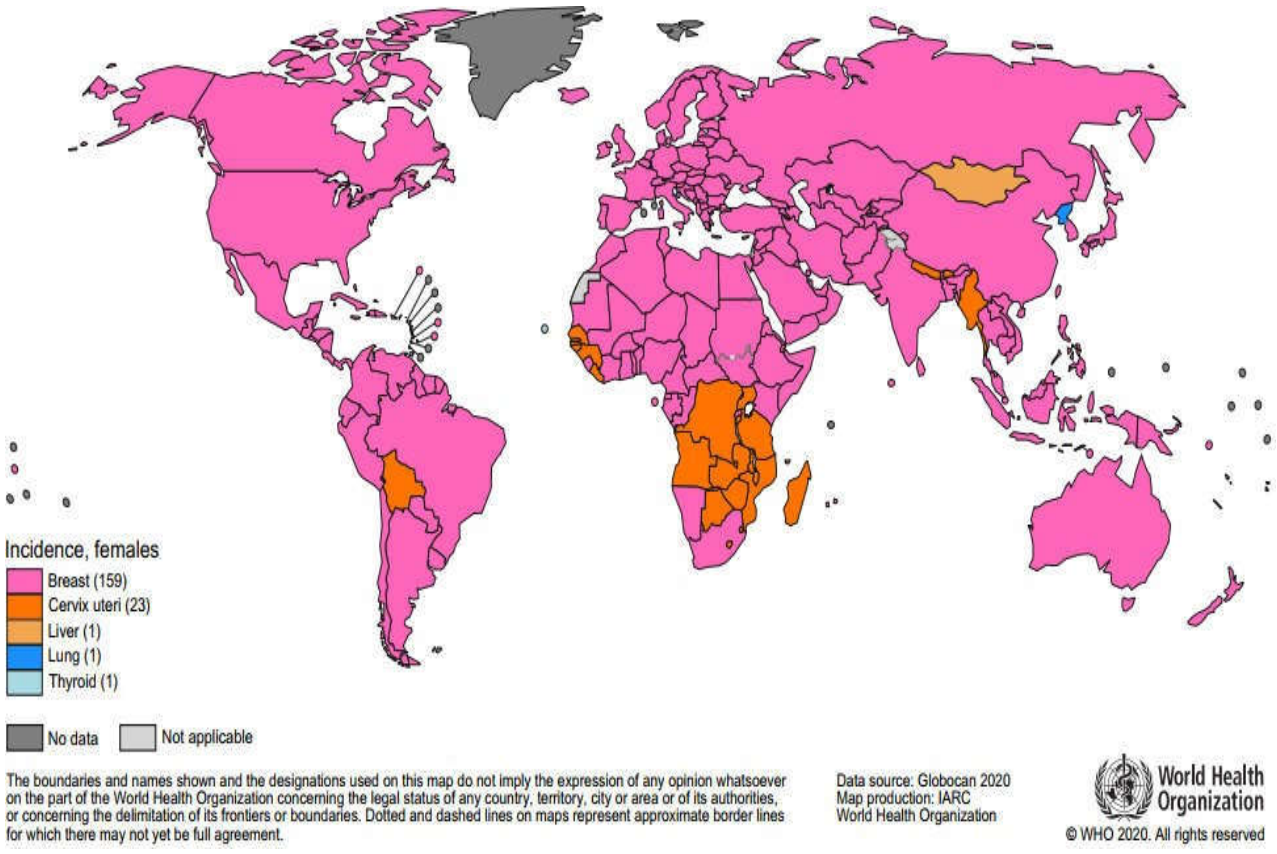

Figure.1: Most common type of cancer Incidence in 2020 in each country among women [2].

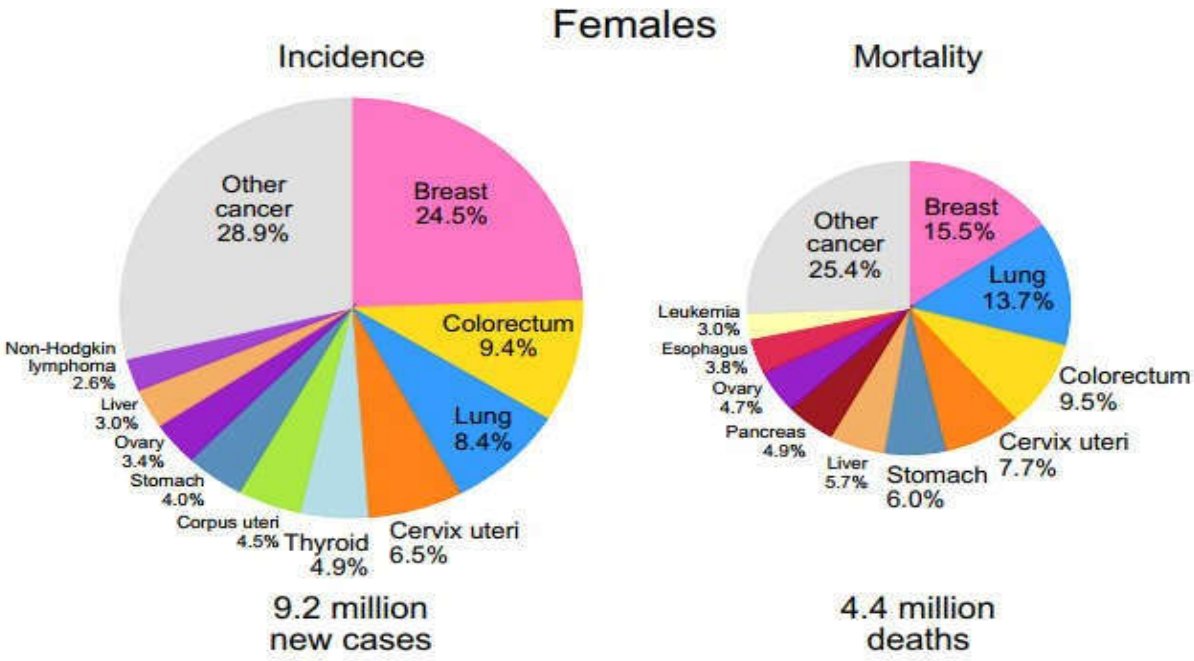

Figure.2: Distribution of cases and cancer death for the top 10 most common cancers in 2020 for women [2].

BC can be identified into five different clinically relevant groups according to the molecular and histological characteristics: (1) luminal A: expressing hormone receptor which is ER (estrogen receptor) and/or PR (progesterone receptor) positive, and HER2 (human epidermal growth factor receptor 2) negative, (2) luminal B: ER and/or PR positive as well as HER2, (3) HER2 positive and overexpressing, both ER and PR molecules are negative,(4) triple-negative breast cancer (TNBC) more likely to occur in young women which is negative or shows a low expression of ER, PR, and HER2, (5) Normal-like breast cancer which is similar to luminal A disease but with low expression of protein Ki-67 [6,7]. The regular therapy for BC in clinical practice includes radiotherapy, surgical ablation, hormone therapy, and chemotherapy that is usually followed by severe side effects. The hormone therapies of BC are mainly established based on the expression of two primary tumor-associated antigens—hormone receptor and epidermal receptor 2. The prevalence, prognosis, and therapeutic options of breast cancers are shown in Table 1 [8].

Table 1. Prevalence, prognosis, and therapeutic options for the breast cancer subtypes [8]

	Hormone Receptor (HR) +/HER2−	**HER2+ (HR+ or HR−)**	**Triple-Negative**
Pathological definition	**≥1%** of tumor cells stain positive for estrogen receptor or progesterone receptor proteins	Tumor cells stain strongly (3+) for Her2 protein or Her2 gene is amplified in tumor cells. Approximately half of ERBB2+ tumors are also HR+	Tumor does not meet any pathologic criteria for positivity of estrogen receptor, progesterone receptor, or HER2
Molecular pathogenesis	Estrogen receptor α (a steroid hormone receptor) activates oncogenic growth pathways	The oncogene HER2, encoding HER2 receptor tyrosine kinase from the epidermal growth factor receptor family, is overactive	Unknown (likely various)
Percentage of breast cancer cases, %	**70%**	**15-20%**	**15%**
Prognosis			
Stage I (5-year breast cancer–specific survival)	**≥99%**	**≥94%**	**≥85%**
Metastatic (media overall survival)	**4-5 Year**	**5 Year**	**10-13 Months**

Table 1. Continued

	Hormone Receptor (HR) +/HER2−	**HER2+ (HR+ or HR−)**	**Triple-Negative**
Typical systemic therapies for nonmetastatic disease *(Agents, route, and duration)*	Endocrine therapy (all patients): • Tamoxifen, letrozole, anastrozole, or exemestane • Oral therapy • **5-10 year** • Chemotherapy (some patients): • Adriamycin/cyclophosphamide (AC) • Adriamycin/cyclophosphamide/ paclitaxel (AC-T) • Docetaxel/cyclophosphamide (TC) • Intravenous therapy • **12-20 week**	Chemotherapy plus Her2-targeted therapy (all patients): • Paclitaxel/trastuzumab (TH) • Adriamycin/cyclophosphamide/ paclitaxel/trastuzumab ± pertuzumab (AC-TH±P) • Docetaxel/carboplatin/trastuzumab ± pertuzumab (TCH±P) • Intravenous therapy • **12-20 week** of chemotherapy; **1 year** of Her2-targeted therapy • Endocrine therapy (if also hormone receptor positive) • Tamoxifen, letrozole, anastrozole, or exemestane • Oral therapy • **5-10 years**	Chemotherapy (all patients): • AC • AC-T • TC • Intravenous therapy • **12-20 week**

1.2 Breast Cancer Immunotherapy

Despite significant progress in diagnosis and treatment in recent years, BC remains a huge potential threat to women's wellness. Therefore, developing novel approaches is urgent and essential, especially for the TNBC which in the absence of therapeutic targets (Hormone and Epidermal Receptors), is not curable with poor response rates and short median overall survival. The only treatment option is chemotherapy [9-11]. Great progress was made in immunotherapy of cancer has been achieved outstanding achievements during the last 20 years, which aims to increase both proliferation and activity of the immune effector cells to increase the production of cytokines or chemokines [12]. The immune system is crucial in the development of BC, including recognizing and eradicating tumor cells [13]. The clinical research data in recent years indicate so far that the immune system plays a vital role in determining both responses to standard therapies and long-term survival in patients with breast cancer [14].

Immune checkpoint molecules are regulators of the immune response against pathogen infections, prevent autoimmunity, transplantations, and tumor immune evasions [15]. The full activation of T cells in the immune system is dependent on two different signals. Cell-to-cell interactions trigger signal one through the antigenic peptide/major histocompatibility complex (MHC) present on the surface of antigen-presenting cells (APCs) binds to the T cell receptor (TCR). Signal two is dependent on the immune checkpoint molecules, including the co-stimulators and co-inhibitors [16, 17]. Immune checkpoint inhibitors/agonists and tumor antigen vaccines are the two main innovative strategies for BC immunotherapy so far. Both these therapies are aimed at immunoediting the tumor microenvironment [18]. Moreover, immune cells (such as CD4+ T helper cells, CD8+ cytotoxic T cells, and natural killer T cells) stimulation aims at the removal of tumor cells by regulating the expression of cytokines or chemokines, is currently being tested as well [19].

1.2.1 The role of Immune Checkpoint Inhibitors in breast cancer treatment

Immune checkpoint inhibitors have been tested in the early and advanced stage of BC patients in clinical trials, particularly in the TNBC subtype. These treatments show promising results in monotherapy and in combination therapy with chemotherapy [20]. Over the years, monoclonal antibodies (mAbs), mainly specific to the immune checkpoint PD-1, PD-L1 and CTLA-4, have achieved great success in cancer therapy (including BC) [21, 22]. PD-1 is a transmembrane receptor expressed by immune cells [23, 24] and induces a robust inhibitory signal to T-cells after binding to PD-L1 and PD-L2 ligands, resulting in exhaustion of T cells during the effector phase of the immune response (Figure.3) [25-27]. Therefore, blocking the interaction of PD-1 with its ligands could greatly help activation of effector T cells for cancer therapy. Humanized anti-PD-1 mAbs (pembrolizumab) and anti-PD-L1 mAbs (atezolizumab, avelumab) were approved for the treatment of metastatic TNBC by FDA in 2020 [28]. CTLA-4 (Cytotoxic T-lymphocyte- associated protein 4/ cluster of differentiation 152, CD152) is the first discovered inhibitory receptor predominantly expressed in intracellular FoxP3+ Treg cells or in activated conventional T cells and absent in naïve conventional T cells [29-31]. However, a small percentage of CTLA-4 protein is still expressed on the plasma membrane that will be upregulated shortly after T-cell activation [32]. The CTLA-4 protein on the T cell surface could bind CD80/CD86 and provide negative feedback to T cell activation (Figure.4) [33]. Two humanized anti-CTLA-4 mAbs (tremelimumab and ipilimumab) specific for BC treatment are in clinical investigation [34, 35].

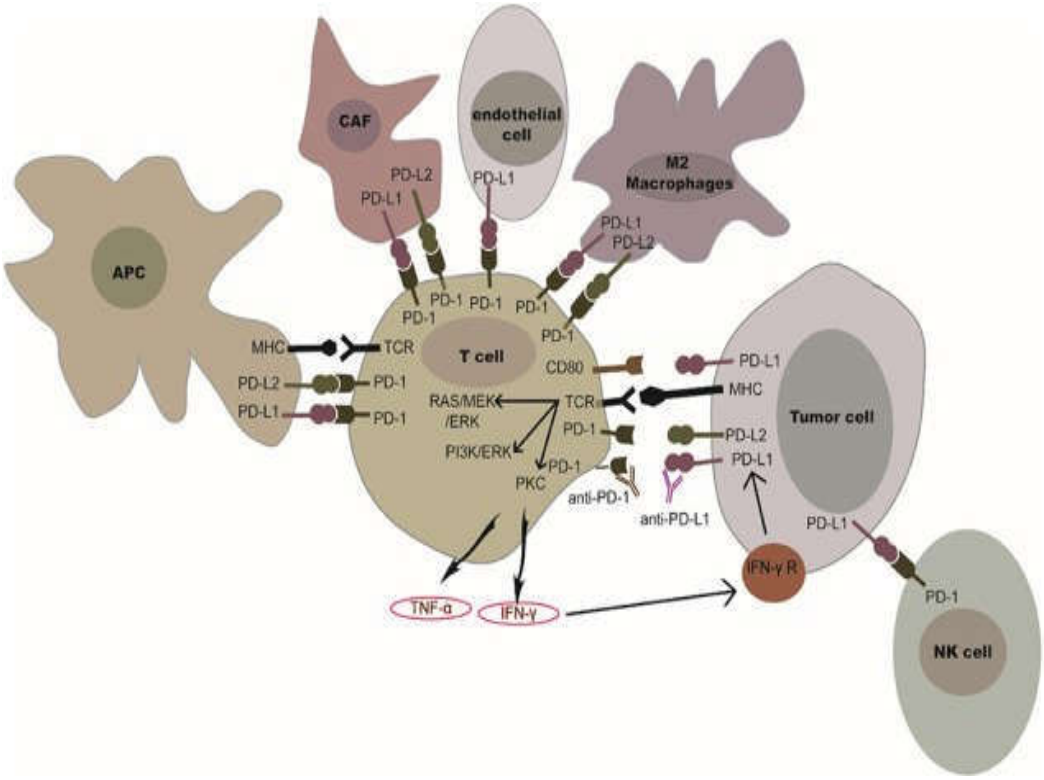

Figure 3. Role of PD-1/PD-L1 or PD-1/PD-L2 in the tumor microenvironment [27].

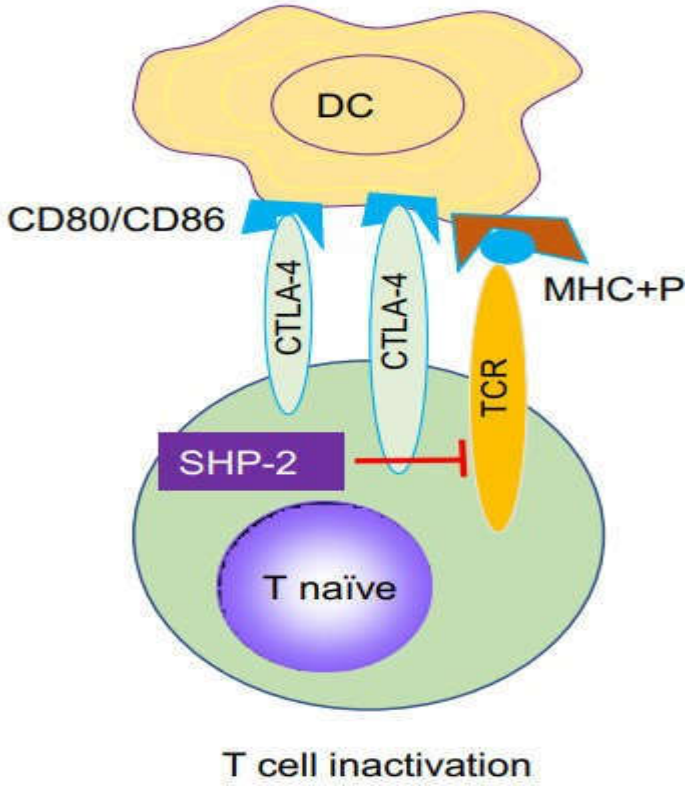

Figure 4. Role of CD80/86 and CTLA-4 receptors in T cell inactivation [33].

1.2.2 Role of Cytokines and Chemokines in breast cancer therapy

Cytokines and chemokines are proteins secreted by immune cells which play critical roles in modulating the tumor microenvironment by recruiting and activating specific subsets of immune cells [36, 37]. Preclinical models and early-stage clinical trials have achieved great success by interfering with some of the cytokine or chemokine expression in the immune system [38, 39]. In addition, several cytokines and chemokines do limit the growth of tumor cells by directly affecting cell proliferation and apoptosis [40, 41]. Chemokines are low molecular weight secretory proteins with four cysteine residues in the conserved structure positions, which could be divided into four subgroups-CXC, CC, CX3C, and C [42, 43]. The chemokine and chemokine receptor signaling pathway plays an intricate role in oncogenesis, in development, and maintaining the inflammatory in breast cancer's microenvironment. Some clinical results show that some chemokines' high expression is significantly related to the growth of BC cells [44, 45]. For instance, the complex of CXCR4 and its receptor CXCL12 promote the growth, invasion, and metastases of the BC cells [46, 47]. Furthermore, drugs targeting chemokine or chemokine receptors have been tested in the clinic for BC treatment Table 2 [48].

Table 2. Drug studies targeting chemokines/chemokine receptors in breast cancer [48]

Receptor	Drug	Response
CCR2	CCX9588 + anti-PD-L1	Reduce the number of MDSCs and inhibit growth and inhibit lung metastasis
CCR5	Maraviroc	Inhibit bone metastasis
CCL2	CNTO888+radiotherapy	Promote angiogenesis and metastasis
CXCR2	CXCR2−/− + PTX	Reduce growth, angiogenesis, and inhibit lung metastasis
CXCR4	Reparixin + PTX	Reduce the number of MDSCs and inhibit metastasis
	Balixafortide + Eribulin	Inhibit metastasis
	GST-NT2 1MP	Decrease growth, adhesion, migration, and reduce metastasis
	AMD3465	Inhibit growth and metastasis
CXCL12-CXCR7	LYG202	Inhibit activation of endothelial cells and angiogenesis

Abbreviation: MDSCs, myeloid-derived suppressor cells

Cytokines are highly inducible, soluble glycoproteins secreted by specific immune cells with a molecular weights average below 30 KDa [49]. It can bind to the cell membrane to activate the intercellular signaling, further regulating the homeostasis of the immune system, including proliferation, differentiation, inflammation, and anti-inflammatory response. Based on the role of the immune response or target cells and primary functions, cytokines could be classified into different categories Table 3 and 4 [50]. As mentioned before, some cytokines have a direct effect on tumor cell growth. For example, interferon-alpha (IFN-α), which was first discovered because of its antiviral properties in 1957, has the ability to inhibit the B16F10 cell growth in vitro [51, 52]. On the other hand, cytokines could (against tumor cells) indirectly induce the anti-tumor effects of immune cells. That is the primary mechanism for cytokine-based immunotherapy in cancer treatment. Although there are limitations for most cytokines used in clinical trials as monotherapy due to its double and conflicting role in carcinogenesis, the Food and Drug Administration (FDA) approved

IFN-α and IL-2 to treat several malignant cancers with mild clinical outcomes. IFN-α was approved for the treatment of stage III melanoma and non-Hodgkin lymphoma [53, 54], while high-dose IL-2 was approved for the treatment of metastatic melanoma and advanced renal cell carcinoma (RCC)3 [55,56]. However, the role of cytokines in breast cancer therapy is still under investigation. For example, overexpression of IL-6 and IL-8 increased the resistance of MCF-7 cells to the chemotherapeutic drug treatments, anti-IL-6 and IL-8 antibodies significantly enhanced the anti-tumor sensitivity drugs in the MCF-7 cells [57]. Meanwhile, antibodies block the interaction of IL-6, and its receptor decreases the cancer stem cell (CSC) population, limiting the growth and metastasis of breast tumor cells [58]. Blocking TGF-ß signaling with inhibitors or antibodies prevents tumor cell growth and metastases as well [59, 60]. Moreover, anti-IL-20 nano-antibody also shows great therapeutic potential for breast cancer treatment [61]. However, IFNs (IFN-α, IFN-β, and IFN-γ) monotherapy and combination therapies showed no significant difference in clinical outcomes compared with conventional treatment [62]. IL-2 has been used to treat advanced breast cancer as well, which I will discuss in the next section separately.

Table 3. Classification of cytokines by immune response [50]

	Family	Members
Adaptive immunity	Common γ chain receptor ligands	IL-2, IL-4, IL-7, IL-9, IL-15, IL-21
	Common β chain (CD131) receptor ligands	IL-3, IL-5, GM-CSF
	Shared IL-2β chain (CD122)	IL-2, IL-15
	Shared receptors	IL-13 (IL-13R–IL-4R complex)
Pro-inflammatory signalling	IL-1	IL-1α, IL-1β, IL-1ra, IL-18, IL-33, IL-36α, IL-36β, IL-36γ, IL-36Ra, IL-37 and IL-1Hy2
	IL-6	IL-6, IL-11, IL-31, CNTF, CT-1, LIF, OPN, OSM
	TNFα	TNFα, TNFβ, BAFF, APRIL
	IL-17	IL-17A-F, IL-25 (IL-17E)
	Type I IFN	IFNα, IFNβ, IFNω, IFNκ, Limitin
	Type II IFN	IFNγ
	Type III IFN	IFNλ1 (IL-29), IFNλ2 (IL-28A), IFNλ3 (IL-28B)
Anti-inflammatory signalling	IL-12	IL-12, IL-23, IL-27, IL-35
	IL-10	IL-10, IL-19, IL-20, IL-22, IL-24, IL-26, IL-28, IL-29

Table 4. Classification of cytokines by the target cells and by the primary functions [50]

	Cytokine	Main sources	Target cell	Major function
Interleukins	IL-1	Macrophages, B cells, DCs	B cells, NK cells, T-cells	Pyrogenic, pro-inflammatory, proliferation and differentiation, BM cell proliferation
	IL-2	T cells	Activated T and B cells, NK Cells	Proliferation and activation
	IL-3	T cells, NK cells	Stem cells	Hematopoietic precursor proliferation and differentiation
	IL-4	Th cells	B cells, T cells, macrophages	Proliferation of B and cytotoxic T cells, enhances MHC class II expression, stimulates IgG and IgE production
	IL-5	Th cells	Eosinophils, B-cells	Proliferation and maturation, stimulates IgA and IgM production
	IL-6	Th cells, macrophages, fibroblasts	Activated B-cells, plasma cells	Differentiation into plasma cells, IgG production
	IL-7	BM stromal cells, epithelial cells	Stem cells	B and T cell growth factor
	IL-8	Macrophages	Neutrophils	Chemotaxis, pro-inflammatory
	IL-9	T cell	T cell	Growth and proliferation
	IL-10	T cell	B cells, macrophages	Inhibits cytokine production and mononuclear cell function, anti-inflammatory
	IL-11	BM stromal cells	B cells	Differentiation, induces acute phase proteins
	IL-12	T cells	NK cells	Activates NK cells

Table 4. Continued

	Cytokine	Main sources	Target cell	Major function
Tumor necrosis factors	TNF-α	Macrophages, Monocytes	Macrophages, Tumor cells	Phagocyte cell activation, endotoxic shock, Tumor cytotoxicity, cachexia
	TNF-β	T-cells	Phagocytes, tumor cells	Chemotactic, phagocytosis, oncostatic, induces other cytokines
Interferons	IFN-α	Leukocytes	Various	Anti-viral
	IFN-β	Fibroblasts	Various	Anti-viral, anti-proliferative
	IFN-γ	T-cells	Various	Anti-viral, macrophage activation, increases neutrophil and monocyte function, MHC-I and -II expression on cells
Colony stimulating factors	G-CSF	Fibroblasts, endothelium	Stem cells in BM	Granulocyte production
	GM-CSF	T cells, macrophages, fibroblasts	Stem cells	Granulocyte, monocyte, eosinophil production
	M-CSF	Fibroblast, endothelium	Stem cells	Monocyte production and activation
	Erythropoietin	Endothelium	Stem cells	Red blood cell production
Others	TGF-β	T cells and B cells	Activated T and B cells	Inhibit T and B cell proliferation, inhibit haematopoiesis, promote wound healing

Abbreviations: BM, bone marrow; DCs, dendritic cells; G-CSF, granulocyte-colony stimulating factors; M-CSF, macrophage colony stimulating factor; Th, T helper cells.

1.3 Interleukin-2 (IL-2)

Interleukin-2 (IL-2) is a glycosylated protein with around 15 kDa molecular weight secreted by activated T cells and comprised of four alpha-helix bundles, belong to a cytokine family in the immune system [63,64]. It plays an essential role in the growth and differentiation of immune cells, especially in that of T cells, B cells, natural killer cells [65]. IL-2Rα (CD25) is the low affinity monomeric IL-2 receptor that exists in a membrane-bound and in a soluble form. However, the IL-2/CD25 complex alone is unable to induce the downstream signaling events [66]. The dimeric IL-2 receptor is comprised of IL-2Rβ (CD122) and IL-2Rγ (CD132) subunits with an intermediate affinity for IL-2 binding. The highest affinity trimeric IL-2 receptor comprises CD25, CD122, and CD132 subunits [67, 68]. In contrast to the monomeric IL-2 receptor, both the dimeric and trimeric receptors could initiate the downstream signal transduction. The CD122 and CD132 subunits are recruited after IL-2 binding to the CD25 subunit, and then subsequent signaling including the phosphoinositide 3-kinase (PI3K) AKT, STAT5, and MAPK pathway will be activated [Figure 5] [69]. These three pathways mediate the cell differentiation, proliferation, activation, survival, and cytokine production of the immune cells through the expression of the IL-2.

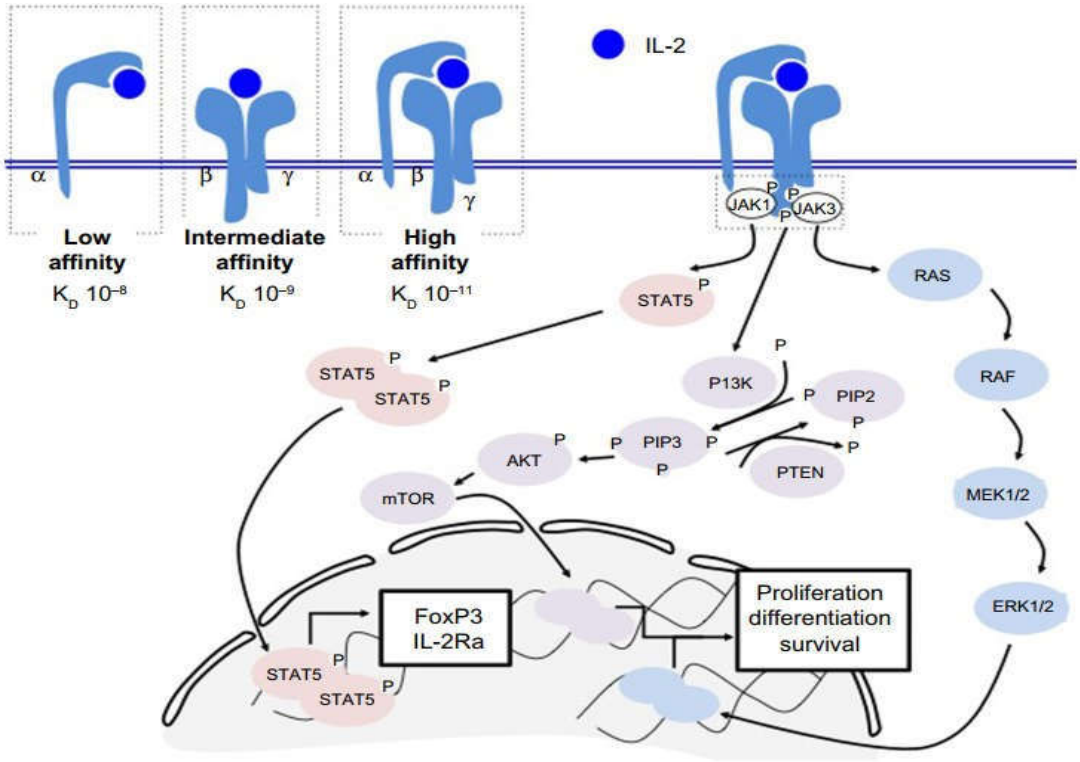

Figure 5. Components of the signaling pathway trigged by IL-2 [69]

1.3.1 Role of IL-2 in cancer therapy

IL-2 was the first cytokine which was successful in applied in cancer treatment. The acceptance of IL-2 in the clinics was not only able to promote the proliferation, differentiation, and activation of T cells and NK cells. Moshe Z. Papa et al. [70] demonstrated the administration of IL-2 in murine models could increase the activity of lymphokine-activated killer (LAK) cells in vivo. This study opened the door for IL-2 as a therapeutic agent in cancer treatment. The first clinical trial of IL-2 therapy was carried in 1985 and demonstrated that IL-2 was capable of mediating tumor regression in human cancer patients [71]. However, the main challenge of IL-2 in the development of cancer immunotherapy was that it affects both CD8+ T cells and CD4+Foxp3+ regulatory T cells (Tregs). Meaning that it plays a dual role in the immune system as an immunostimulant and immunosuppressive agent. Conversely, IL-2 therapy for autoimmune diseases requires Treg activation, without stimulation of effector T cells. The CD8+ T cells and NK (T) cells are immune cell populations that can boost the immune system and express the dimeric receptor with low affinity to IL-2, resulting in a high concentration of IL-2 required for their activation and proliferation [72]. After activation, the naïve cells are differentiated into either effector or memory T cells which express high-affinity trimeric IL-2R [73]. Moreover, IL-2 driven T cells differentiation depends on the strength and duration of the IL-2 signal. While the Tregs, which enable to dampen immune responses, express the trimeric receptors, with a high affinity for the IL-2 [74]. The Tregs normally have high-affinity IL-2 receptors can be promoted by a low level of IL-2 to create a more effectively corresponding response [75]. Due to this effect, the low-dose (LD) IL-2 could preferentially induce and activate the CD4+Foxp3+ Tregs in vivo, strengthening the immunosuppressive functions of Tregs [76, 77]. Therefore, IL-2 administration is dose-dependent for immunotherapy. After some subsequent studies, FDA approved high-dose (HD) IL-2 to treat patients with renal cell carcinoma in 1992 and stage IV (metastatic) melanoma in 1998 [78]. Although HD IL-2 monotherapy showed promising results in metastatic melanoma and in renal cell carcinoma patient treatment, still not the most optimal and standard treatment for cancers due to the insufficient response of patients regarding overall survival and severe toxicity. Thus, the investigation of IL-2 in cancer therapy still needs to be continued, especially the combination treatment with other methods.

1.3.2 Cancer treatment with combination of IL-2 and peptide vaccines

Many combination therapies of IL-2 with other agents have been extensively investigated in the clinic in the past two decades. One of the most promising treatment strategies is IL- 2 combined with peptide vaccines. Among others, IL-2 combined with immune checkpoint inhibitors or with other cell-based immunotherapy is interesting [79]. As mentioned before, the activation and proliferation of CD4+/CD8+ T cells could be induced by the administration of HD IL-2 in vivo. Therefore, IL-2 could have a synergistic effect with cancer peptide vaccines in treating tumors [80]. In a phase II trial, Smith et al. [81] demonstrated that HD IL-2 plus the gp100 peptide vaccine in fact had a higher response rate than IL-2 monotherapy in patients with metastatic melanoma. In this trial, the overall objective response rate of patients receiving IL-2 alone was 13% lower than the patients who received IL-2 with gp100 peptide vaccine was 16%. The subsequent phase III trial further illustrated that IL-2 plus gp100 peptide vaccine treatment not only had a higher overall clinical response than IL-2 alone (16% vs. 6%) but also showed on prolonged in the progression-free survival (median 2.2 vs. 1.6 mo; p=0.008) and in overall survival (median 17.8 vs. 11.1 mo; p=0.06) compared with the IL-2 monotherapy group in the patients with advanced melanoma [82]. These two studies confirmed that the addition of IL-2 could enhance the effect of peptide vaccine therapy in melanoma treatment. Recently, Hussein Sultan et al. [83] proved that the sustained persistence of IL-2 signals expands the population of peptide-specific CD8+ T cells and prevents PD-1 inhibition of the effector cells. This excellent research pointed to the mechanism of the potential of IL-2 and peptide vaccine combination therapy.

1.3.3 Breast cancer therapy with IL-2

IL-2 monotherapy was unsuccessful in breast cancer treatment due to the low efficiency and high toxicity, similarly to other cancers mentioned before. Therefore, new therapeutic methods to enhance the effectiveness of IL-2 against breast cancer are needed to continue to be investigated. In a pilot study, Tanya Repka et al. [84] reported that combination therapy of trastuzumab and IL-2 did induce a partial response in patients with her2-overexpressing metastatic breast cancer. Jessica Marlind et al. [85] constructed a fusion protein (F16-IL2) composing the human IL-2 fused to human antibody fragment scFv (F16), which significantly reduced the growth of breast tumors compared with the recombinant IL-2 therapy alone.

1.4 Tumor antigen/peptide vaccines in breast cancer therapy

1.4.1 Tumor-associated peptides in Breast cancer

It was demonstrated that tumor antigens could elicit autologous immune response involving CD4+ T-helper cells, CD8+ cytotoxic T-lymphocytes (CTLs), and antibodies secreted by B cells against the cancer cells. Generally, the CTLs induced tumor antigen-related peptides play an important role in cancer immunotherapy. Tumor-Associated Antigens (TAAs) are predominantly self-proteins aberrantly overexpressed in tumors but are also expressed at lower levels in healthy tissues and non-cancerous cells [86]. Thus, epitopes derived from TAAs could be good sources of peptide vaccines for cancer treatment. There are three main types of TAAs: (i) Tissue differentiation antigens are usually only found at particular phases of differentiation of tissues. For example, NY-BR-1 is a differentiation antigen of the mammary gland, which can be recognized by CTL clones [87]. (ii) Cancer-Testis (CT) antigens which are ordinarily silent in healthy adult tissues while activated in tumor cells [88,89]. (iii) Self-antigens are expressed at low levels in normal tissues but over-expressed in tumors, which can reach the threshold for T cell recognition to break the immunological tolerance. Moreover, the tumor cells always express unique antigens, mutated in cancer cells which are also called neo-antigens or tumor-specific antigens (TSAs) [90]. Breast tumor-associated antigens are one of the most wildly investigated antigens Table 5 [91]

Table 5. Breast tumor-associated antigens [91]

Peptide antigen	Source of peptide
Differentiation antigens	
NY-BR-1	Serologically defined breast cancer antigen 1
WT1	Wilm's tumor suppressor gene 1
Cancer/testis antigens	
MAGE	Melanoma-associated antigen
GAGE	G antigen
BAGE	B antigen
XAGE	X antigen
NY-ESO-1	New York esophagus antigen 1
Survivin	Inhibitor of apoptosis (IAP) family
hTERT	Human telomerase reverse transcriptase
Antigens overexpressed in tumors	
HER2	Human epidermal growth factor receptor 2
MUC1	Hypoglycosylated in adenocarcinomas
p53	Tumor suppressor protein
CEA	Carcinoembryonic antigen
Sialyl Tn	Carbohydrate associated with the MUC-1 aberrant mucin
Mutanome antigens	
Patient-specific ('private epitopes')	Based on tumor exome sequencing

1.4.2 Tumor peptide vaccines in breast cancer

A peptide-based tumor vaccine is an agent that can elicit tumor antigen-specific immune response for cancer therapy or prevention [92]. Tumor cells could be recognized and directly killed by activated CD8+ or CD4+ T cells in the immune system after the tumor antigens are processed and presented by antigen-presenting cells (APCs) through MHC class I (for CD8+ T cells) and MHC class II (for CD4+ T cells) molecules (Figures 6,7) [93,94]. BC is traditionally regarded as a low immunogenic cancer which means a lack of tumor-infiltrating lymphocytes in the tumor microenvironment (non-inflamed tumor) [95,96]. However, some new studies in recent years are convincing that BC can be divided into “inflamed” tumors and “non-inflamed” tumors according to the different molecular subtypes [97, 98]. For example, Triple-negative breast cancer (TNBC) could be viewed as the most “inflamed” breast cancer subtype. So far, the peptide-based vaccine is one of the most common research therapy strategies for breast cancer because of its efficiency, and dozens of breast cancer antigens have been defined [99]. Breast cancer peptide-based vaccines are currently tested to avoid relapse in patients at high risk, despite having a good response with standard therapy. Some clinical results suggest that peptides-based vaccines are a promising approach for BC therapy, although it is at an early stage [100]. To date, the antigens of peptide-vaccines for BC mainly belong to tumor-associated antigens (TAAS). H2NVAC is a multi-epitope HER2 peptide vaccine that can induce a T cell-mediated immune response against Her2-overexpressing Ductal Breast Carcinoma in Situ [101]. The multi-epitope folate receptor alpha (FRa) peptide vaccine has been proven safe as an agent in cancer treatment and promising in combination with GM-CSF and cyclophosphamide for treating patients with Triple-Negative Breast Cancer [102]. The AE37 peptide vaccine is a vaccine containing the fusion protein of Ii-Key hybrid of the MHC class II peptide (LRMK) and AE36 (HER2 aa: 776–790) [103]. The phase II clinical trial with AE37 peptide and Pembrolizumab combination therapy for Triple-negative Breast Cancer is ongoing [104].

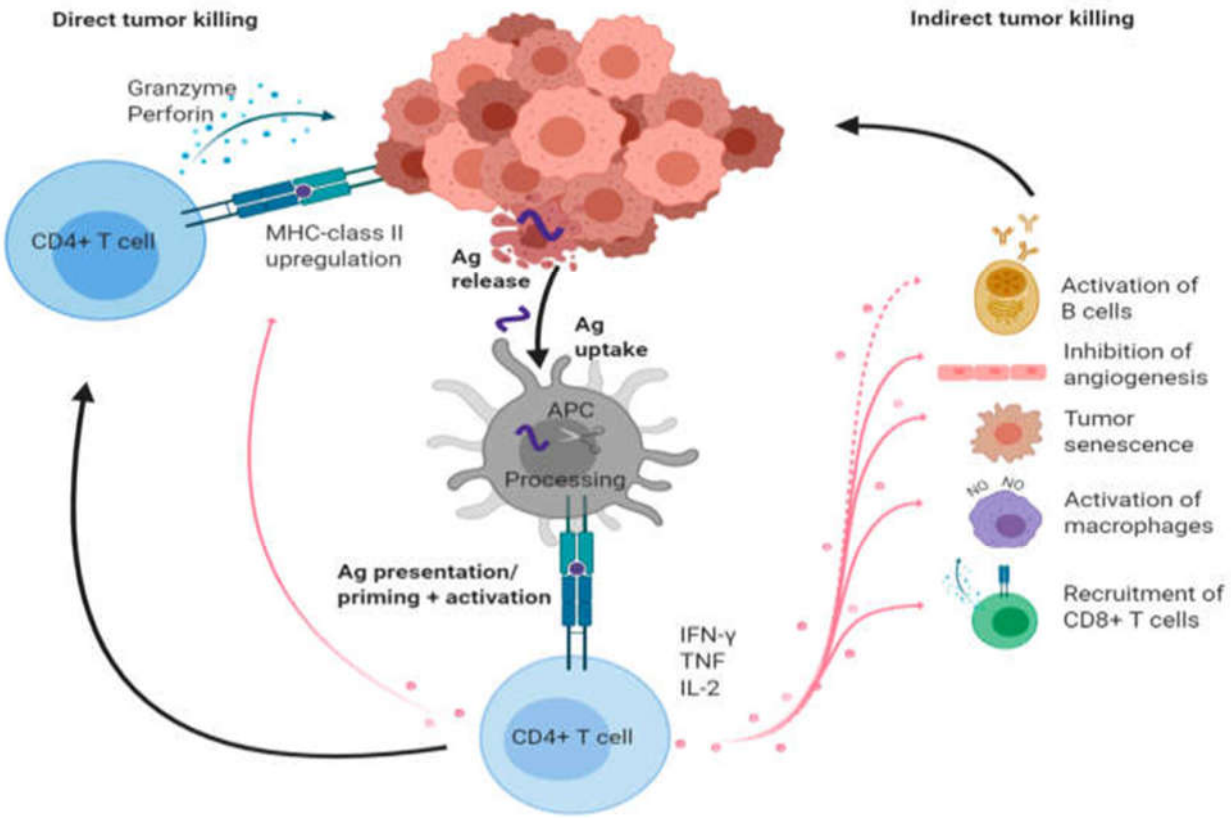

Figure 6. Overview of CD8+ Cytotoxic T cell tasks in antitumor immunity [93].

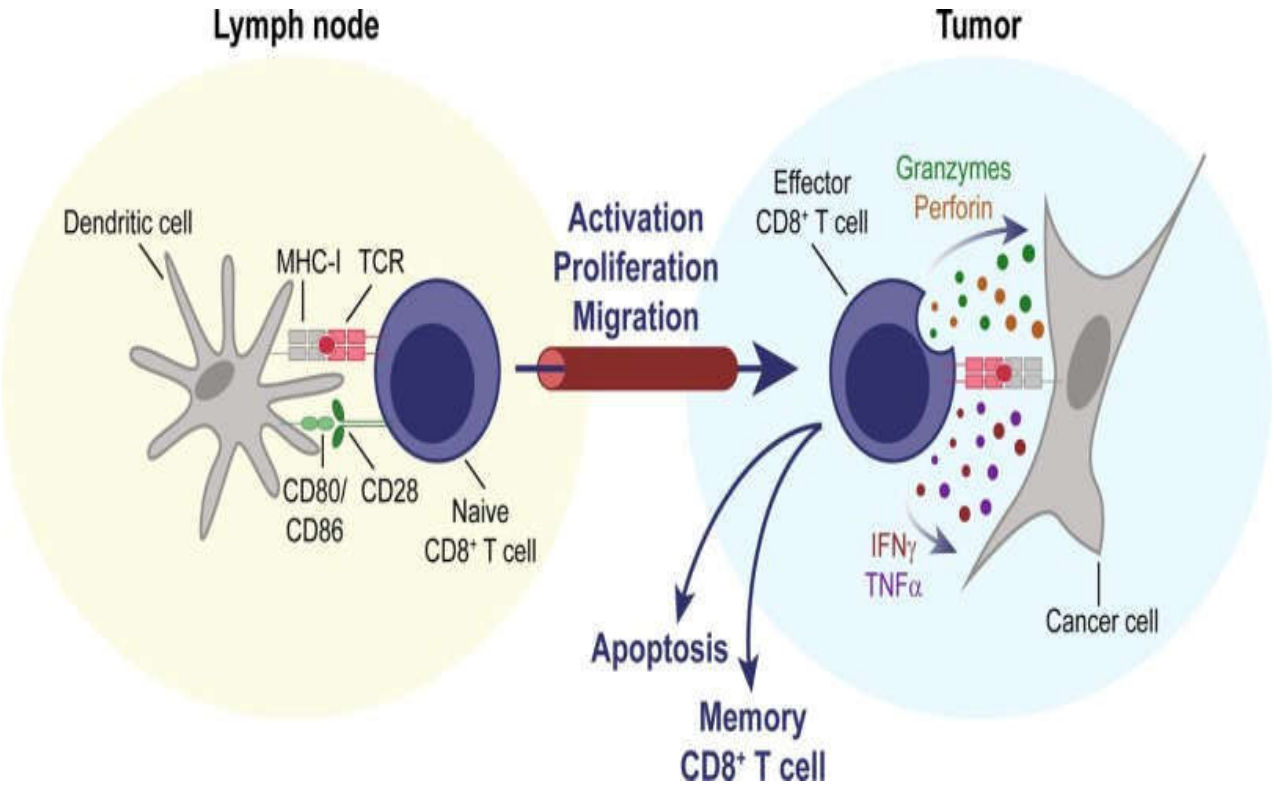

Figure 7. Overview of CD4+ T helper cell tasks in antitumor immunity [94].

1.4.3 Background information on MuLVgp70 protein, on AH1 peptide and on AH1-A5 peptide

Murine leukemia virus (MuLV), which can induce leukemia in mice, is one of the first discovered mammalian retroviruses found in the 1950s and is one of the simplest retroviruses due to its minimal coding capacity [105,106]. Gp70 is a MuLV endogenous viral envelope glycoprotein that is silent in normal tissues and located at many different sites in the mouse genome. However, gp70 can be reactivated in cancer cell lines like B16 and CT26 [107]. Francesca Scrimieri et al. [108] demonstrated gp70 expressed in many murine tumor cell lines with different levels using the quantitative real-time PCR (RT-qPCR) assays (Table 6). Although Gp70 is highly expressed in some murine tumors, and it is expressed lower in normal adult tissues [109]. Thus, gp70 could be an optimal antigen source for the peptide vaccine in mouse tumor models. AH1 (SPSYVYHQF) peptide is a linear epitope derived from MuLV Gp70 amino acids 423–431 and presented by the major histocompatibility complex (MHC) class I Ld molecule (H2-Ld) [110]. Multiple studies demonstrated AH1 peptide was able to inhibit the growth of CT26 murine colorectal carcinoma in the mouse model [111-113]. Furthermore, some studies showed AH1 specific CD8+ T cells could induce the apoptosis of the 4T1 mammary cell line in vitro [114]. AH1-A5 (SPSYAYHQF) peptide is an AH1 peptide variant that has a mutant amino acid in position 5 of the AH1 peptide (Val to Ala) [115]. Although AH1-A5 has similar MHC binding affinities with AH1 peptide, H-2Ld-AH1-A5 complex binds TCR with higher affinity than H-2Ld-AH1; meanwhile, AH1-A5 peptide could not only improve cytolytic activity mediated by an AH1-Specific T Cell Clone in vitro but also improve T cell immunity to AH1 peptide and CT26 tumor in vivo [116].

Table 6. Gp70 mRNA expression levels in various murine tumor cell lines analyzed by RT-qPCR assays [108]

Cell Line	Type	Origin	Mean*	SD*
ALL302	Leukemia		33.81	0.05
4T07	Breast cancer	Breast	16.47	0.09
4T1	Breast cancer	Breast	16.26	0.15
67NR	Breast cancer	Breast	14.79	0.14
A17	Cervical cancer	Cervix	27.14	0.16
B16 F0	Melanoma	Skin	16.00	0.07
B16 F10	Melanoma	Skin	15.49	0.14
CT26	Colon carcinoma	Colon	15.35	0.01
EL4	Lymphoma	T lymphocyte	24.23	0.07
ICN1	T-cell acute lymphoblastic leukemia	Thymocytes	25.15	0.12
K7	Osteosarcoma	Bone	14.24	0.09
K7M2	Osteosarcoma	Bone	14.49	0.03
MM1	Medulloblastoma	Cerebellum	28.16	0.12
NBL 947.4	Neuroblastoma	Neural crest	33.00	0.23
NBL 975A2	Neuroblastoma	Neural crest	27.24	0.25
NIH-3T3	Fibroblast	Embryo	n.d.	19
P0	Cervical cancer	Cervix	29.49	0.17
P815	Mastocytoma	Mast Cell	18.55	0.07
RMS 76–9	Rhabdomyosarcoma	Muscle	14.07	0.16
RMS M3–9-M	Rhabdomyosarcoma	Muscle	18.17	0.03

*n = 3; n.d., non-detectable.

1.4.4 Background information on SPARC protein and peptides derived from SPARC protein

SPARC (Secreted protein acidic and rich in cysteine), also known as osteonectin, basement-membrane-40, or BM-40, is a non-structural extracellular matricellular glycoprotein secreted by endothelial cells, fibroblasts, and cardiomyocytes [117,118]. Although SPARC is often considered a secrete protein, it is also expressed on the basement membrane and cytoplasm [119,120]. The

function of SPARC is regulating extracellular matrix (ECM) reorganization, cell adhesion, and proliferation in the tissue [121]. Therefore, SPARC may play a crucial role in cancer development and metastasis. Furthermore, SPARC is always associated with highly aggressive tumors like melanomas and gliomas [122,123]. Meanwhile, SPARC may function as a tumor suppressor in some other cancer types, such as ovarian, neuroblastomas, and colorectal cancers [124]. Breast cancer has been identified with a high-level expression of SPARC and is considered as a marker of poor prognosis and recurrence [125,126]. However, the roles of SPARC in breast cancer were reported with contradictory results. Wong and colleagues revealed that loss of SPARC had no significant effects on tumor initiation, progression, angiogenesis, or metastasis in murine mammary tumor models [127]. Overexpression of SPARC in MDA-231 cells does not increase cell proliferation, apoptosis, migration, and aggregation [128]. In contrast, SPARC overexpression in 4T1 cells by retroviral vectors reduced tumor growth and metastasis [129]. Yoshiaki Ikuta et al. [130] identified two peptides from BALB/c mouse SPARC protein which belong to H2-Kd-restricted cytotoxic T lymphocyte (CTL) epitopes Table 7. In addition, they reported that peptides DYIGPCKYI and MYIFPVHWQF could induce epitope-specific CTL reactions in BALB/c mice without causing autoimmune diseases [130]. Furthermore, Mitsuhiro Inoue et al. [131] demonstrated that cytotoxic T lymphocytes (CTLs) from the peripheral blood mononuclear cells stimulated by these two peptides in vitro exhibited cytotoxicity specific to cancer cells expressing both SPARC and HLA-A24 (A*2402). These results paved the way for the epitopes derived from SPARC as potential cancer vaccines.

Table 7. Peptides derived from mouse SPARC protein

Source of peptides	Position	Peptide sequence	T cell Specificity	Mouse Haplotype	Mouse Strains	TAA
S1 SPARC	143–151	DYIGPCKYI	CD8+	H2-Kd	BALB/c	Yes
S2 SPARC	225–234	MYIFPVHWQF	CD8+	H2-Kd	BALB/c	Yes

1.5 Oncolytic Vaccinia Virus Strains

1.5.1 Overview of Oncolytic Viruses

Viruses employed as first cancer therapeutic agents in clinical trials began in 1949, 22 patients suffering from Hodgkin's disease were treated by administering the hepatitis B virus [132]. In 1952, Southam and Moore using Egypt 101 virus treated 34 patients with advanced unresponsive neoplastic disease, four patients showed successful tumor regression [133]. After these early clinical studies, many different human viruses were applied in the clinic for cancer treatment during the next few decades. Meanwhile, the concept of oncolytic virotherapy was becoming more and more popular as a promising therapeutic approach. Oncolytic viruses (OVs) are genetically engineered or wild-type viruses that can enter replicate in tumor cells and lyse tumor cells without or with limited harm to the healthy cells and the normal tissues. Over the past 20 years, OVs have gradually come at the forefront of research in cancer therapy. Oncorine (H101) was the first oncolytic virus applied in clinical tumor therapies in human history. It was approved by China Food and Drug Administration Department (CFDA) to treat nasopharyngeal carcinoma in combination with chemotherapy in 2005 [134-136]. In 2015, the US-FDA approved T-VEC (A genetically engineered Herpes Simplex Virus-Talimogene, Laherparepve, an HSV- based oncolytic virus) for different types of cancer treatment [137]. Moreover, several viruses are currently under investigation and are undergoing clinical trials as oncolytic viral vectors to treat various types of advanced cancers Table 8 [138].

Table 8. Oncolytic viruses in clinical trials [138,139].

Cancer type	Expressed therapeutic molecule	Type of viral vector and combination therapy	Response
Brain	IL12	HSV-1	Phase I design
	None	HSV-1 G207+ radiation	Phase I safety
	None	HSV-1 G207	Phase IB, anti-tumor activity
	None	HSV-1 G47δ	Fast-track approval
	None	NDV Ulster	Long-term survival in patients
Bladder	GM-CSF	Ad	Good tolerance, anti-tumor activity
	GM-CSF	Ad	Close to approval
	None	VV	Safe delivery in Phase I
Head and neck	None	NDV73T	Improved survival rate in patients
	None	VV GL-ONop	Improved survival in patients
	p53	Ad	Approved drug
	p53	Ad E1B55K deletion	Approved drug
	None	Reolysin (Reovirus) + paclitaxel/CPlat	No toxicity in Phase I/II
	None	Pelareorep (Reovirus)	Close to drug approval
Kidney	IL12	SFV + liposomes, PEG	Tumor targeting, clinical safety
	None	NDV PV701	Objective responses in Phase I
	GM-CSF	VV-JX594	Phase I evaluation
Liver	GM-CSF	VV-JX594	Close to drug approval
Melanoma	IL12	SFV + liposomes, PEG	Tumor targeting, clinical safety
	None	NDV73T	Improved survival in patients
	GM-CSF	HSV1	Approved drug
	None	Reolysin (Reovirus)	Safe delivery, Phase II
	None	CVA21	Anti-tumor activity in Phase I/II
	None	CVA21	Immuno-response in Phase II
	None	CVA21+ pembrolizumab	Response in Phase IB

Table 8 continued

Cancer type	Expressed therapeutic molecule	Type of viral vector and combination therapy	Response
Pancreatic	None	Reolysin (Reovirus) + paclitaxel/CPlat	Safe delivery, Phase II
Prostate	None	AAV-CG7870	Decreased serum PSA in Phase I
	CD/HSV-TK	Adenovirus	Decreased serum PSA in Phase I
	PSMA	VEE	Neutralizing antibodies in Phase I
	None	Pelareorep (Reovirus)	Repeated delivery in Phase I
	Prostate-specific antigen (PSA)	VV	Immuno-response in Phase I
Ovarian Cancer	None	VV, GL-ONC1	Entering phase III clinical trial

Abbreviations: Ad, adenovirus; CD, cytosine deaminase; CPlat, carboplatin; CV, Coxsackie virus; GM-CSF, granulocyte-macrophage colony-stimulating factor; HSV-TK, herpes simplex virus thymidine kinase; NDV, Newcastle disease virus; PEG, polyethylene glycol; PSMA, prostate-specific membrane antigen; PSA, PS antigen; SFV, SemlikiForest virus; VEE, Venezuelan equine encephalitis; VV, vaccinia virus

1.5.2 Overview of vaccinia virus

Vaccinia virus (VACV) is an enveloped double-stranded DNA virus with a broad host range and belongs to the member of the Poxviridae family [140]. VACV has approximately 200 Kbp length of genome, which encodes around 250 proteins. The gene transcription of VACV can be classified in real-time in three consecutive stages: early, intermediate and late. Each stage has specific promoters and transcription factors [141]. VACV was employed as a smallpox vaccine and has been widely researched for decades, which led to the eradication of the variola virus (the human poxvirus) in the late 1970s, which is the first deracinated virus in human history [142]. The entire life cycle of VACV occurs and is complete within the cytoplasm of infected cells. After the viral particle enters into the host cells through virion fusion with the cell membrane, VACV forms four different types of virions [143]: intracellular mature virus (IMV) particles are first assembled virions in the cytoplasmic virus factories, which is the place initiate the replication of the VACV DNA, and each factory begins as a single viral infecting particle [144]; intracellular enveloped virus (IEV) derived from IMV, and are wrapped by a double layer of endosomes and trans-Golgi network (TGN) membrane; cell-associated enveloped virus (CEV) was viral particles fused with the cell plasma membrane; extracellular enveloped virus (EEV) is the formation of virus released from the infected cells and mediates the long-range dissemination of virus in vitro and probably in vivo Figure 8.

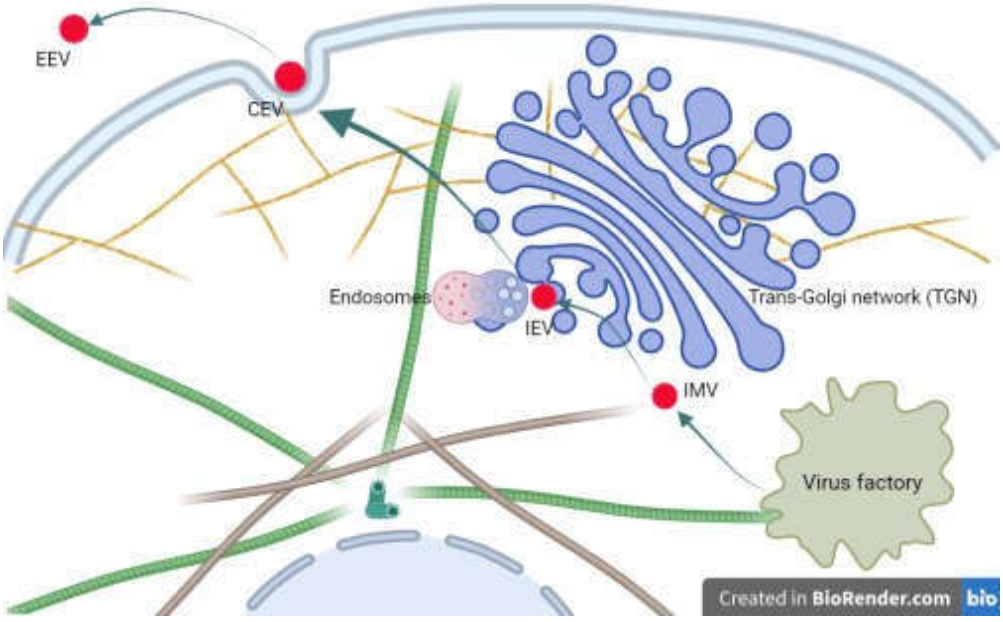

Figure 8. Overview of the VACV life cycle

1.5.3 Vaccinia virus as an oncolytic agent

VACV is one of the most promising oncolytic viruses. Different isolations have been extensively used as oncolytic vectors for cancer therapies due to their inherent features of natural tumor tropism, lyse tumor cells, and spread through tumor tissue as well as active anti-tumor immunologic reactions [145,146]. VACV holds excellent promise as an oncolytic agent mainly because of its safety, large foreign DNA size carrying capacity (up to 25 kb), and natural oncolytic capability [147-150]. Furthermore, VACV is one of the safest viruses the viral genome cannot integrate into the host cell genome and possesses an excellent safety record as a vaccine for eradicating smallpox disease in human history, as described above. VACV provides a large transgene addition capacity and carries multiple genomic insertion locations without reducing the viral replication. Meanwhile, the methods of genetic modification of VACV are simple, convenient, and well developed. Moreover, deleting specific VACV genes or inserting foreign genes could significantly improve the tumor selectivity based on the natural tumor tropism of the wild-type vector.

1.6 Real-Time Fluorescence Imaging System-IncuCyte®S3

IncuCyte®S3 is a live-cell imaging system developed by Bioscience. It can provide instant and real-time cell distribution images from the different types of plates, which help derive physiologically relevant information about the cells, such as cell confluence or migration. Furthermore, based on these parameters, real-time kinetic data can be obtained [151].

2. Materials and Methods

2.1 Materials and Equipment

2.1.1 Equipment

Name of the instrument	Manufacturer
Autoradiography films	Fuji
Axiovert 40 CFL	Zeiss
Biofuge fresco	Heraeus
Biofuge pico	Heraeus
BioPhotometer	Eppendorf
ChemiDoc XRS+ System	BioRad
Centrifuge 5424 R	Eppendorf
CO_2-Incubator ICO150med	Memmert/ Eppendorf
EWJ 300-3	Kern
Heracell 150i	Thermofisher
Herasafe KS 12	ThermoFisher
L46 Power Mixer	Labinco
Mega Star 3.0R	VWR
Mini-Sub Cell GT	BioRad
Mastercycler X50s	Eppendorf
Mini Trans-Blot Cell	BioRad
Multi Casting chamber	Bio-Rad
Trans-Blot Turbo Transfer System	Bio-Rad
Semi-Dry Blot apparatus	Peqlab
Multichannel pipette	Eppendorf
PowerPac Basic	BioRad
Polymax 2040	Heidolph

Name of the instrument	Manufacturer
Recirculating chiller DLK 402	Fryka
Rocking platform	VWR
450 Sonifier	VWR Branson
Sunrise Microplate reader	Tecan
Semi-Dry Blot apparatus	Peqlab
Cell Counting Slides	BIO-RAD
Thermomixer comfort	Eppendorf
TC20 Automated Cell Counter	BioRad
UVette 220 - 1600 nm	Eppendorf
Vortex VX100	Labnet
Water bath	Fisher scientific
IncuCyte®S3	Bioscience, Sartorius

Software

FreeCAD software for viral plaques counting; Graphpad Prism 8.0 for Statistical analyses; Flowjo, BD.

Incucyte®S3 Software: (v2018B,https://www.essenbioscience.com/en/products/software/incucyte-s3- software-v2018b/).

2.1.2 Reagents

Dulbecco's Modified Eagle's Medium-high glucose (Thermo Fisher Scientific, Waltham, MA, USA, 11965092), RPMI 1640 Media (Thermo Fisher Scientific, Waltham, MA, USA, 31870082),Opti-MEM™ I Reduced Serum Medium (Thermo Fisher Scientific, 31985062), Fetal Bovine Serum (Merck, Darmstadt, Germany, F4135),Penicillin Streptomycin (Thermo Fisher Scientific, 15070063), TurboFectin8.0 (Origene, Rockville, MD, USA, TF81001),Hexadimethrine bromide (Merck, Darmstadt, Germany, H9268-5G), Blasticidin solution (InvivoGen, San Diego, CA, USA,

ant-bl-05).Ultracel-100 regenerated cellulose membrane 15 mL sample volume (Merck, Darmstadt, Germany, UFC910024), Nunc™ 50 mL conical sterile polypropylene centrifuge tubes (Thermo Fisher Scientific, 339652), safe-lock protein oBind tubes (Eppendorf, Hamburg, Germany, 925000090), 96-well plate (Corning, New York, NY, USA, 3596),Corning®1–200 µL universal fit pipette tips (Merck, Darmstadt, Germany, CLS4860-960EA), cell scrapers (Cell treat, Pepperell, MA, USA, 229310), laboratory markers (Edding, Ahrensburg, Germany, 8015 F 0.75 m Black). DPBS (no calcium, no magnesium) (14190250, ThermoFisher); ACK Lysing Buffer (A1049201, ThermoFisher); Cell Staining Buffer (420201, BioLegend)

Antibodies： Anti-Mouse IgG HRP produced in goat (Sigma-Aldrich, A4416); DyLight 649 Goat anti-mouse IgG (BioLegend, 405312); Monoclonal ANTI-FLAG M1 (Sigma Aldrich, F3040); Monoclonal ANTI-FLAG M2 (Sigma-Aldrich, F3165); anti-mouse SPARC antibody (R&D, AF942-SP); APC anti-mouse CD279 (PD-1) Antibody (135210, biolegend); APC Rat IgG2a, κ Isotype Ctrl Antibody (400511, biolegend); APC anti-mouse CD3ε Antibody (100312, biolegend); APC Armenian Hamster IgG Isotype Ctrl Antibody (400911, biolegend); Alexa Fluor® 488 anti-mouse CD8a Antibody (100723, Biolegend); FITC Rat IgG2a, κ Isotype Ctrl Antibody (400505, Biolegend); FITC anti-mouse CD4 Antibody (100406, Biolegend); FITC Rat IgG2b, κ Isotype Ctrl Antibody (400605,Biolegend); Purified Rat Anti-Mouse CD16/CD32 (Mouse BD Fc Block™) Clone 2.4G2 (RUO) (553141,BD)

Self-made buffers and solutions：

Coating buffer, pH 9.6

8.4g	$NaHCO_3$
3.56g	Na_2CO_3
Add ddH2O to final volume of 1.0L	

ECL solution buffer A

1mL	Luminol
0.44mL	Coumaric acid
10mL	Tris-HCl 1M, pH 8.5,
Add ddH2O to final volume of 100 mL	

ECL solution buffer B

64µL	30% hydrogen Peroxide
10 mL	Tris-HCl 1M, pH 8.5,

Add ddH2O to final volume of 100ml

PBS/T (0.1 %)

500mL	PBS
0.5mL	Tween 20

Ripa-buffer

0.88g	NaCl
0.1mL	Nonidet P-40 (1%)
0.05 mL	Sodium deoxycholate (0.5%)
0.01 mL	SDS (0.1 %)
5 mL	Tris 50 mM, pH 7.4,

Add ddH2O to final volume of 10 mL

SDS-page running buffer, pH 8.3

25mL	10x TTS Buffer
0.25g	SDS

Add ddH2O to final volume of 1L

TBE-buffer 5x

60.55g	Tris-base
30.90g	Boric acid
3.70g	EDTA

Add ddH2O to final volume of 1L

TBS

1.21g	Tris-base
4.38g	NaCl

Add ddH2O to final volume of 500 mL

TBS/T

250µL	Tween20
500mL	TBS

Terrific Broth medium

47.0g	Terrific broth
4mL	Glycerol

Add ddH2O to final volume of 1 L

Terrific Broth agar

14.1 g	terrific broth
4.5 g	Agar
1.2 mL	Glycerol

ddH2O to final volume of 300 mL

1XTransfer-buffer

200 mL	Transfer buffer 5 x
200 mL	Ethanol
600 mL	ddH2O

Tris-HCl 1M, pH 8.5

121.14 g Tris-base

Adjust pH with HCl to 8.5

Add ddH2O to final volume of 1 L

Tris-HCl 2.5 M, pH 8.8

302.85g Tris-base

Adjust pH with HCl to 8.8

Add ddH2O to final volume of 1 L

Tris-HCl 50 mM, pH 7.4

6.06g Tris-base

Adjust pH with HCl to 8.8

Add ddH2O to final volume of 1 L

Restriction Enzymes:

XbaI	#15226-038 [Invitrogen life technologies, Carlsbad, CA USA]
NheI	#15444-011 [Invitrogen life technologies, Carlsbad, CA USA]
BamHI	#15201-031 [Invitrogen life technologies, Carlsbad, CA USA]
NotI	#15441-017 [Invitrogen life technologies, Carlsbad, CA USA]
SacI	#R0156S [New England Biolabs, Ipswich, MA USA]
BglII	#15213-028 [Invitrogen life technologies, Carlsbad, CA USA]
NaeI	#R0190S [New England Biolabs, Ipswich, MA USA]
SmaI	#15228-018 [Invitrogen life technologies, Carlsbad, CA USA]
EcoRI	#15202-021 [Invitrogen life technologies, Carlsbad, CA USA]
SphI-HF	R3182SBioLabs

2.1.3 Kits

Name	Manufacturer
QIAGEN Plasmid Plus Kits	QIAGEN
QIAquick PCR Purification Kit Thermo fisher	QIAGEN
QIAquick Gel Extraction Kit	QIAGEN
DNeasy Blood & Tissue Kits	QIAGEN
MojoSort™ Mouse CD8 T Cell Isolation Kit	Biolegend
Pierce BCA Protein Assay Kit	ThermoFisher
CloneEZ PCR Cloning Kit	GenScript Trans-Blot Turbo
RTA Mini Nitrocellulose Transfer Kit	BioRad
IL-2 Mouse Uncoated ELISA Kit with Plates	ThermoFisher

2.1.4 Chemicals

Chemical/Reagent	Manufacturer	Catalog number
10x TTS Buffer	BioRad	1610744
1kb Plus DNA Ladder	Invitrogen	10787018
2x Phusion Master Mix	ThermoFischer	F531L
4x Laemmli Sample buffer	BioRad	1610747
Acrylamide/Bis-acrylamide, 30 % solution	Sigma-Aldrich	A3574
Agar	Sigma-Aldrich	A9414
Agarose Sigma-Aldrich A9539 Ampicillin	Sigma-Aldrich	A9393
APS	Roth	9592.2
Boric acid	Sigma-Aldrich	B6768
BSA	Roth	8076.4
CutSmart Buffer	BioLabs	B7204S
DMEM	Gibco	41965039
DPBS	Gibco	14190144
EDTA	Roth	8043.2

Ethanol	Sigma-Aldrich	32221-M
FBS	Biochrom	S0615
Gel Loading Dye, Purple (6x)	BioLabs	B7024s
GelRed	Biotium	41003
Glycerol	Sigma-Aldrich	49782
HCl	Sigma-Aldrich	258148
Isopropanol	Sigma-Aldrich	I9516
Methanol	Sigma-Aldrich	34860
Milk powder	Roth	T145.3
NaCl	Sigma-Aldrich	S7653
Nonidet P-40 solution (10%)	Sigma-Aldrich	98379
Opti-MEM	Gibco	31985062
P/S	Gibco	15140122
SDS-pellets	Roth	CN30.3
Sodium carbonate	Merck	106392
Sodium deoxycholate	Sigma-Aldrich	D6750
Sodium hydrogen carbonate	Merck	106329
TEMED	Sigma-Aldrich	T9281
Terrific Broth, modified	Sigma-Aldrich	T0918
TMB Stop Solution	BioLegend	423001
TMB Subastrate Reagent Set	BioLegend	421101
Tris base	Sigma-Aldrich	T1503
Trypsin-EDTA (0.25 %)	Gibco	25200056
Turbofectin 8.0	OriGene	TF81001
Tween20	Roth	9127.1
β-Mercaptoethanol	Applichem	A1108

Chemically synthesized peptides

The peptides SPARC 143-151: DYIGPCKYI (1-2 mg); SPARC 225-234: MYIFPVHWQF (1-2 mg); AH1-A5: SPSYAYHQF (1-2 mg) are synthesized by the company Peptide Specialty Laboratories GmbH (Im Neuenheimer Feld 515, 69120 Heidelberg, Germany) and the purity levels of at least 90% to 95%. The peptide AH1 6-14: SPSYVYHQF (1 mg) was purchased from the company Eurogentec (Catalog: AS-64798, 34801 Campus Drive Fremont, CA 94555, USA), the purity is over 95%

2.1.5 Cell lines and viruses

Cell line

DH5α-competent cells were purchased from Thermo Fisher Scientific. African green monkey kidney fibroblasts cell line (CV-1) was obtained from the American Type Culture Collection (ATCC; CCL-70). Mouse mammary carcinoma N2C cell line was kindly provided by Professor Mario P. Colombo (Fondazione IRCCS Istituto Nazionale dei Tumori, Milano, Lombardia, Italy). HEK 293T cell line was purchased from the German Collection of Microorganisms and Cell Cultures GmbH (DSMZ no.: ACC 635). The mouse mammary gland carcinoma 4T1 (ATCC; CRL-2539) cell line and melanoma B16F10 cell line (ATCC; CRL-6475) were obtained from the American Type Culture Collection. The generation of the stable cell lines N2C-pTet- turboFP635-EF-1a-Egfp has been described previously, and 4T1-EF-1a-turboFP635 stable cell line was constructed followed this article (). All of the cell lines were propagated in Dulbecco's modified Eagle's medium (DMEM; 11965092, Thermo Fisher Scientific) supplement with 10% Fetal Bovine Serum (FBS, F4135, Sigma) and 1% penicillin-streptomycin (P4333, Sigma)

Plasmids and constructions

Plasmid pTet-turboFP635-EF-1a-eGFP-PKG-BSD was constructed from the pTet- IRES-eGFP plasmid (kindly provided by Professor Maria Li Lung, Department of Clinical Oncology, Li Ka Shing Faculty of Medicine, the University of Hong Kong (Hong Kong, China). First, the turboFP635 gene was inserted into the pTet-IRES-eGFP plasmid at the Pme I restriction site. Second, the Human elongation factor-1 alpha (EF-1a) promoter gene was inserted into the plasmid at the Pst I and BmgBI restriction sites, and then the PKG promoter-Blasticidin fusion gene was inserted at the SalI restriction site. tTA_BFP (#58854) plasmid was purchased from Addgene (Watertown, MA, USA). The pLV-Exp-Bsd-EF1a-Turbo plasmid was constructed from pLV-Exp-Bsd-EF1A-eGFP. The eGFP DNA fragment of the plasmid pLV-Exp-Bsd-EF1A-eGFP was replaced by the TurboFP635 gene after digesting with the BsrGI restriction enzyme. The pSC65 plasmid was obtained from Genelux Corporation, San Diego Science Canter, 3030 Bunker Hill Street, San Diego, CA 92109, USA. To construct the shuttle vector, the LacZ fragment was deleted in the PSC65 plasmid by

double digestion through Xho I and EcoR I restriction enzymes and replaced with the eGFP gene to generate the pSC65-eGFP plasmid. The pSC65-eGFP plasmid was constructed using Xho I and EcoR I restriction enzymes double digest plasmid PSC65 then inserted the eGFP gene. To construct the plasmid pSC65-eGFP-mIL2, the mIL-2 gene fragment was inserted into the pSC65 plasmid through the BglII restriction site. The pIg-TurFP635 plasmid was provided by Dr. Duong Hoang Nguyen, Stemimmune, San Diego, CA, United States. For the plasmid pIg-TurFP635-4T1-peptides construction, a 4T1 tumor-associated antigen peptides fusion protein gene segment was inserted into the pIg-TurFP635 through the Sph I restriction site. The primers for the plasmid construction and viruses identification are shown in Table S1.

Virus strains

Vaccinia virus strain LIVP (L1) was derived from LIVP (Lister strain, Institute of Viral Preparations, Moscow, Russia). Vaccinia virus strain GLV-1h109 virus was derived from the oncolytic vaccinia virus GLV-1h68 by inserting the glaf-1 gene encoding the GLAF-1 antibody under the control of the vaccinia virus promoter (p7.5) into the J2R locus (Figure 15). C1-opt1 was Copenhagen (C1) strain thymidine kinase (TK) deleted and inserted with Turbo-FP635 under the control of vaccinia synthetic early/late promoter- Psyn (E/L) provided by Tanja Auth, StemVac GmbH, Bernried, Germany Figure S1.

2.1.6 Animals

The female BALB/c mice of 5- to 6-week-old were purchased from Charles River, Sulzfeld, Germany.

2.2 Methods

2.2.1 Recombinant Vaccinia virus construction and purification

Day 1: Seed 3-4 x 10^5 CV-1 cells with 2ml complete growth medium per well in 6-well plate to reach 80% confluence in the next day. Day 2: Aspirate medium from a confluent monolayer of cells, then infect the cells with 4 x 10^4 pfu vaccinia virus in one well for 2 hours at 37°C, agitate the plate every 30mins. Transfect 1ug pmaxGFP plasmid with TurboFectin 8.0 into virus uninfected wells and 3-4ug shuttle plasmid into the virus-infected wells, incubate at 37°C for two days, then using the IncuCyte®S3 whole well imaging function check the fluorescence signal for transfection efficiency. Day 4: Aspirate the medium and use the scraper to harvest the infected cells in 1ml FBS Free DMEM frozen in -80°C for backup use, meanwhile seed 4-5 x 10^4 CV-1 cells with 100ul complete growth medium per well into the six 96-well plate to obtain 100% confluence on the next day. Day 5: After ultrasonic processing, the viral stock from the former step, add 0.25ul into the 61ml FBS free DMEM medium, then use the multichannel pipette add 100ul DMEM medium per well into the 96-well plates. Put all the 96-well plates into IncuCyte®S3 to set up a scan schedule that initiates the plate scanning after one and half days. After all the plates are scanned, suspend the scheduled program. Check the images and marker the plaques under the standard optical microscope, then pick out the positive clones with pipette tips in 200ul DMEM/PBS for second round purification (suggest using 6 or 24 well plates for the next few rounds purification), purify the recombinant virus.

2.2.2 Western blotting

Western blotting (immunoblotting) is a widely used laboratory technique to detect specific protein molecules in tissue and cell samples. In this study, I used it to detect virus-mediated expression of tumor-associated peptides and mIL-2 in infected 4T1 tumor cells. The details of the Western blot experiment in this work were described by Syed R. Haider et al. (152). The proteins in the samples were separated in 10% acrylamide gel, and the gels were used by semi-dry blotting onto the PVDF membrane. To block the non-specific sites, the membrane was incubated with 1 x TBS 5 % milk powder for one h at room temperature. Then a directly labeled antibody or an unlabeled primary antibody was incubated overnight at 4°C. After washing three times with 1 x TBS 0.5 % Triton-X 100 on the next day, the membrane was incubated with the respective secondary antibody for one h at room temperature. Then the membrane was incubated with TMB and scanned in the Bio-Rad ChemiDoc XRS+ system.

2.2.3 Elisa assay

The Elisa assay used here was to detect the bioactivity of mIL-2 protein in virus-mediated expression in 4T1 cell cultures. The mIL-2 capture antibody was coated to the 96-well ELISA plate with 100 µl/well in the coating buffer by incubating overnight at 4°C. Then the remaining binding sites were blocked with 200 µL of 5% Non-fat powdered milk TBST. After that, the samples in appropriate dilutions were added to the plate for one hour incubation at room temperature, followed by added mIL-2 detection antibody for another one-hour incubation at room temperature. Then100 µL/well of HRP substrate 3,3',5,5'-tetramethylbenzidine (TMB) was supplemented into the plate. And the plate was incubated at room temperature until a blue color could be detected. The reaction was stopped by adding 100 µL per well of 1 M H_2SO4 solution, followed by the measurement of absorbance at 450 nm in an ELISA reader.

2.2.4 VACV amplification and purification

In this study, all the Vaccina virus strains were amplified in CV-1 cells and purified through the sucrose gradient method [153]. After 80% of CV-1 cells were infected by the virus in 145 mm^2 cell culture dishes, the infected cells were collected and resuspended in 14 ml of cold 10 mM Tris·Cl, pH 9.0. Then the cell suspension was homogenized in a glass Dounce homogenizer, centrifuged to remove the cell nuclei, and the supernatant was saved. The remaining cell pellet was resuspended, centrifuged again, and then combined with the supernatant from the former step to get more viruses. The supernatant was processed through sucrose gradient centrifugation to get purified virus. After that, the sample of the virus was aliquoted at −80°C

2.2.5 Virus titration assay

Day 1: Seed 6x 10^5 wild type CV-1 and CV-1-EF-1a-turboFP635 cells with 2ml 10% FBS DMEM growth medium per well in three 6-well plates to reach 100% confluence in the next day. Day 2: Thaw the viral samples (under the running tap water or in the 37℃-heating water bath) and ultrasonic with full power in 1 min, then prepare the virus (Lister 1.1.1, L1c-Ig-Turbo and GLV-1h109) dilution as the following table 9:

Table 9. Protocol for virus dilution

Dilutions	**Recipe**		
10^{-2} dilution	5 µl from virus stock	495 µl DMEM-5% FBS	
10^{-3} dilution	100 µl from dilution 10^{-2}	900 µl	DMEM-5% FBS
10^{-4} dilution	100 µl from dilution 10^{-3}	900 µl	DMEM-5% FBS
10^{-5} dilution	100 µl from dilution 10^{-4}	900 µl	DMEM-5% FBS
10^{-6} dilution	100 µl from dilution 10^{-5}	900 µl	DMEM-5% FBS
10^{-7} dilution	100 µl from dilution 10^{-6}	900 µl	DMEM-5% FBS
10^{-8} dilution	100 µl from dilution 10^{-7}	900 µl	DMEM-5% FBS

Remove the medium from the cell culture wells, infect the cells with 250 µl viral solution from dilution 10^{-5} to 10^{-7} in duplicate, incubate the plate at 37℃, 5% CO2 for 2 hours, gently shaken every 20 mines. Aspirate the infection medium, then add 2 ml of DMEM 10% FBS CMC culture medium to

incubate another two days for further analysis. For the Image visualization, after two days of virus infection, the plates are directly scanned on green or red fluorescence channels using a whole well image program by the Incucyte®S3. The cell lesions (plaques) were photographed at high resolution. Then use the Incucyte®S3 self-contained program to simply process the image remove the background to get the distinct picture. After the image visualization, the pictures were analyzed by FreeCAD software for the plaque counting. In the case of low virus concentration wells, the number of viral plaques could be determined directly on the Incucyte®S3 software.

2.2.6 Construction of stable cell lines

(a) Lentivirus Production, Cultivation of HEK 293T Cells

One or two days before transformation, plate $2X10^6$ HEK293T cells in a 10 cm dish in 10 mL of DMEM supplemented with 10% heat-inactivated fetal bovine serum (FBS) and 1% penicillin-streptomycin and let the cells grow until reach 70–80% confluence.

(b) Prepare DNA/Lentivirus Mixture

In a sterile Eppendorf tube, mix 10 µg Transfer Vector PLV-EF-1a-TurboFP635 for 4T1-Turbo stable cell line construction (Schematic presentation, Figure 1; Plasmid map, Appendix A) and 5 µg (0.5 µg/µL) packaging vectors (5 µg PMD2.G and 5 µg psPAX2) in 1.2 mL of Opti-MEM I medium. Add 40 µL of turbofectin 8.0 (Origene) to the mixture and mix by pipetting. Incubate the mixture for 30 min at room temperature.

(c) Transfection of HEK 293T Cells

Add the mixture prepared in step 3.1.1.2 dropwise to the HEK 293T cells and gently rock the plate back and forth and from side to side to distribute the complex evenly. Incubate the cells in a CO_2 incubator at 37℃ overnight (12 h). Replace the overnight culture medium with fresh DMEM medium supplemented with 2–5% heat-inactivated FBS and 1% penicillin-streptomycin. Collect the virus-containing medium at 36-, 48-, and 60-hours post-virus-transfection into a Falcon 50 mL conical centrifuge tube and keep it at 4℃.

(d) Harvest of Lentivirus

Centrifuge the falcon tubes at 500× g for 10 min to remove the cell debris. Pass the collected supernatants through a 0.45 μM filter and concentrate the virus using Amicon Filter at 3000rpm for 10–20 min at 4 ◦C. Store the lentivirus stokes at -80◦ C.

(e) Lentivirus Infection of 4T-1 and N2C cells.

Seed 4T1 cells and N2C cells with different volumes of lentivirus and DMEM complete +10 μg/mL polybrene medium respectively in 6 well plate (Table 10), after 72 h incubation, the medium was replaced with 10 μg/mL Blasticidin (InvivoGen) containing DMEM medium for another one week. Then replace the Blasticidin containing medium with DMEM complete medium and keep the clones growing for a period of time, pick out the positive monoclones.

Table 10. Components of the infection medium

Dilution	Volume of Lentivirus (μL)	Volume of DMEM complete + 10 μg/mL polybrene (μL)
0	0	500
1:5	300	200
1:10	150	350
1:50	30	470
1:100	15	485
1:500	3	497

2.2.7 Mouse Spleen cell isolation (Isolation of splenocytes from mouse spleens)

The rVACVs injected or PBS injected mice were sacrificed after ten days of vaccination, then spleens were taken out into a 10cm cell culture dish containing 5 ml of ice-cooled complete RPMI medium and crushed using a plunger of the 10-ml syringe until without mostly fibrous tissue remains in the dish (Figure 9). To get the single cell suspension of splenocyte, the cell suspension was pipetted into a 70 µm Nylon cell strainer to filter cells and get rid of the tissue debris (Figure 9). After that, the filtered cell suspension was washed with complete RPMI medium by centrifugation. Then resuspend cells in 3 ml of ice-cold ACK buffer to lyse the red blood cells and incubate the sample at room temperature for 5 min with occasional shaking. The lysis reaction was stopped by adding 7 ml complete RPMI medium. Lastly, the cells were washed with complete RPMI medium twice and resuspended in 5 ml of complete RPMI medium. Then put the sample on ice for the remainder of the experiment.

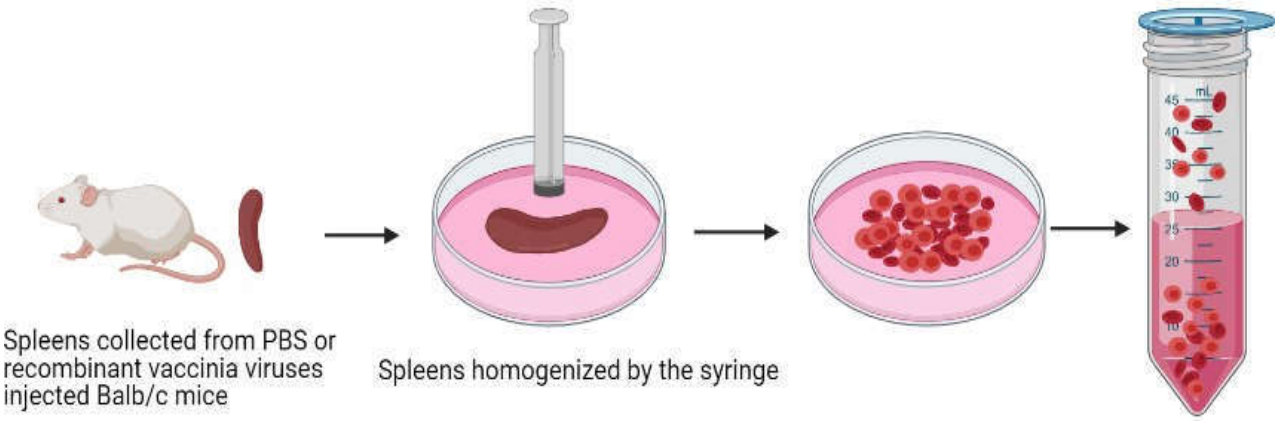

Figure 9. Isolation procedure for splenocytes

2.2.8 Flow Cytometry- Cell-Surface Staining

Splenocyte pellet was resuspended in the Cell Staining Buffer at 5-10 x 10^6 cells/ml and distributed 100µl/well of cells (5-10 x 10^5 cells/tube) into a 96 well plate. For Fc receptor blocking, 100µl/well Anti-Mouse CD16/CD32 antibody (10µg/ml) was added to the plate after removing the cell staining buffer. After the non-specific sites blocking,100µl/well of appropriately pairs of conjugated antibodies (CD3+CD4+; CD3+CD8+; CD4+PD-1+; CD8+PD-1+) and corresponding isotypes were added to the plate (The cell-surface staining and isotype antibodies were prepared as the table 11). After 15-20 minutes of incubation, the cell pellet was resuspended in 0.2 ml of Cell Staining Buffer after being washed twice to perform the flow cytometric analysis.

Table 11. List of antibodies used in flow cytometry

Antibody Name	Isotype	Application Dilution
APC anti-mouse CD279 (PD-1) Antibody	Rat IgG2a, κ	0.2 µg per million cells in 100 µl volume
APC Rat IgG2a, κ Isotype Ctrl Antibody		0.2 µg per million cells in 100 µl volume
APC anti-mouse CD3ε Antibody	Armenian Hamster IgG	0.5 µg per million cells in 100 µl volume
APC Armenian Hamster IgG Isotype Ctrl Antibody		0.5 µg per million cells in 100 µl volume
Alexa Fluor® 488 anti-mouse CD8a Antibody	Rat IgG2a, κ	0.2 µg per million cells in 100 µl volume
FITC Rat IgG2a, κ Isotype Ctrl Antibody		0.2 µg per million cells in 100 µlvolume
FITC anti-mouse CD4 Antibody	Rat IgG2b, κ	0.2 µg per million cells in 100 µl volume
FITC Rat IgG2b, κ Isotype Ctrl Antibody		0.2 µg per million cells in 100 µl volume
APC anti-mouse IFN-γ R β chain Antibody	Armenian Hamster IgG	0.5 µg per million cells in 100 µl volume

2.2.9 Detection of IFN-γ by Flow Cytometry

To induce the expression of IFN-γ, the stimulation medium was prepared as follows conditions:

a. Cells without peptides stimulation in complete RPMI medium with IL-2=100 U/ml and 10μg/ml anti-mouse CD28 antibody as the negative control.

b. Cell stimulation with 1:1000 Cell Activation Cocktail (without Brefeldin A) in complete RPMI medium with IL-2=100 U/ml as the positive control.

c. Cell stimulation with 1ug/ml peptides mixture ($SPARC_{143-151}$, $SPARC_{225-234}$, AH_{16-14}, AH1-A5) stimulation in complete RPMI medium with 100 U/ml IL-2 and 4μg/ml anti- mouse CD28 antibody.

After that, 4 x 10^5 CD8+ T cells per well were seeded into a 96-well U-bottom cell culture plate. Then 200μl per well prepared stimulation medium was added to the plate for IFN-γ induction. After three days of incubation, the IFN-γ was blocked in the cytoplasm by adding Brefeldin A to perform the flow cytometric analysis.

2.2.10 Isolation of CD8+ T cells

After the preparation of single splenocyte pellet suspensions from the spleen of PBS or rVACV injected mice, the cells were filtered with a 70μm cell strainer and washed one time with the MojoSort™ Buffer. To deplete the non CD8+ T cells, biotin antibody cocktail was added by incubation with magnetic Streptavidin Nanobeads. Then the magnetically labeled fraction was retained by magnetic separator, and the CD8+ T cells were collected by decanting the liquid in a clean tube.

2.2.11 Activation and expansion of epitope-specific CD8+ T cells

First, prepare CD8+ T cell activation medium as the follows:

a. Negative control medium: Complete RPMI medium with 160 U/ml IL-2 and 6 ug/ml anti-mouse CD28 antibody.

b. Activation medium: Complete RPMI medium with 1ug/ml peptide mixture,160 U/ml IL-2 and 6 ug/ml anti-mouse CD28 antibody.

Secondly, aliquot 1 x 10^5 cells/ml 50μL isolated CD8+ T cells per wells into a U-bottom 96-well plate, then add 150μL of activation medium. Lastly, place the plate into the CO_2 incubator and culture the cells for four days to get the CD8+ effector T cells.

2.2.12 Co-cultivation assay of activated CD8+ T cells with target tumor cells

After determining the cell count, 1 x 10^3 per well target cells (4T1-EF-1a-turboFP635 and N2C-pTet- turboFP635-EF-1a-Egfp stable cell line has been described previously) with complete RPMI medium were added to a flat bottom 96-well plate for overnight incubation. Then 4-5 x 10^3 effector T cells (i.e., epitope pre-activated or inactivated CD8+ T cells) with flesh activation medium or negative control medium were added to the plate containing the target cells. After that, the plates were put into the IncuCyte®S3 and set up a scan schedule that scan the plate once every 4 hours with the red or green fluorescent signal. Lastly, analysis the data with Incucyte®S3 Software (v2018B).

3. Results

3.1 Characterization of recombinant Vaccinia virus strains expressing tumor-associated peptides and mouse IL-2 in cell culture

3.1.1 Generation of recombinant Vaccinia virus (rVACV) strains using homologous recombination

Homologous recombination (HR) plays a critical role in repairing DNA double-strand breaks and other forms of damages (154). Using the method of HR to produce genetically modified VACV was developed in the 1980s and is still widely used in academic research and clinical applications (155, 156). This approach requires a shuttle plasmid containing the foreign gene and the plaque selection marker gene under the control of their respective VACV promoters, flanked by a DNA sequence from a nonessential region of the viral genome (157, 158). HR occurs between the VACV genome and the two homologous segments flanking the foreign and marker gene in the plasmid, and then the foreign gene is inserted into the aforementioned nonessential region of the VACV genome in vivo (159). Fluorescent proteins are frequently used as plaque selection markers for the purification of the engineered rVACV. Here, we used enhanced green fluorescent protein (eGFP) and far-red fluorescent protein (TurboFP635/Turbo) as fluorescent markers to visualize, isolate, and purify the new recombinant viral strains. L1c-Ig-Turbo is a L1 derivate virus that a TurboPF635 encoding gene was inserted into the space between locus 157 and locus 158. L1c-Ig-Turbo-TK-Egfp (LVP-R-G) was derived from L1c-Ig-Turbo and replaced the TK gene with an eGFP encoding fragment under the control of the p7.5 promoter. For the rVACV strain L1c-Ig-Turbo-TK-Egfp-mIL2 (LVP-R-G-mIL2) construction, the mouse Interleukin 2 (mIL-2) gene under the control of the Psyn (E/L) promoter was inserted into the TK locus and used eGFP as a marker gene for purification. For the rVACV strains of L1c-Ig-Turbo-SPARC/gp70-peptides-TK- eGFP (LVP-R-G-SPARC/gp70-peptides) and L1c-Ig-Turbo-SPARC/gp70-peptides-TK-Egfp-mIL2 (LVP-R-G-SPARC/gp70-peptides-mIL2) construction, a segment of SPARC/gp70-peptides fusion protein gene under the control of the Psyn (E/L) was inserted into the space between locus 157 and locus 158 of the VACV L1 genome to generate the strain L1c-Ig-Turbo-SPARC/gp70-peptides (LVP-R-SPARC/gp70-peptides). Then the

fragment of the eGFP gene controlled by the p7.5 promoter was inserted into the TK locus to generate the strain LVP-R-G-SPARC/gp70-peptides. To construct the LVP-R-G-SPARC/gp70-peptides-mIL-2, a DNA fragment of the mIL-2 gene linked to the Psyn (E/L) promoter and eGFP gene under the control of the P7.5 promoter was inserted into the TK locus of L1c-Ig-Turbo-SPARC/gp70-peptides. The diagrams of newly created rVACV genetic structures are presented in Figure 10. The inserted SPARC/gp70-peptides structure and their sequence information are shown in Figure 11 and Table 12. All the inserted gene fragments were sequenced after amplifying and isolating the novel rVACV strains. All the primers for the sequencing of rVACVs are shown in Table S1. All the novel virus strains were sucrose gradient purified for the viral titer determination to use in animal experiments.

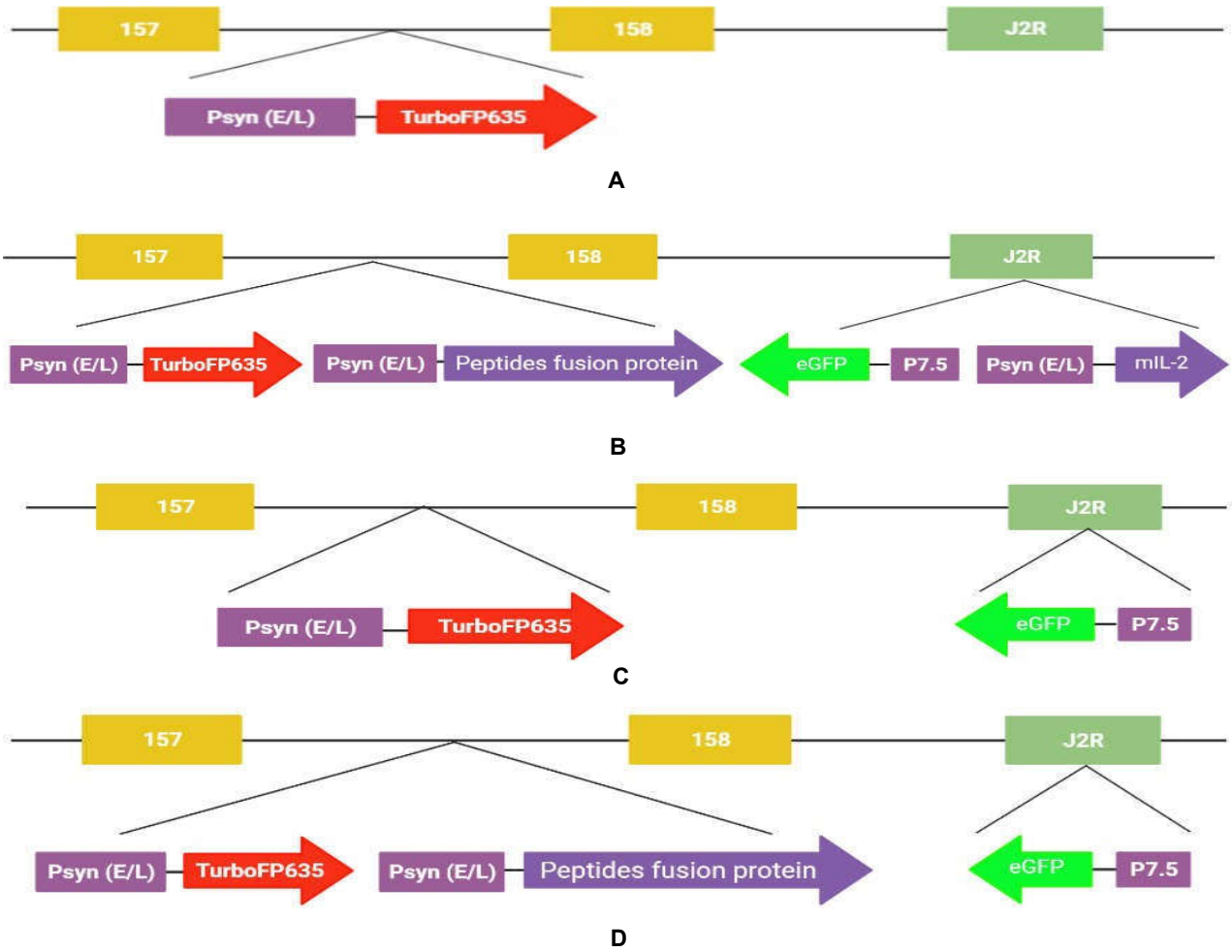

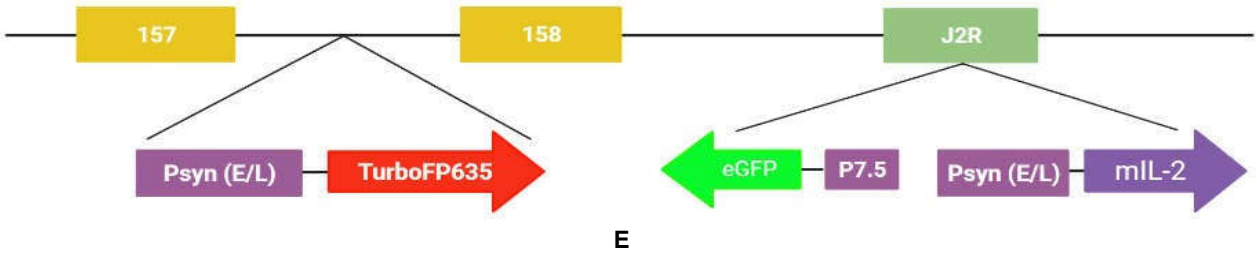

Figure 10. Genetic map of recombinant vaccinia virus strains. **A:** L1c-Ig-Turbo; **B:** L1c-Ig-Turbo-SPARC/gp70 peptides-TK-Egfp-mIL-2(LVP-R-G-SPARC/gp70 peptides-mIL-2); **C:** L1c-Ig-Turbo-TK-Egfp (LVP-R-G); **D:** L1c-Ig-Turbo-SPARC/gp70 peptides-TK-eGFP (LVP-R-G-SPARC/gp70 peptides); **E:** L1c-Ig-Turbo-TK-Egfp-mIL-2(LVP-R-G-mIL-2)

Figure 11. Schematic representation of tumor-associated fusion peptide design

Table 12. Amino Acid sequence of fusion protein elements

Elements	Protein Sequence
IgK leader sequence	METDTLLLWVLLLWVPGSTGD
AH1	SPSYVYHQF
S1	DYIGPCKYI
S2	MYIFPVHWQF
AH5	SPSYAYHQF
Linker	GGGGSGGGGS
3XFlag	DYKDHDGDYKDHDIDYKDDDDK

To visualize the replication of the virus, 4T1 cancer cells were infected with rVACV strains C1-opt1, LVP-R-G-mIL2, and LVP-R-G-SPARC/gp70-peptides-mIL2 at an MOI of 0.1 in 6-well plates. After two hours of incubation, the infection medium was replaced with a fresh growth medium, and cells were maintained in a 5% CO_2 incubator at 37°C for another two days. Then the 6-well plates were scanned by the IncuCyte®S3 via the fluorescent channel to generate the images Figure 12-14. As the results shown in the pictures, the newly constructed viral strains have the ability of infection,

replication, and lysis in the 4T1 tumor cell line. And the infection patterns are the same among these three viral strains.

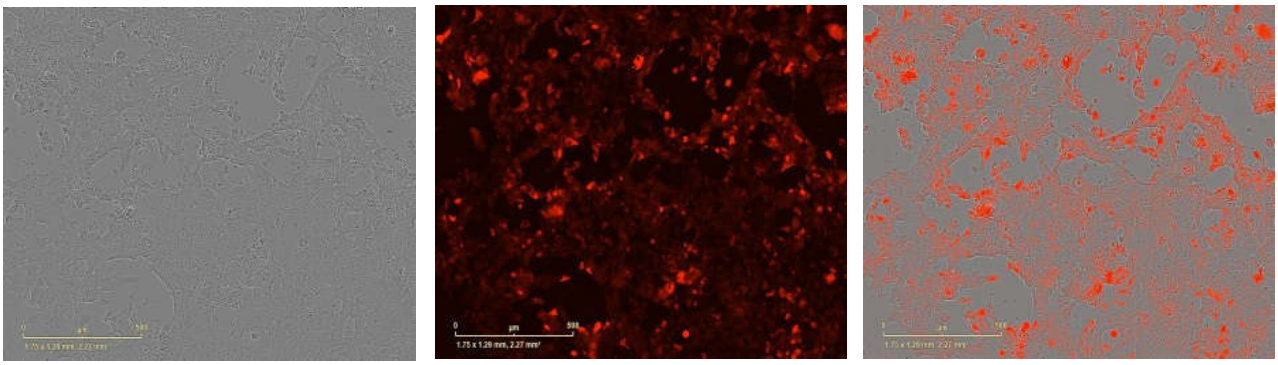

A B C

Figure 12. Images of C1-opt1 infected 4T1 cells. (**A**) Image of C1-opt1 infected 4T1 cells detected by bright phase. (**B**) Image of C1-opt1 infected 4T1 cells detected by red fluorescence signal. (**C**) Image of C1-opt1 infected 4T1 cells, merge. All the scale bars represent 500μm.

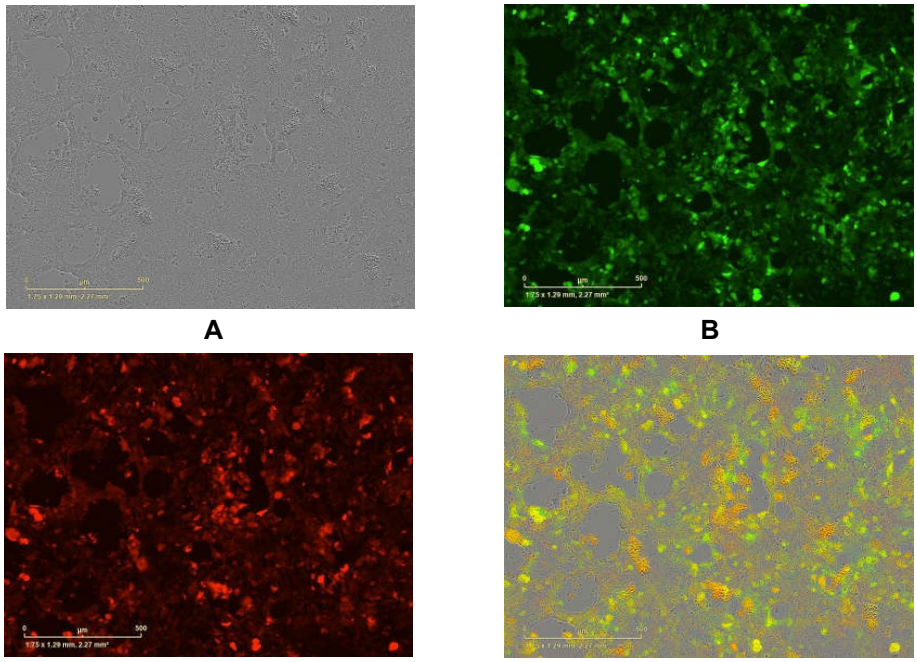

A B C D

Figure 13. Images of LVP-R-G-mIL-2 infected 4T1 cells. (**A**) Image of LVP-R-G-mIL-2 infected 4T1 cells detected by bright phase. (**B**) Image of LVP-R-G-mIL-2 infected 4T1 cells detected by green fluorescence signal. (**C**) Image of LVP-R-G-mIL-2 infected 4T1 cells detected by red fluorescence signal. (**D**) Image of LVP-R-G-mIL-2 infected 4T1 cells, merged. All the scale bars represent 500μm.

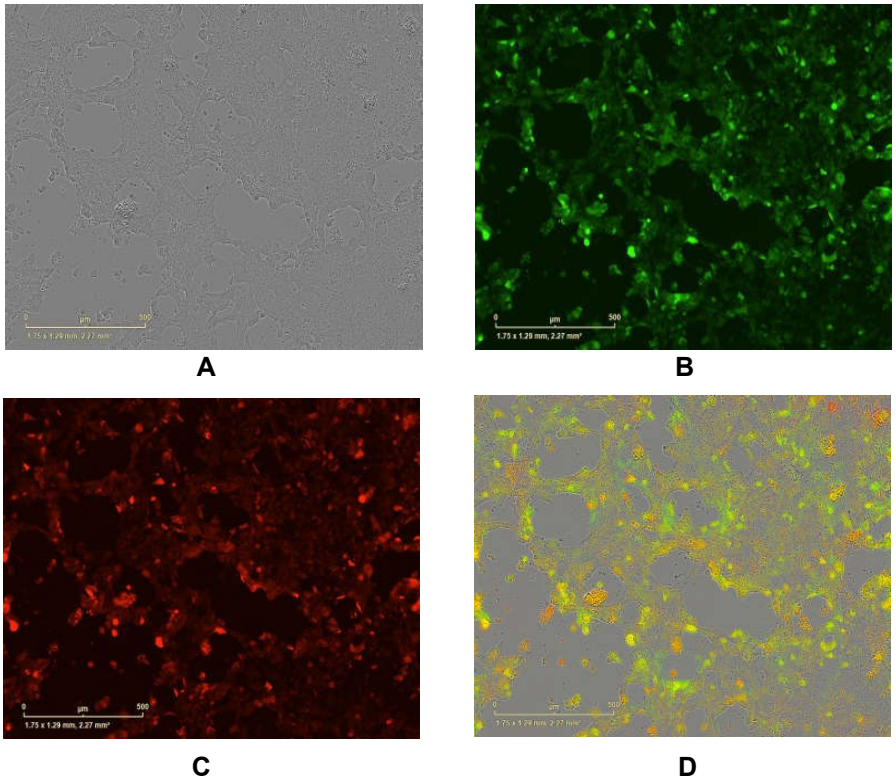

Figure 14. Images of LVP-R-G-SPARC/gp70 peptides-mIL-2 infected 4T1 cells. (**A**) Image of LVP-R- G-SPARC/gp70 peptides-mIL-2 infected 4T1 cells detected by bright phase. (**B**) Image of LVP-R-G- SPARC/gp70 peptides-mIL-2 infected 4T1 cells detected by green fluorescence signal. (**C**) Image of LVP-R-G-SPARC/gp70 peptides-mIL-2 infected 4T1 cells detected by red fluorescence signal. (**D**) Image of LVP-R-G-SPARC/gp70 peptides-mIL-2 infected 4T1 cells, merged. All the scale bars represent 500µm.

3.1.2 Identification of rVACVs expressing SPARC/gp70-peptides and mIL-2 in 4T1 cell cultures.

All the isolated and purified rVACVs were amplified in CV-1 cells for the in vitro experiment. To confirm the expression of SPARC/gp70-peptides and mIL-2,4X10^5 4T1 cells were seeded in 6-well plates and overnight incubated. Then infected respectively with rVACVs GLV- 1h109, C1-opt1, L1c-Ig-Turbo-SPARC/gp70-peptides-TK-eGFP, L1c-Ig-Turbo-TK-Egfp-mIL2, and L1c-Ig-Turbo-SPARC/gp70-peptides-TK-Egfp-mIL2 (MOI=10). After two days of incubation, the infected cells were harvested and lysed in 250µl RIPA lysis buffer. The target protein expression in the lysates was analyzed by Western blot with 20µl per pocket Figure 15. The flag tag fusion protein expressed by GLV-1h109 is approximate 30 kDa [160]. And the molecular weights of SPARC/gp70-peptides

are 15 kDa; the mouse IL-2 is 20 kDa. According to the results of Western blot, both newly constructed virus strains L1c-Ig-Turbo-TK-Egfp-mIL2 and L1c- Ig-Turbo-SPARC/gp70-peptides-TK-Egfp-mIL2 are expressing the mIL-2 protein; the virus strains L1c-Ig-Turbo-SPARC/gp70 peptides-TK- eGFP and L1c- Ig-Turbo-SPARC/gp70-peptides-TK-Egfp-mIL2 are expressing the SPARC/gp70-peptides.

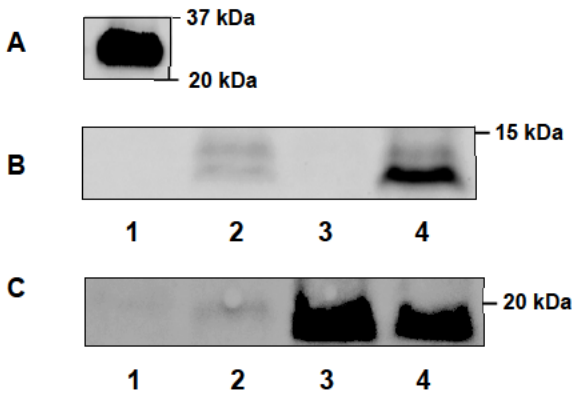

Figure 15. Detection of SPARC/gp70-peptides and mIL-2 in 4T1 cell cultured by Western blot analyses. (**A**) and (**B**) The membrane was incubated with anti-Flag antibody, (**C**) The membranes were incubated with anti-mIL-2 antibody. (**A**): 4T1 cells infected with GLV-1h109; (**B**) and (**C**): Line 1: 4T1 cells infected with C1-opt1, Line 2: 4T1 cells infected with L1c-Ig-Turbo-SPARC/gp70 peptides-TK- eGFP, Line 3: 4T1 cells infected with L1c-Ig-Turbo-TK-Egfp-mIL2, Line 4: 4T1 cells infected with L1c- Ig-Turbo-SPARC/gp70-peptides-TK-Egfp-mIL2.

3.1.3 Detection of mIL-2 expression in cells by ELISA

Due to the low oncolytic efficiency of VACV in mouse cell lines, it's necessary to confirm the expression of secreted mIL-2 in the supernatant of infected cells. To prepare the samples of secreted mIL-2 from rVACV,3-4X10^5 4T1 cells were seeded into the 6-well plates to reach 80% conference in the next day, then infected with rVACVs strains at MOI=0.5 and followed by taking 200µl aliquots from the supernatant of each sample at different time points (0,12,24,48,72 hours). For Elisa assays, one monoclonal anti-mIL-2 antibody was coated in a 96-well plate for 4°C overnight incubation. Add 100µl samples per well into the plate on the next day after blotting the plate and put the plate at 4°C for overnight incubation. Then the plates were washed three times, incubated with detection anti-mIL-2 antibody at room temperature for 2 hours. After that, the TMB

Horseradish Peroxidase color development was added to the plate for incubation and for further OD450 detection. The Elisa curve is shown in Figure 16. The Elisa result confirmed that the newly constructed Vaccina virus successfully expresses the mIL-2 protein. Meanwhile, the virus expressed mIL-2 can be recognized by the commercial mouse IL-2 kit, which means the Vaccina virus expressed mIL-2 has potential biological functions.

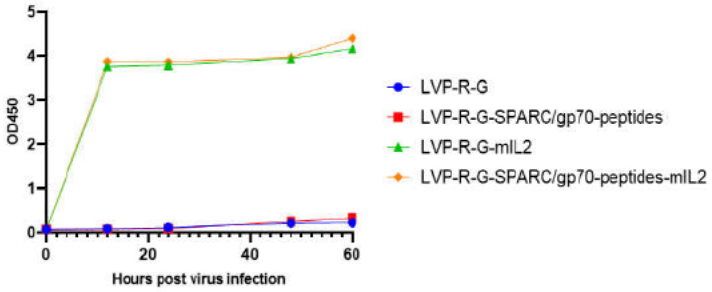

Figure 16. Detection of mIL2 in 4T1 cells infected with engineered rVACV strains by Elisa. 4T1 cancer cells were infected with different strain of rVACVs at different time point of incubation and aliquots of supernatant were collected for Elisa analysis

3.1.4 Detection of SPARC protein expression in 4T1 and N2C cancer cell lines

S1 and S2 peptides are MHC I molecular H2-Kd binding peptides, which were derived from mouse SPARC protein. Thus, for the successful activation of T cells in vivo in animal models and in vitro in cell cultures, expression of SPARC in 4T1 and N2C mammary cancer cell are required. To investigate the expression of SPARC protein in 4T1 and N2C mammary cancer cell lines. $2X10^5$ 4T1 cells and N2C cells were seeded in 6-well plates. After four days of incubation, cells were harvested and lysed in 250µl RIPA lysis buffer, then analyzed the expression of SPARC protein by Western blot with 20µl per pocket Figure 17. The molecular weight of SPARC is 40kDa [161]. The Western blot result in here demonstrated that both 4T1 and N2C mammary cell lines are expressing the SPARC protein.

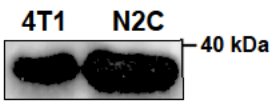

Figure 17. Expression of SPARC in 4T1 and N2C mammary cancer cell lines after infection with rVACV strains detected by Western blotting.

3.2 Construction of eGFP and TurboFP365 expressing stable cell lines

In order to test the prospective cytotoxic T lymphocyte killing assay, two fluorescent strains of mammary cancer cell lines were generated Figure 18. The N2C-pTet-TurboFP635-EF-1a-eGFP stable cell line was previously constructed, and the function of Tet-off TurboFP635 expression was verified by transfected with the tTA_BFP plasmid [151]. In this study, we selected the monoclone 3A4 for further assay. For 4T1-turboFP365 stable cell line construction, the mixture of pLV- Exp-Bsd-EF1a-Turbo plasmid and lentiviral packaging vectors (PMD2.G and psPAX2) were transfected into HEK 293T cells seeded in a 10 cm dish one day before, and the lentivirus was collected and concentrated using Amicon Ultra Centrifugal Filters. Then wild-type 4T1 cells were infected with the lentivirus for 72 hours, and cells that integrated the lentivirus were selected by addition of blasticidin containing medium in 6 well plates. After that, the B2 positive monoclonal cells were picked. The genomic structure of these two stable cell lines is shown in Figure 19.

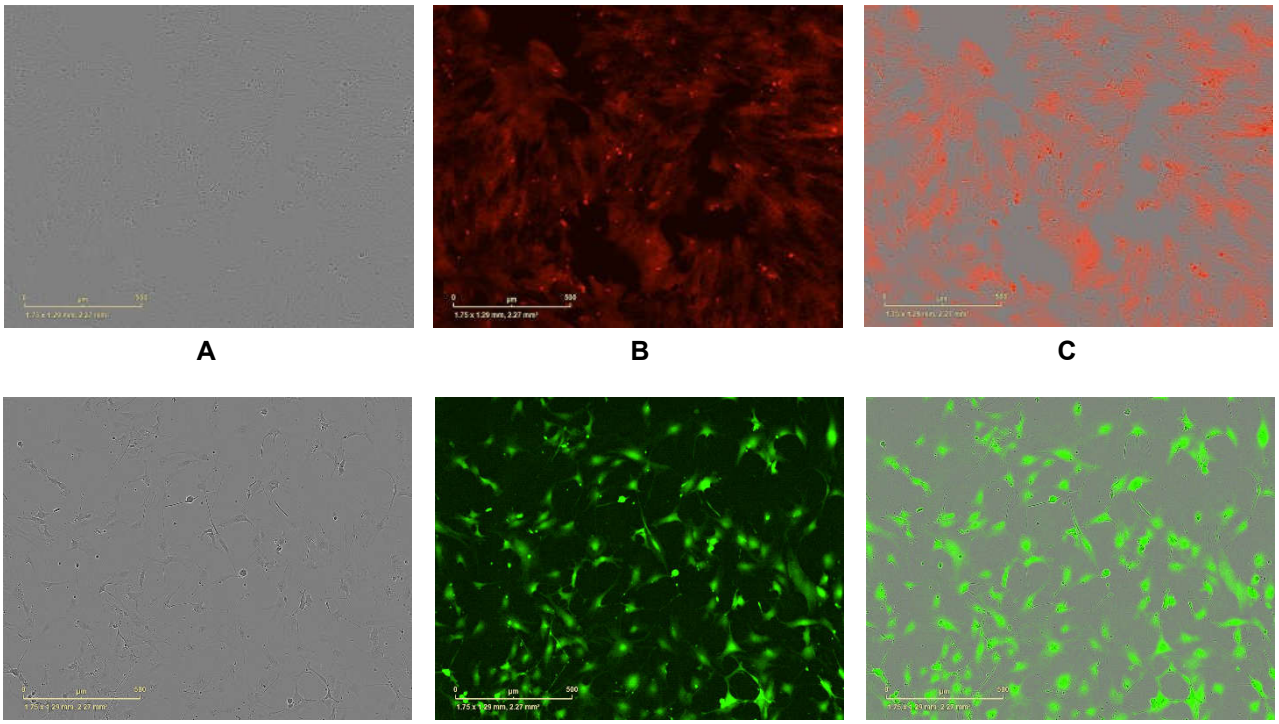

Figure 18. Images of 4T1 and N2C fluorescent labelled cells. (**A**) Image of 4T1-turbo B2 monoclonal cells detected in bright phase. (**B**) Image of 4T1-turbo B2 monoclonal cells detected by red fluorescence signal. (**C**) Image of 4T1-turbo B2 monoclonal cells, merge. (**E**) Image of N2C-eGFP 4A3 monoclonal cells detected by bright phase. (**F**) Image of N2C

eGFP 4A3 monoclonal cells detected by red fluorescence signal. (**G**) Image of N2C-eGFP 4A3 monoclonal cells, merge. All the scale bars represent 500μm.

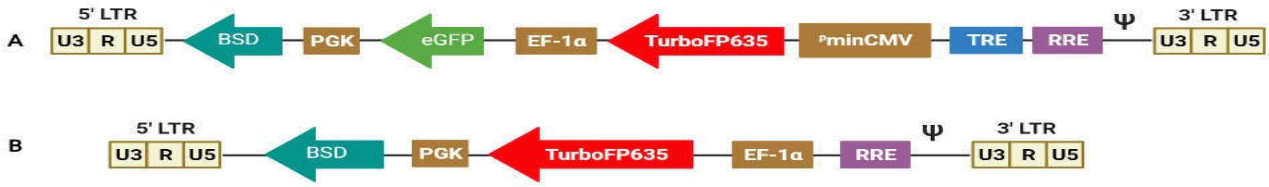

Figure 19. Schematic presentation of stable cell lines constructed by lentiviral vector. (**A**) N2C- pTet-turboFP635-EF-1a-Egfp cell line and (**B**) 4T1-EF-1a-turboFP635 cell line.

In general, the fluorescent protein eGFP and TurboFP635 were stably integrated into the host cell N2C and 4T1, respectively. The entire stable cell lines generation and subsequent analysis of the fluorescent signal expression were performed by IncuCyte®S3.

3.3 4T1 and N2C cell line growth curves induced by mIL-2

As previously reported, IL-2 does directly inhibit the growth of human breast cancer cell lines in vitro [162]. To test the potent growth inhibition activity of IL2 in mouse mammary cancer cells, we used IncuCyte®S3 to monitor the proliferation of 4T1 and N2C cells in medium with the different concentrations of mIL-2 and in real-time. First, $2X10^4$ 4T1 and N2C cells were seeded in two individual 24 well plates in one day, and the growth medium was replaced with mIL-2 containing medium. Then a schedule was set to evaluate cell confluence in real-time with IncuCyte®S3. At last, create the cell proliferation curves through the self-contained software of IncuCyte®S3.Our results show that mIL-2 does inhibit both of the 4T1 and N2C cells growth with linearizing increasing with different concentrations in vitro Figure 20.

Fig 20/A

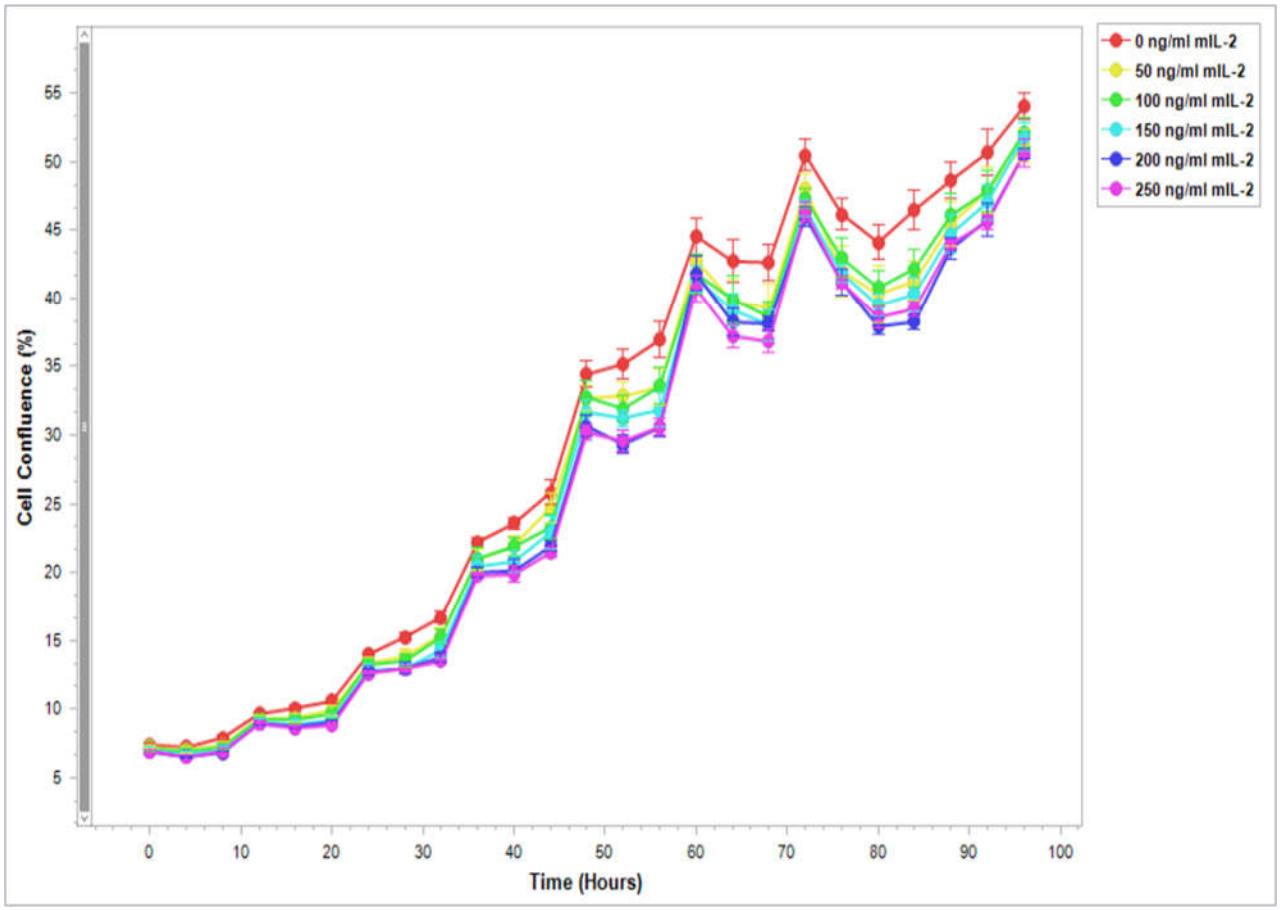

A

Fig 20/B

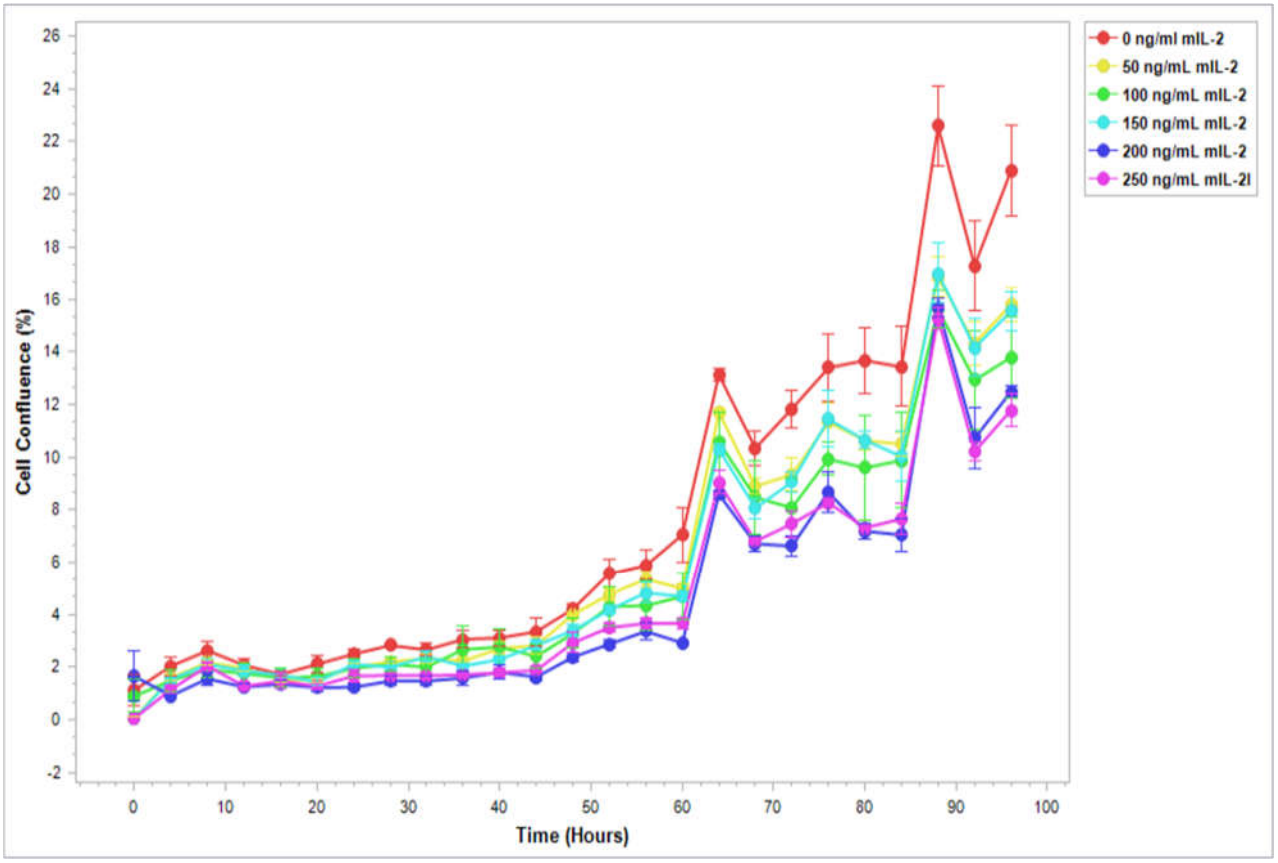

B

Figure 20. Effect of mIL-2 on the viability of 4T1 and N2C mammary cancer cell lines, the cell growth was monitored by the IncuCyte®S3, then the growth curve was created by IncuCyte®S3 software v2018B. (**A**) 4T1 cells were cultured with the medium containing different concentration of mIL-2 (0ng/ml, 50ng/ml, 100ng/ml, 150ng/ml, 200ng/ml, and 250ng/ml) for four days, continuously. (**B**) N2C cells treated with various doses of mIL-2 the same as 4T1 cell.

3.4 Tumor therapy of 4T1 tumor bearing mice with rVACVs expressing tumor antigens and mIL-2

3.4.1 Both Vaccinia virus strains expressing mIL-2 alone and mIL-2 plus tumor antigens significantly enhanced tumor regression in a syngeneic mouse model

To establish the tumor model, 1 x 10^5 mammary carcinoma 4T1 cells were administered to the right dorsal flank of regions of 5- to 6-week-old female BALB/c mice. After 13 days, animals were separated into four groups, and five of the mice were injected intravenously (tail vein) with 100µl PBS as a control group. The other three groups were treated with intravenous injection of 100µl (1× 10^8 pfu/ml) different strains of rVACVs respectively: C1-opt1 (n=5), LVP-R-G-mIL2 (n=10), and

LVP-R-G- SPARC/gp70-peptides-mIL2 (n=10) was shown in Figure 21. For evaluating the toxicity of the rVACV cancer vaccine therapy and the survival efficiency, the mouse body weight and tumor volumes were measured and monitored every three days after the PBS and virus injections until the day of termination (Mice were sacrificed when the tumors reached a volume of about 1500 mm3). The results are shown in Figure 22. All animal studies were run according to protocols approved by the animal facility of Universität Würzburg.

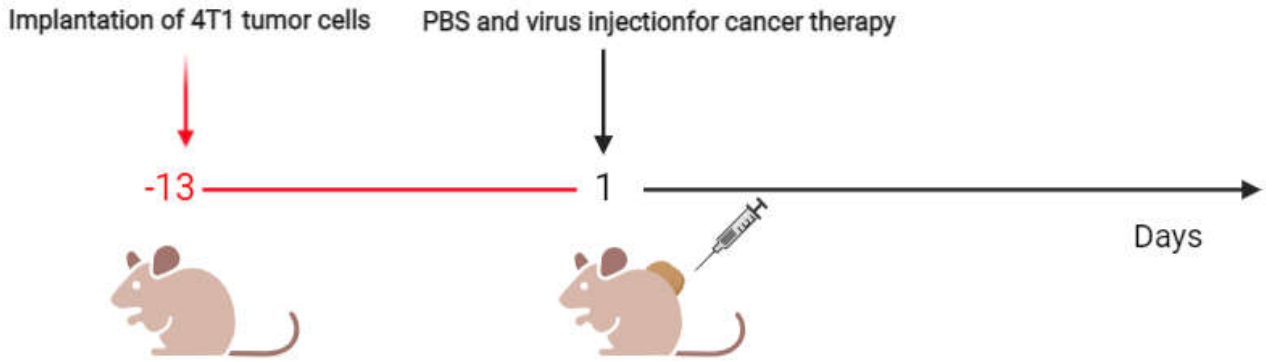

Figure 21. Schedule of tumor cells implantation and rVACV administration for tumor therapy in 4T1 tumor- bearing BALB/c mice.

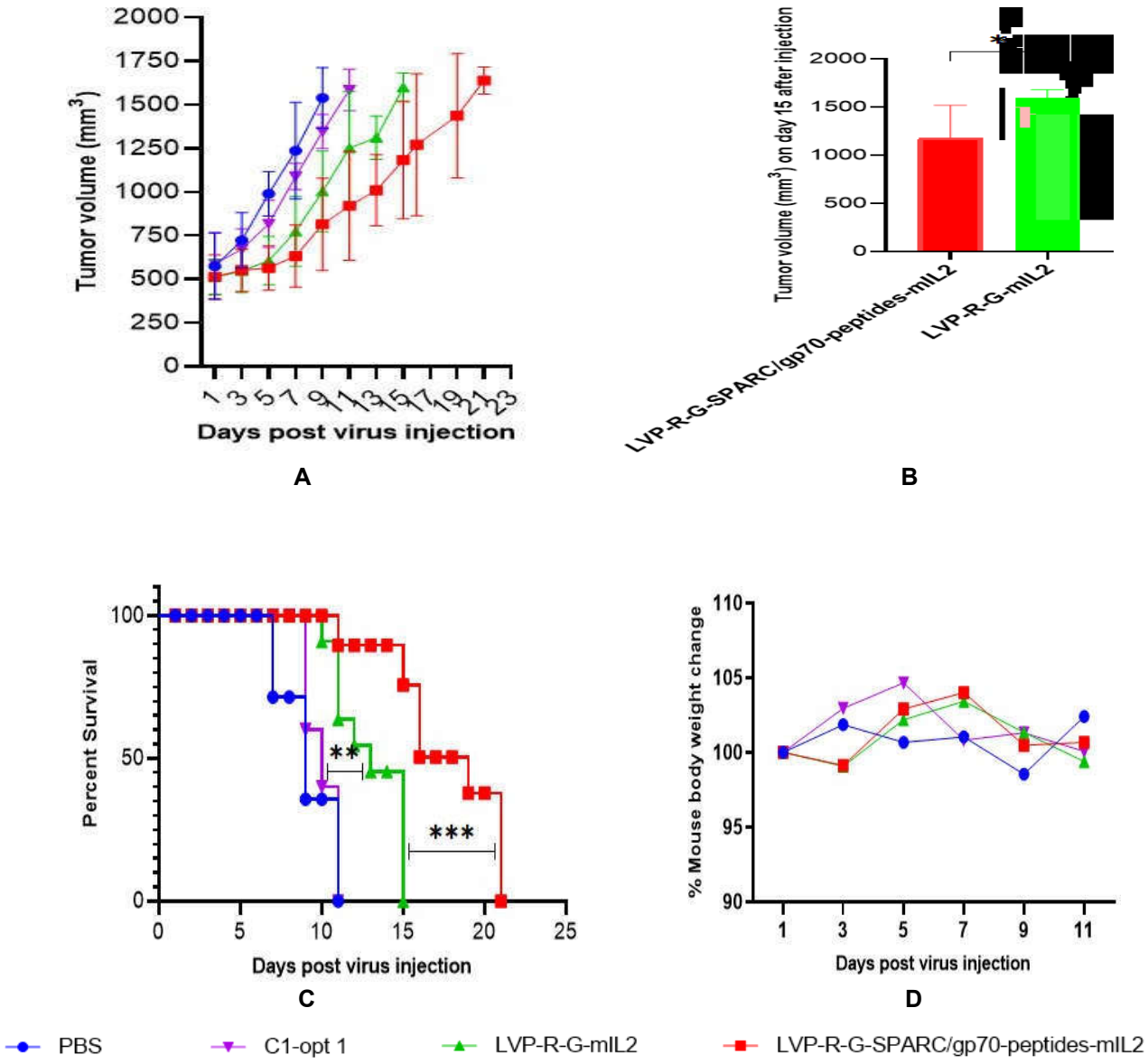

Figure 22. Tumor growth, body weight loss curve and comparison between survival time of the groups. **(A)**. Effects of rVACVs treatment on 4T1 tumor-bearing BALB/c mice after IV application **(B)** Day 15th Tumor volume of LVP-R-G-SPARC/gp70- peptides-mIL-2 and LVP-R-G-mIL-2 injected mice**.** The statistical significance was calculated by the t-test, * indicates P<0.05. **(C)** Kaplan-Meier survival curve following therapy initiation using sacrificing animals as the terminal event. The comparison of survival between the three different treated groups was statistically evaluated by Kaplan-Meier and log-rank (Mantel-Cox) tests (Graphpad Prism, San Diego, CA). P<0.05 was considered statistically significant. ** indicates P<0.01, *** indicates P<0.001. **(D)** Effect of different treatments on the weights of 4T1 tumor-bearing BALB/c mice.

The animal experiment data proved that the mIL-2 plus tumor-associated antigens expressing VACV vector shows a better anti-cancer response than the mIL-2 alone expressing vector. The

former could significantly inhibit tumor growth compared with the latter. Moreover, the results confirmed our previous unpublished data that the mIL-2 expression driven by Psyn (E/L) promoter in the VACV lister strain did enhance the tumor regression in the 4T1 mouse model.

3.4.2 Analysis of CD4+ and CD8+ T cells in lymphocytes from the vaccinated mice after treatment with different rVACVs

There are two broad subtypes of T cells that have been identified by the expression of either the CD4 or CD8 T cell receptor (TCR) on their cell surface [163]. CD4+ T cells help regulate the immune response by stimulating other immune cells, mainly including six principal subsets according to their function and phenotype: T helper 1, 2, 17 and 22 (Th1, Th2, Th17, Th22), regulatory T cells (Treg), and T follicular helper cells (Tfh) [164]. CD8+ T cell is normally considered a uniform population of cells that recognize antigens presented by MHC Class I molecules, named CD8+ cytotoxic T cells that are indispensable for defense against pathogens and tumor surveillance [165]. In the last decade, T cell-based immunotherapy has shown promising results in cancer immunotherapy, and the activated T cell population in vivo plays a central role in inhibiting tumor growth [166]. As mentioned in the previous chapter, IL-2 could promote T cell expansion of both CD4+ (Mainly Tregs) and CD8+ T cells (including the effector and memory cells) in vivo [167]. In the IL-2 based tumor therapy model, contrary to the CD4+ Tregs, the IL-2 induced CD8+ T cells greatly promote tumor growth inhibition. To investigate cell populations of CD4+ and CD8+ T cells in lymphocyte fraction, the isolated splenocytes from different strains of rVACVs vaccinated mouse was analyzed by FACS after the tumor volume reached around 1500mm^3. The results showed that both CD4+ and CD8+ cell populations were expanded in the mIL-2 administered mouse groups, while the ratio of CD4+/CD3+ and CD8+/CD3+ did not have any significant significance change. Furthermore, we also investigated the expressions of PD-1 in both CD4+ and CD8+ T cell populations, and the results are shown in Figure 23. This animal experiment demonstrated that the mIL-2 expressed by the Lister strain of VACV under the control of Psyn (E/L) promoter remarkably increased both CD4+ and CD8+ T cell populations in vivo and did not affect the expression of PD-1 molecule on CD4+ or CD8+ T cells.

Fig 23

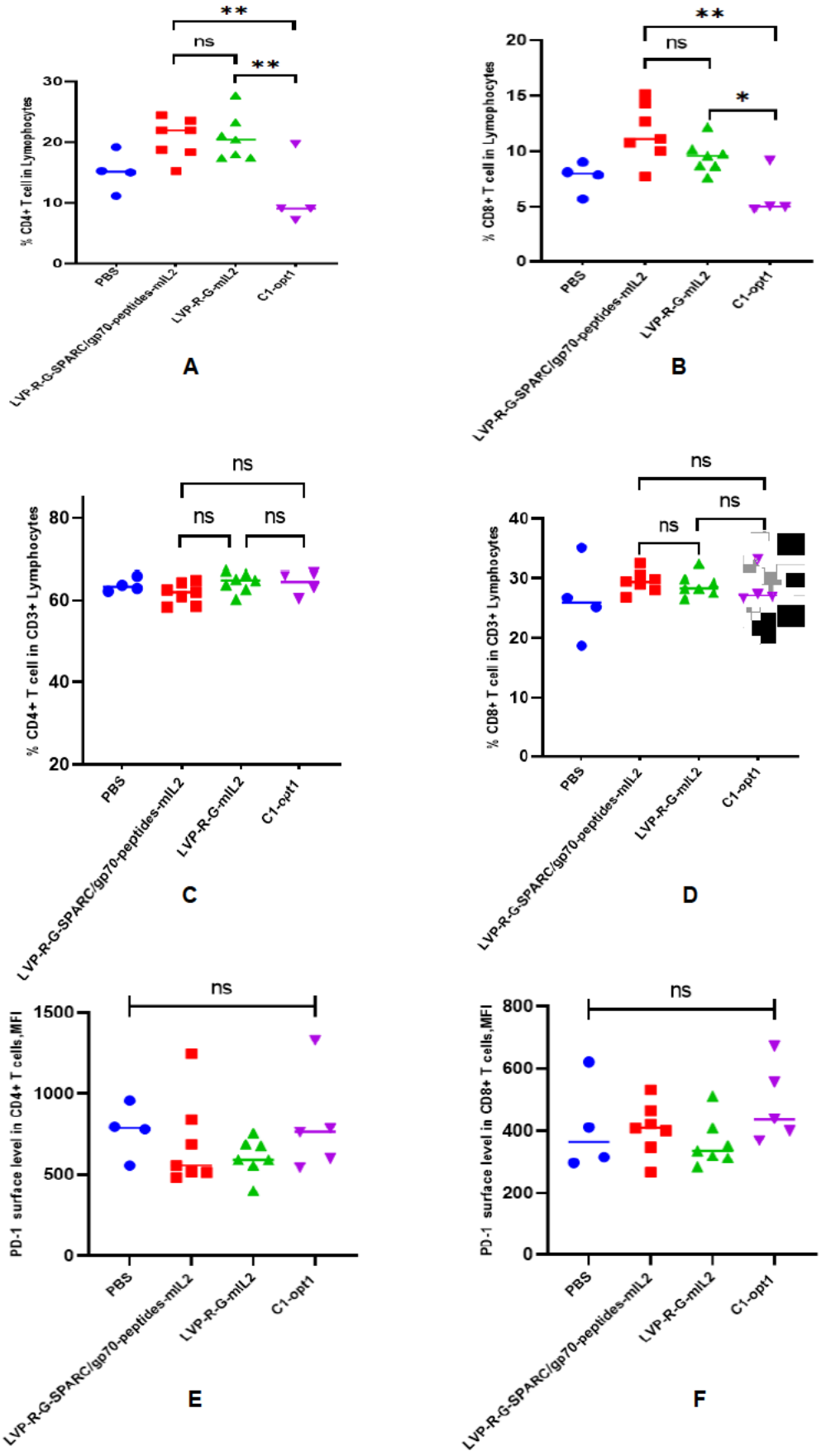

PBS C1-opt 1 LVP-R-G-mIL2 LVP-R-G-SPARC/gp70-peptides-mIL2

Figure 23. FACS analysis of splenocyte preparations from mice after injection with PBS or with rVACV Strains. (**A**) Percent [%] of CD4+cells in splenic lymphocyte populations. (**B**) Percent [%] of CD8+ cells in lymphocytes population. (**C**) Percent [%] of CD4+cells CD3+ lymphocytes population. (**D**) Percent [%] of CD8+cells CD3+ lymphocytes population. (**E**) PD-1 expression as mean fluorescence intensity (MFI) on CD4+ T cells. (**F**) PD-1 expression as mean fluorescence intensity (MFI) on CD8+ T cells. The statistical significance was calculated by Ordinary one- way ANOVA test, * indicates P<0.05 was considered statistically significant. ** indicates P<0.01, p values > 0.05 are not significantly different (ns). Detection of IFN-γ expression of antigen-specific CD8+ T lymphocyte by flow cytometry

3.4.3 Detection of IFN-γ expression in antigen-specific CD8+ T lymphocytes by flow cytometry

The cellular immune system plays a crucial role in the immunological anti-tumor effects, besides the antibody-mediated humoral immune system. Therefore, the study of specific T cells is critical to understanding the anti-tumor reaction of the cellular immune system. Tumor-associated antigen-specific CD8+ T cells are existing in the lymphocyte of cancer patients, and there are various methods for monitor T cell specific responses. Identifying tumor antigen-specific T cells mainly depends on the functional analyses after stimulating the cells with recall antigens in vitro. The antigen-specific T lymphocyte activation can be evaluated by different approaches such as T cell proliferation, MHC-tetramer staining, extracellular or intracellular cytokine staining [168]. In this study, to assess the antigen-specific CD8+ T cells, we analyzed IFN-γ expression through flow cytometry to quantify the ratio of GP70 and SPARC-specific CD8+ cells in the T lymphocyte fraction. The results are shown in Figure 24. The data in Fig.25 show that a fraction of CD8+ cells from peptides expressing vaccina virus injected mice secrete IFN-γ after specific peptide mixture stimulation. In contrast, CD8+ T cells from the control group did not produce abundant IFN-γ. These findings demonstrated that the structure of peptides fusion protein preserves the function of the T cell epitope.

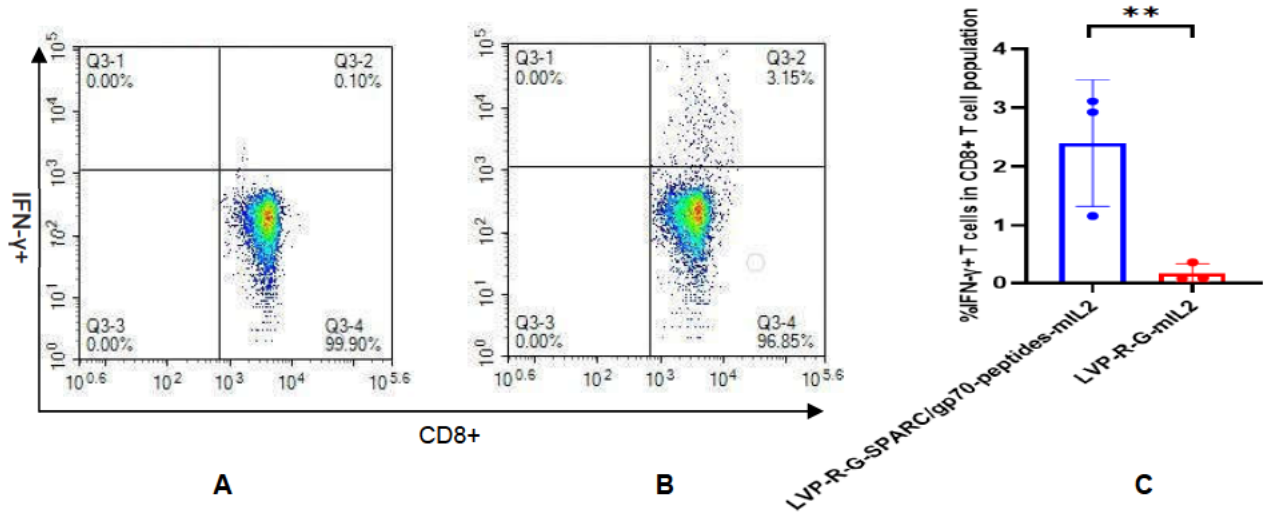

Figure 24. Comparison of IFN-γ produced by CD8+ T lymphocytes isolated from rVACVs injected mice. (**A**) IFN-γ detection of CD8 T lymphocytes isolated from LVP-R-G-mIL-2 vaccinated mice induced by peptides mixture. (**B**) IFN-γ detection of CD8 T lymphocytes isolated from LVP-R-G-SPARC/gp70-peptides-mIL-2 vaccinated mice induced by peptides mixture. (**C**) Comparison of IFN-γ expression by CD8+ T lymphocytes of LVP-R-G-mIL-2 and LVP-R-G-SPARC/gp70-peptides-mIL-2 vaccinated mice. The statistical significance was calculated by Ordinary two-way ANOVA test, * indicates P<0.05 was considered statistically significant. ** indicates P<0.01, p values > 0.05 are no significantly different (ns).

3.4.4 Detection of H2-kd and H2-Ld MHC I molecule expression in 4T1 and N2C mammary cancer cell lines

As mentioned before, S1 and S2 peptides are MHC I H2-Kd molecule binding epitopes. In addition, AH1 and AH1-A5 are MHC I molecule H2-Ld binding peptides. To investigate the expression of H2-Kd and H2-Ld in two strains of mammary cancer cell lines, $2X10^5$ (4T1, N2C) cells were seeded in two 6-well plates. After three days' incubation, cells were harvested by treated with 0.25% trypsin-EDTA and analyzed by flow cytometry using anti-H2-Kd and anti-H2-Ld specific antibodies. The results demonstrate that both 4T1 cells and N2C cell lines in our hand were expressing H2-Kd and H2-Ld MHC I molecules Figure 25, which means these two mammary cell lines are optimal cell candidates for Vitro and Vivo analysis in our experiment design.

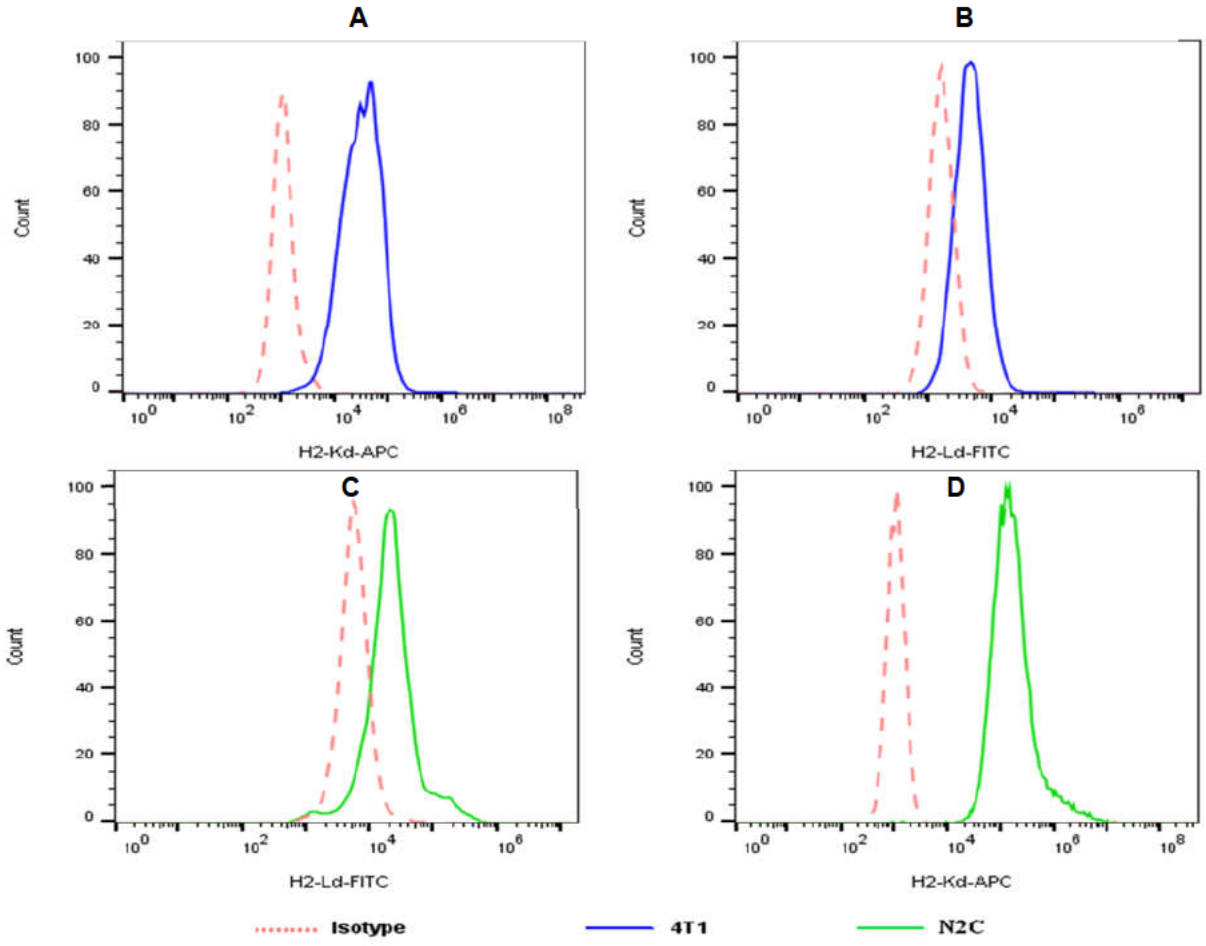

Figure 25. Detection of H2-Kd and H2-Ld expression in 4T1 and N2C cell lines. (**A**) H2-Kd expression in 4T1 cells. (**B**) H2-Ld expression in 4T1 cells. (**C**) H2-Ld expression in N2C cells. (**D**) H2-Kd expression in N2C cells.

3.4.5 Co-culture assays to assess specific anti-tumor CD8+ T cell cytotoxicity

The CD8+ T cell-mediated cytotoxicity plays the most critical role in the anti-tumor immune responses of the peptide-based vaccines. Therefore, ex vivo testing of interactions of tumor cells and the T cell is pivotal for evaluating the effectiveness of the cancer vaccines [169]. Antigen-specific cytotoxic CD8+ T cells can recognize and kill cancer cells through the T cell/tumor cell engagement, which is caused by the interaction between T cell receptors (TCRs) and the tumor antigens in the context of major histocompatibility complex I (MHC I) molecules [170]. Techniques such as flow cytometry and ELISpot assay have been used to measure the cytotoxic activity of the CD8+ T lymphocytes (CTLs) through different cell surface markers or effector cytokines. Here, we developed a co-culture assay to assess the T cell cytotoxicity meanwhile visualizing the cell-killing using a real-time imaging platform-IncuCyte®S3.In this method, the CD8+ T cells were isolated and purified from the spleens of rVACVs vaccinated mice, then co-cultured with two strains of fluorescent (red and green) mammary cancer cell lines (4T1-turbo, N2C-eGFP) in the context of peptides mixture and anti-CD28 antibody in 96-well plates. The plates were monitored by the IncuCyte®S3 to generate images at the different time points, then videos and specific lysis curves were created Figure 26-33.

Fig 26

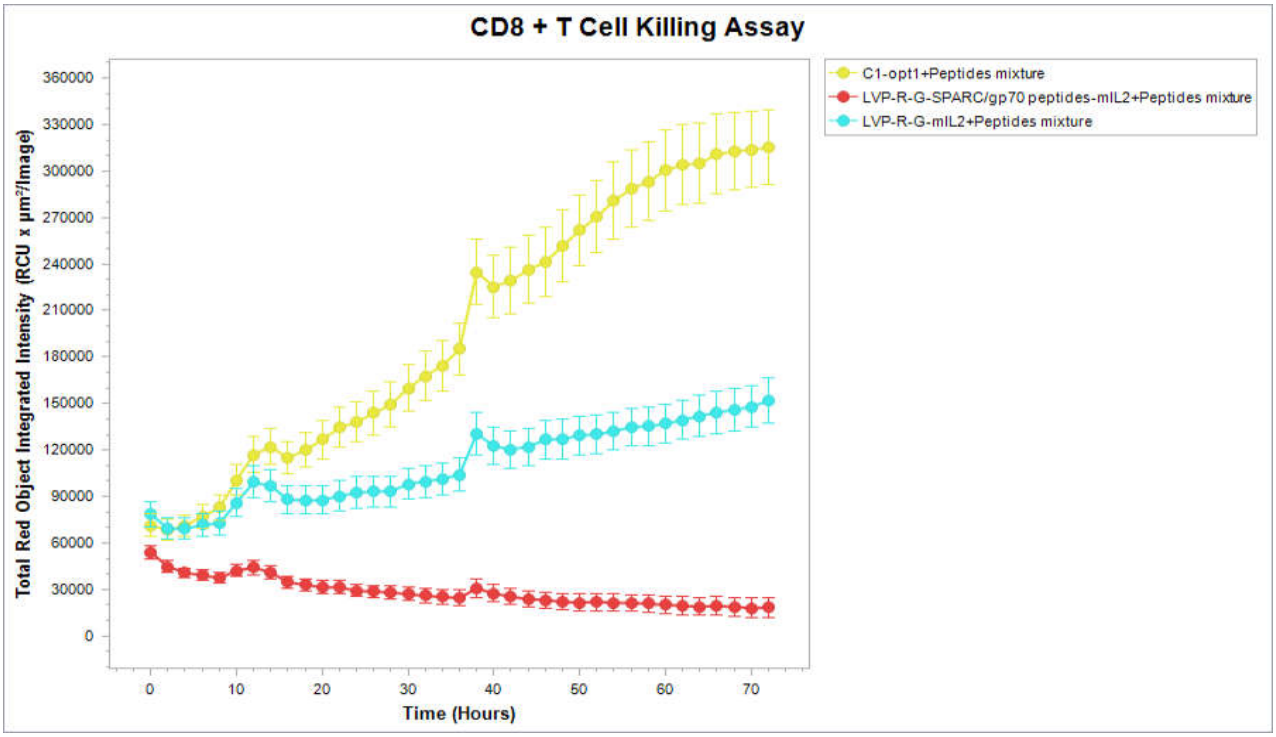

Figure 26. Effect of cytotoxic CD8+ T cells on the 4T1-turbo cell line. CD8+ T cell was isolated and purified from C1-opt1, LVP-R-G-mIL-2, and LVP-R-G-SPARC/gp70-peptides-mIL-2 vaccinated mice, then co-cultured with 4T1-turbo cells in the medium contained with peptides mixture and anti-CD28 antibody. The cell proliferation curve was created through the red florescent signal.

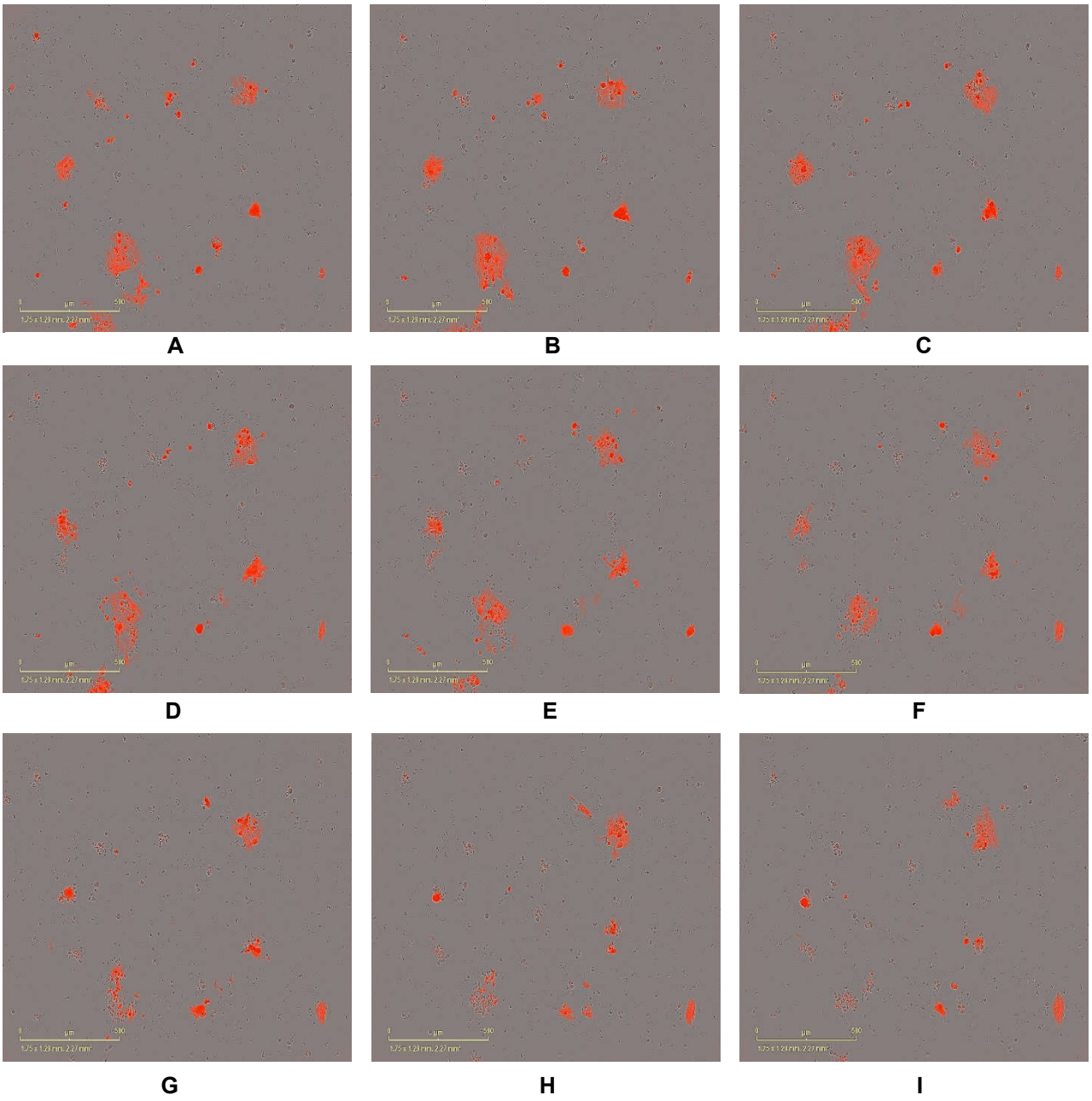

Figure 27. Effect of cytotoxic CD8+ T cells on the 4T1-turbo cell line. CD8+ T cells were isolated and purified from LVP-R-G-SPARC/gp70-peptides-mIL-2 vaccinated mice, then co-cultured with 4T1 cells in the medium contained with peptides mixture and anti-CD28 antibody. The plate was scanned by the IncuCyte®S3 at the different time points. (**A**) Co-culture after 4 hours. (**B**) 8 hours. (**C**) 12 hours. (**D**) 16 hours. (**E**) 20 hours. (**F**) 24 hours. (**G**) 28 hours. (**H**) 32 hours. (**I**) 36 hours.

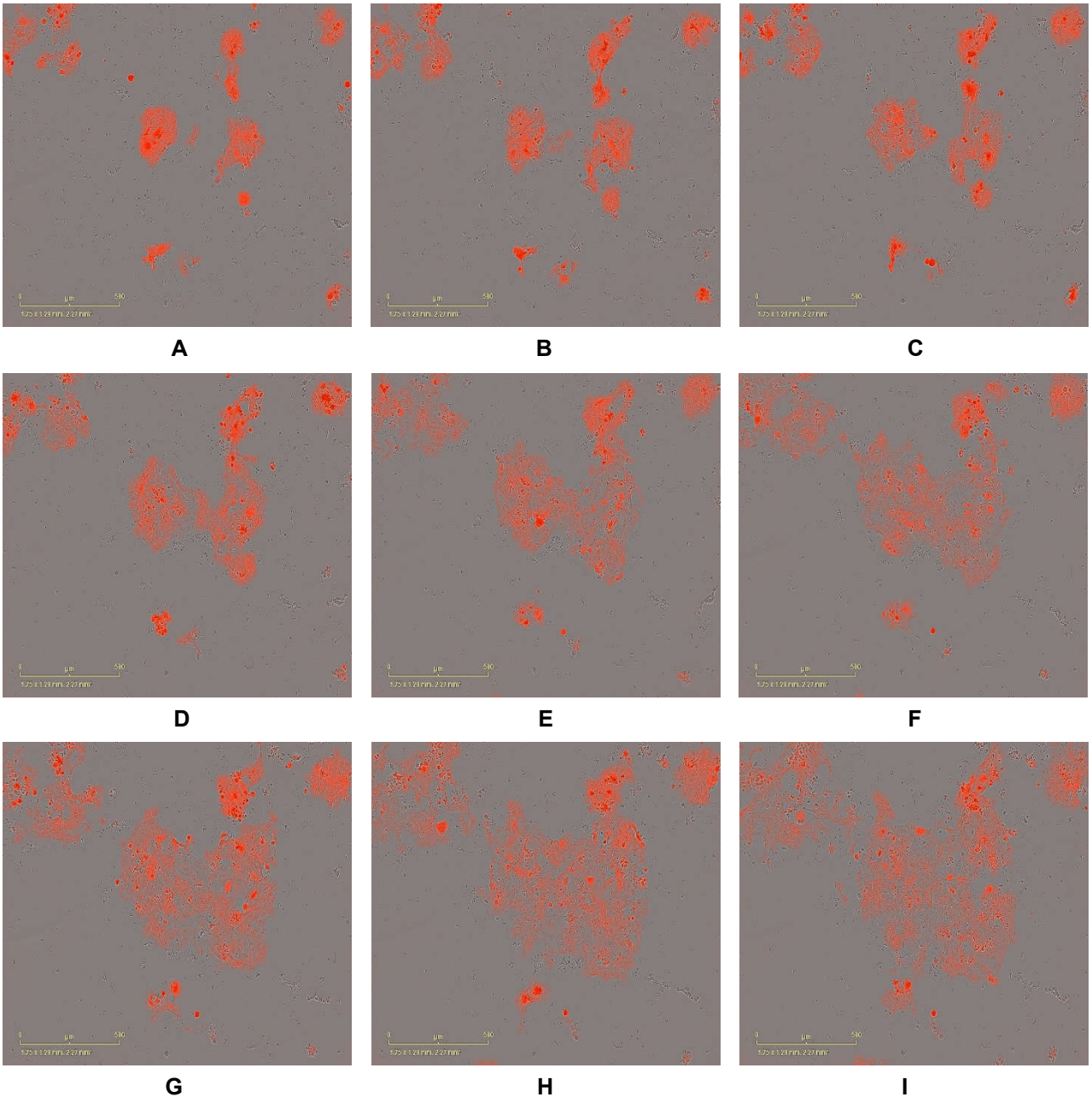

Figure 28. Effect of cytotoxic CD8+ T cells on the 4T1-turbo cell line. CD8+ T cells were isolated and purified from LVP-R-G-mIL-2 vaccinated mice, then co-cultured with 4T1 cells in the medium contained with peptides mixture and anti-CD28 antibody. The plate was scanned by the IncuCyte®S3 at the different time points. (**A**) Co-culture after 4 hours. (**B**) 8 hours. (**C**) 12 hours. (**D**) 16 hours. (**E**) 20 hours. (**F**) 24 hours. (**G**) 28 hours. (**H**) 32 hours. (**I**) 36 hours.

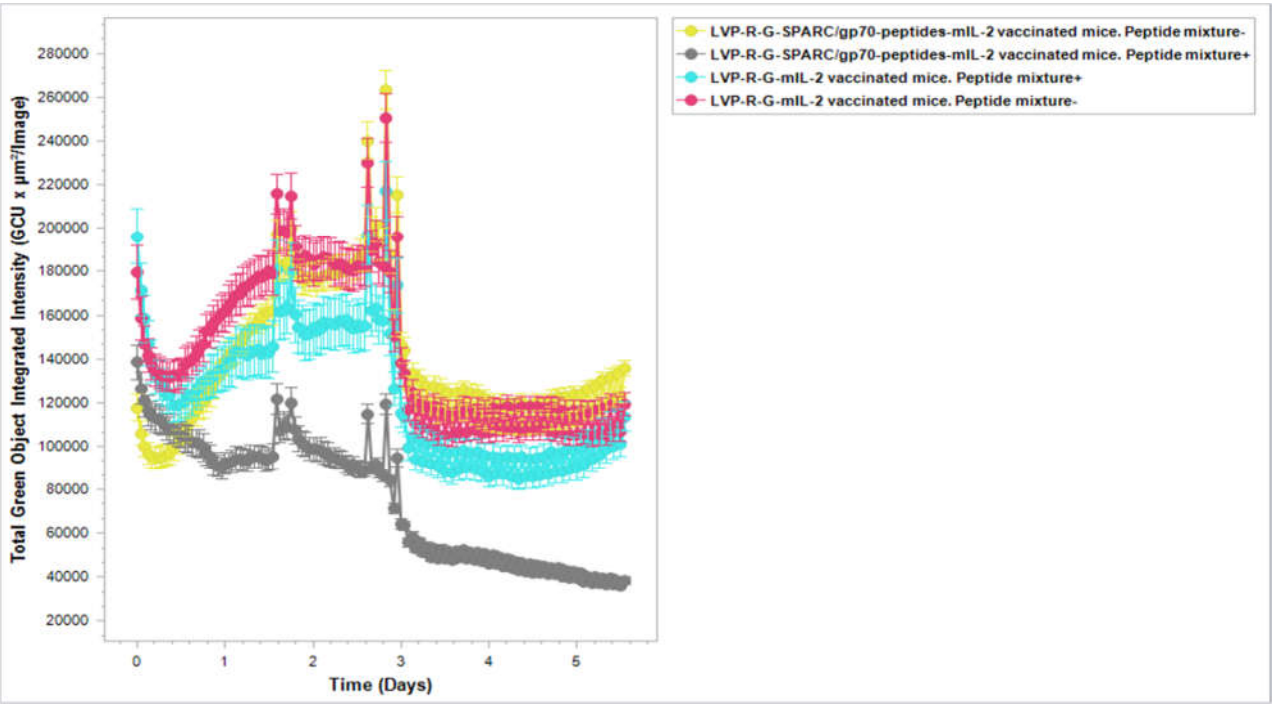

Figure 29. Effect of cytotoxic CD8+ T cells on the N2C-eGFP cell line. CD8+ T cells were isolated and purified from LVP-R-G-mIL-2, and LVP-R-G-SPARC/gp70-peptides-mIL-2 vaccinated mice, then co-cultured with N2C-eGFP cells in the medium contained with anti-CD28 antibody and with or without peptides mixture. The cell proliferation curve was created through the green florescent signal.

Fig 30

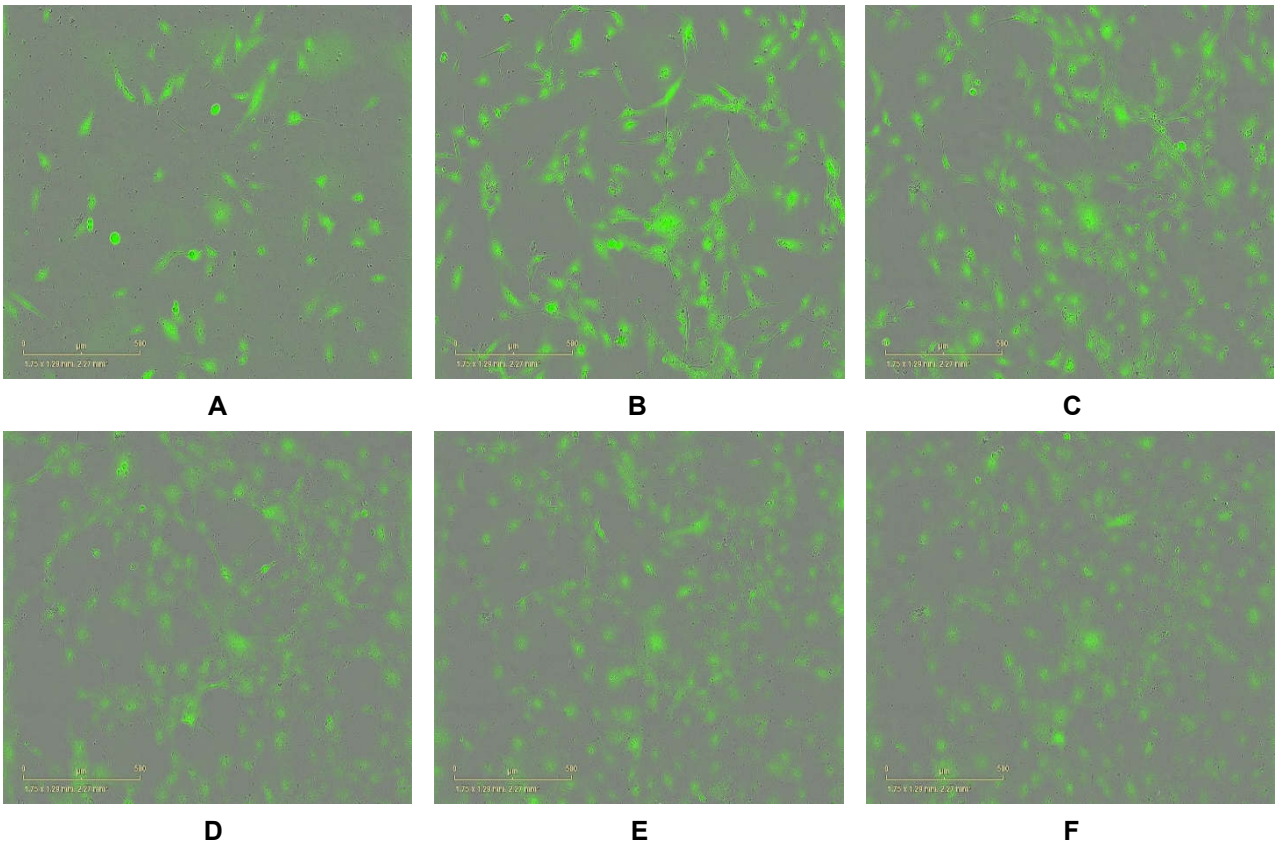

Figure 30. Effect of cytotoxic CD8+ T cells on the N2C-eGFP cell line. CD8+ T cells were isolated and purified from LVP-R-G-SPARC/gp70-peptides-mIL-2 vaccinated mice, then co-cultured with N2C-eGFP cells in the medium contained with anti-CD28 antibody and without peptides mixture. The images were created through the green florescent signal by the IncuCyte®S3 at the different time points. (A) Co-culture after 0 hours. (B) 36 hours. (C) 60 hours. (D) 84 hours. (E) 108 hours. (F) 132 hours.

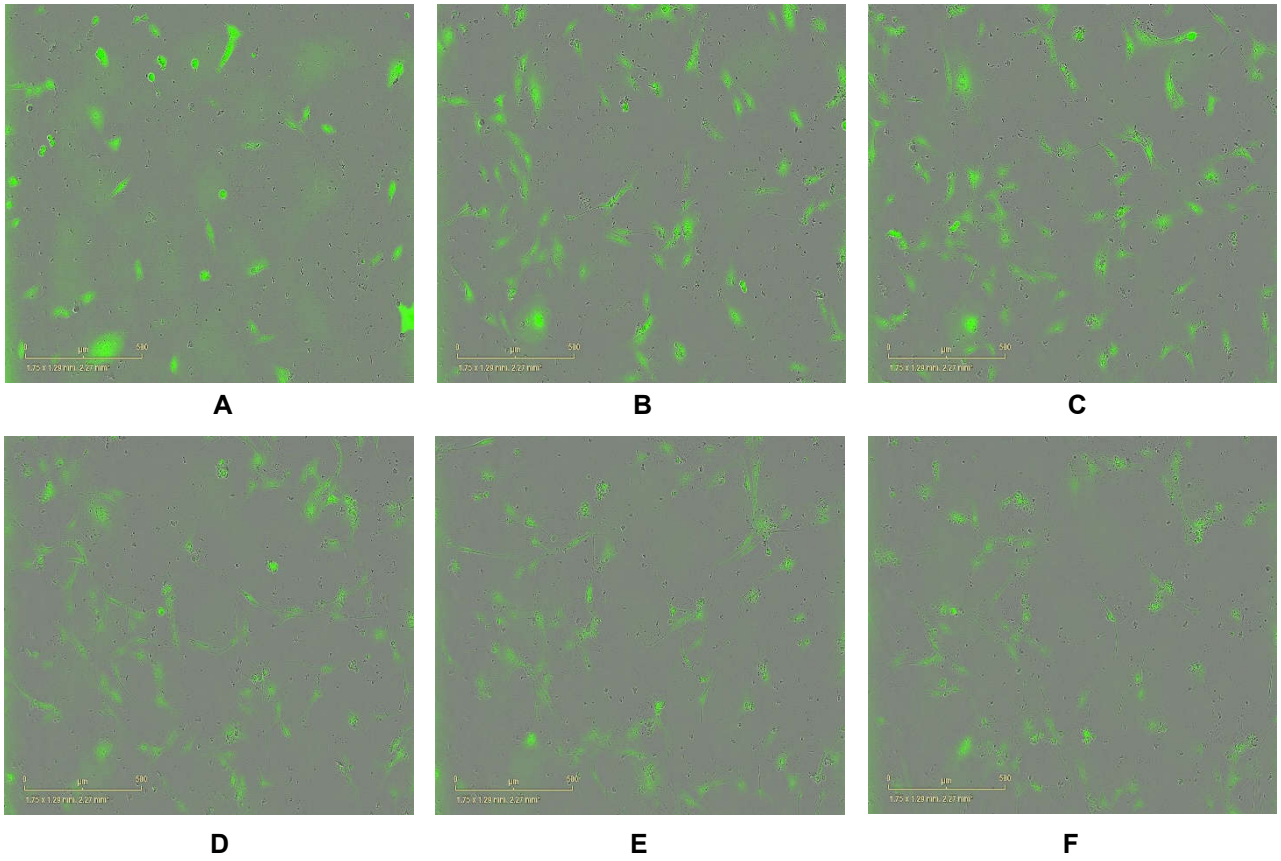

Figure 31. Effect of cytotoxic CD8+ T cells on the N2C-eGFP cell line. CD8+ T cells were isolated and purified from LVP-R-G-SPARC/gp70-peptides-mIL-2 vaccinated mice, then co-cultured with N2C-eGFP cells in the medium contained with anti-CD28 antibody and peptides mixture. The images were created through the green florescent signal by the IncuCyte®S3 at the different time points. (A) Co-culture after 0 hours. (B) 36 hours. (C) 60 hours. (D) 84 hours. (E) 108 hours. (F) 132 hours.

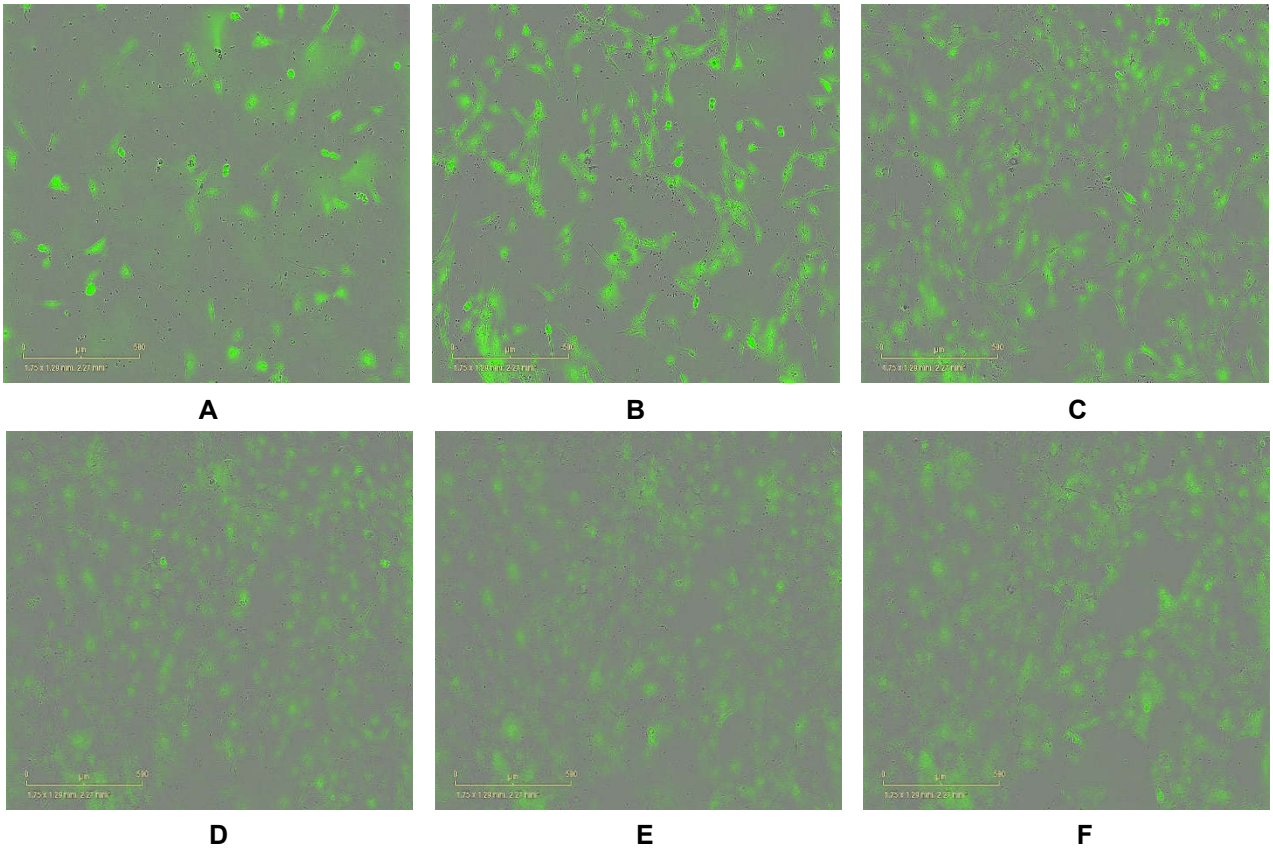

Figure 32. Effect of cytotoxic CD8+ T cells on the N2C-eGFP cell line. CD8+ T cells were isolated and purified from LVP-R-G-mIL-2 vaccinated mice, then co-cultured with N2C-eGFP cells in the medium contained with anti-CD28 antibody and peptides mixture. The images were created through the green florescent signal by the IncuCyte®S3 at the different time points. (A) Co-culture after 0 hours. (B) 36 hours. (C) 60 hours. (D) 84 hours. (E) 108 hours. (F) 132 hours.

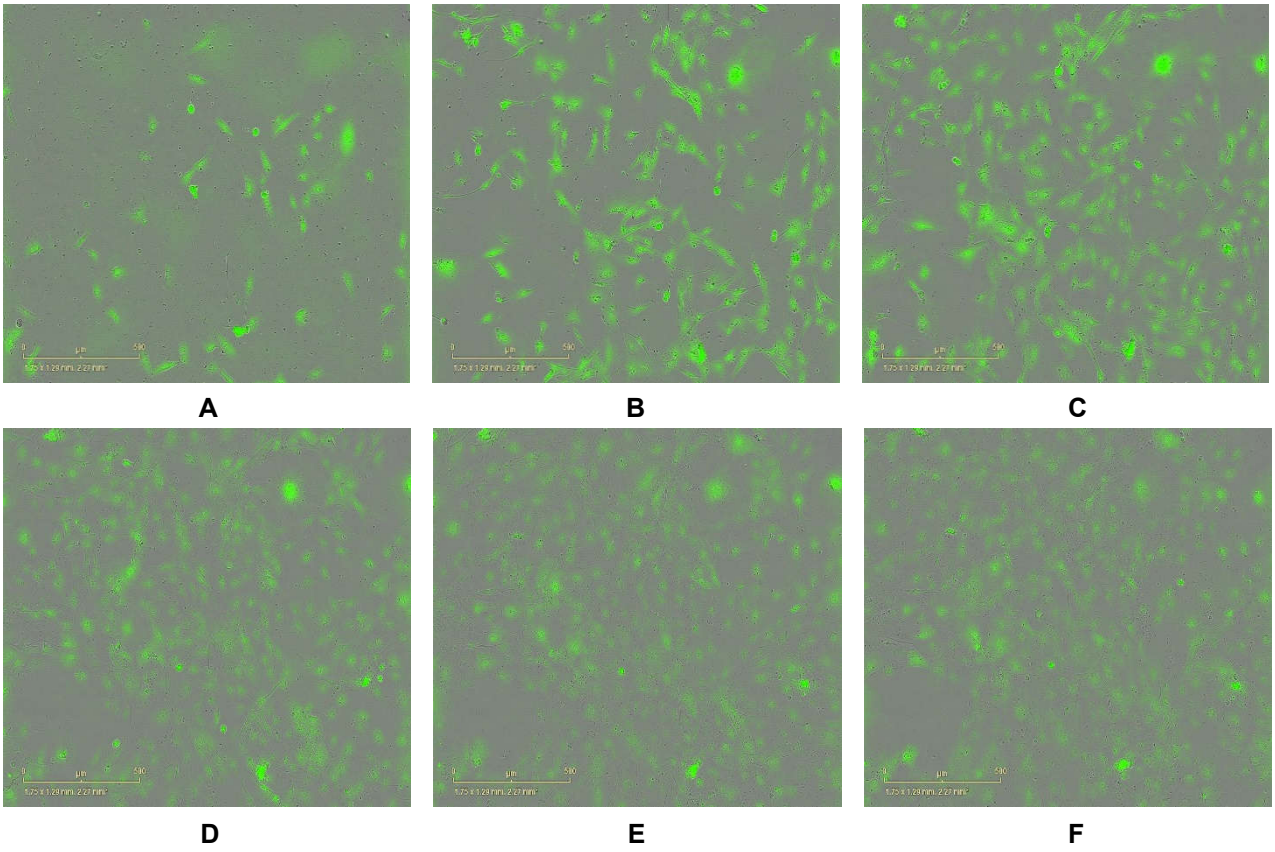

Figure 33. Effect of cytotoxic CD8+ T cells on the N2C-eGFP cell line. CD8+ T cell were isolated and purified from LVP-R-G-mIL-2 vaccinated mice, then co-cultured with N2C-eGFP cells in the medium contained with anti-CD28 antibody and without peptides mixture. The images were created through the green florescent signal by the IncuCyte®S3 at the different time points. (A) Co-culture after 0 hours. (B) 36 hours. (C) 60 hours. (D) 84 hours. (E) 108 hours. (F) 132 hours.

The results show that both fluorescent-labeled 4T1 and N2C cells were lysed by peptide-mediated cytotoxic CD8+ T cells. CD8+ T cells isolated from peptide expressing rVACVs injected mice did kill the target cancer cells under the corresponding chemical peptides contained medium. The killing efficiency was significantly higher than that of cancer cells cultured with CD8+ T cells which were isolated from non-peptide expressing rVACVs injected mice. The target cells killing curve results were consistent with the images captured by IncuCyte®S3 in real-time Figure 27,28,31,33. Meantime, we also investigated the cytotoxic functions of CD8+ T cells in eGFP labeled N2C cells with or without peptide-mediated. The CD8+ T cells isolated from peptide expressing rVACVs injected mice did not kill the target cancer cells without the peptide but significantly inhibited cell growth with the incubation of peptides Figure 30 and 31.

4. Statistical Analysis

All the data analyses and graphics were performed using Graphpad Prism 8.0 software. Statistical significance was determined by unpaired Student's t-tests. Results are presented as mean ±SD (*, $P < 0.05$; **, $P < 0.01$; ***, $P < 0.001$; ****, $P< 0.0001$, ns: not significant).

5. Discussion

Triple-negative breast cancer (TNBC) is a breast cancer subtype with negative expression (or low expression) of ER, PGR, and HER2. It is more aggressive than other forms and is associated with worse outcomes. This disease is more likely to be diagnosed in women older than 35 years old, and with a poor prognosis, despite optimal adjuvant treatments [171,172]. Patients with TNBC have limited benefit from the targeted therapy due to the lack of hormone receptors such as ER, PGR, and HER2 amplification. Thus, chemotherapy remains the main systemic option in the clinic because TNBC was found sensitive to the chemotherapy. Therefore, surgery and chemotherapy are the current standard of care (SOC) treatment for TNBC. However, the median overall survival (OS) for this disease is only 10.2 months, even treated with current therapies and always followed by rapid relapse [173]. Therefore, finding novel efficient treatment approaches for patients with TNBC are urgent.

Immunotherapy is one of the most promising treatment strategies for TNBC, which has greatly prolonged the overall survival in patients with other solid tumors. Up to now, immune checkpoint inhibitors (ICIs) are the most successful immunotherapeutic agents for TNBC treatment. TNBC frequently overexpresses programmed cell death-ligand 1 (PD-L1) in both tumor and immune cells [174,175]. Therefore, some antibodies targeting the PD-1/PD-L1 signal pathway were approved by the US Food and Drug Administration (FDA) as first-line therapy for patients with TNBC and had good clinic results, especially when combining with chemotherapy [176]. In addition, TNBC has more tumor-infiltrating lymphocytes (TILs) in its tumor microenvironment than other breast cancer subtypes, which would lead to better responses to vaccines and ICIs [177,178]. Cancer vaccines that can improve the cytotoxicity and proliferative capacity of tumor-infiltrating lymphocytes (TILs)

constitute another novel strategy to the TNBC therapy. These vaccines strengthen the recognition of cytotoxic T lymphocytes with the cancer cells through presenting breast cancer immunogenic peptides to T cells. For instance, both PVX-410 vaccine (NCT03362060, NCT02826434) and folate receptor a vaccine (NCT03012100) improved disease-free survival in TNBC patients [179,180]. Although IL-2 monotherapy was not as successful as expected to improve the patients' survival, the combination therapy of IL-2 and other anti-cancer agents showed encouraging clinic results, especially combined with the peptide vaccines, as mentioned before. The mechanism of this combination treatment was revealed by Hussein Sultan et al. [83]. Virotherapy is a new approach for cancer treatment developed in recent years. VACV is one of the most common DNA viruses studied in advanced cancer therapy. Gholami et al. engineered a strain of rVACV armed with anti-Vascular endothelial growth factor (VEGF) single-chain antibody and harbors three viral gene deletions, which effectively local control the growth of TNBC xenografts [181].TG4010 is a therapeutic cancer vaccine based on a Modified Vaccinia Ankara (MVA) vector, expressing MUC1 and IL-2 [182]. TG4010 combined with first-line chemotherapy showed promising results in a phase 2b/3 clinic trial of non-small-cell lung cancer (NSCLC) treatment [183]. Considering all these facts, in this study, we utilized the vaccinia virus as an oncolytic vector to co-express the tumor-associated antigens and mIL-2 cytokine for mouse triple-negative mammary cancer immunotherapy.

The Generation of recombinant novel vaccinia virus (rVACV) strains by homologous recombination and the titer determination

Recombinant vaccinia virus generation and viral titer determination are fundamental experimental techniques in oncolytic virus studies. In the Ph.D. thesis research period, I developed a modified method for fluorescent rVACV generation as well as a rapid VACV viral titer measurement using a multi-well plate imaging system, IncuCyte®S3. Our methods make the research of the oncolytic vaccinia virus much more effective and easier to undertake. The methods were developed based on the VACV-Lister strain but also could be helpful for other orthopoxviruses. Our laboratories constructed one of the first precisely engineered Vaccinia virus strains with fluorescent gene

insertion 17 years ago. After many rounds of human tumor xenograft therapy experiments in mice, we completed 4 phase I human clinical trials in the US and Europe and a phase II platinum-resistant human ovarian cancer trial in the US, which was successfully completed very recently. Now, this FDA-approved oncolytic virus is used in phase III ovarian trials (under patient recruitment). If successful, many novel VACV with specific payloads will be generated in the future for cancer treatments using oncolytic immune therapy. If optimized, our modified virus titer determination methodology can be routinely carried out on tumor samples taken from VACV treated cancer patients as well as on liquid biopsies [184,185].

Expression of fusion protein of four tumor-associated peptides by engineered Vaccina virus strains

In this study, we selected four peptides as immunogens to be expressed by VACV to elicit the peptide-specific cytotoxic T lymphocytes response. On the basis of published literature, all those four peptides are optimal vaccine candidates. The AH-1 epitope is a gold standard for CT26 and 4T1 mouse tumor model therapy. AH1-A5 peptide is derived from AH1 peptide, in which Ala in position 5 of AH1 was replaced by Val and even had a better immune response than AH1 peptide. The S1 and S2 peptides are H2-Kd-restricted epitopes from tumor-associated antigen SPARC, which can stimulate antitumor immunity without causing autoimmune disease in mouse mammary tumor models [130]. Our unpublished data support that the mIL-2 expression drive by a synthetic early and later promoter in the TK location of the VACV Lister strain could bring benefit to the 4T1 and B16F10 mouse tumor models. Thus, we also constructed a Lister strain rVACV co-expressing mIL-2 and a fusion protein containing AH1, AH1- A5, S1, and S2 peptides, which has been shown in the part of results. The mIL-2 gene was inserted into the thymidine kinase locus (TK, J2R) of VACV, as this is a common attenuating mutation site [186]. For the structure of peptides fusion fragment design, we connected the AH1, AH1-A5, S1, and S2 peptides through a flexible linker (GGGGS) 2 and tagged with a flag peptide at the C terminal of the sequence, and mouse Ig Kappa leader sequence was located at the N terminal of the sequence that could help cells to secrete the fusion protein into the extracellular. Brittany A. Umer et al. [187] recently proved that even minor

changes to the VACV genome could impact the immune reaction for the efficiency of tumor therapy. Therefore, to avoid the alteration of immune response based on our former model, we inserted the fusion protein DNA fragment into a VACV “no expression” intergenic region between the intergenic locus 157 and intergenic locus 158. All the foreign proteins expressed of rVACV were identified through either by western blots or by fluorescent microscopy. According to the amino acid sequence, the molecular weight of peptides fusion protein is around 12 kDa, which includes the leader sequence. However, the molecular weight observed on the blot membrane is around 15Kda and with double bands. One possible explanation could be that the fusion protein contains serine, threonine and tyrosine, which may be phosphorylated after expression from VACV, which led to a higher molecular weight and an extra band. Based on these findings, we can predict that the phosphorylated fusion peptide is able to induce the activity of cytotoxic CD8+ effector T cells, according to the ex vivo data presented above, and therefore the structure of the fusion protein provides a new pattern for the tumor antigen-based peptide vaccine design.

Construction of stable cell lines

For the N2C-eGFP stable cell line construction, we developed a modified limited dilution method to screen the monoclonal stable cell lines. Compared to the traditional way, the modified method is able to ensure that the selected cell colonies are originated from a single cell and can rescue some optimal positive monoclonal cells from the polyclones as well [151].

Toxicity concerns related to virus-mediated over-expression of mIL-2 and tumor antigens in mouse tumor model

IL-2 is the first effective cytokine for human cancer immunotherapy. Although the mechanism of IL-2 therapy in humans is unclear, it seems due to its ability to widespread expansion of T cells and maintain functional activity. The curative effect of IL-2 in cancer treatment is dose-dependent, HD IL-2 was always necessary to achieve clinical efficacy. Many studies showed low-dose (LD) IL-2 mainly increases the number of CD4+ Treg cells. However, Treg cells drive dominant tolerance by inhibiting anti-tumor responses mediated by multiple types of activated cells. Our former

unpublished data showed the in vivo biological function of VACV expressed mIL-2 not only virus strain but also promoter dependent. We used two different VACV strains as a vector to express the mIL-2 in the J2R locus driven by three other promoters, synthetic early/late promoter, synthetic late promoter, and intermediate early/late promoter individually. We found that only the Lister strain of rVACV containing the mouse IL-2 gene fragment under the control of synthetic early/late promoter can inhibit tumor growth in the 4T1 mouse model. Therefore, based on this vector, we introduced several 4T1 tumor-associated antigens, which are under the control of synthetic early/late promoter, into the space between the intergenic locus 157 and intergenic locus 158. Recently, some studies have shown that the treatment of IL-2 could enhance therapeutic anticancer peptide vaccines, and the combination therapy of peptide vaccine plus IL-2 was demonstrated to significantly improve the cancer patients' overall survival in the clinic [81, 82]. Here, we constructed an rVACV vaccine strain that co-expressing tumor-associated antigens and mIL-2 cytokine to investigate the anti-tumor activity in a 4T1 tumor-bearing syngeneic BALB/c mouse model. In this experimental setting, we administered the PBS and virus intravenously through the mouse tail vein to avoid the difficulty of intratumoral injection because the 4T1 solid tumors were too hard to inject. Our data demonstrated that the mIL-2 expressing rVACV could help expand both CD4+ and CD8+ T cell populations in vivo, while did not change the ratio of CD4+/CD3+ and CD8+/CD3+, that's one of the explanations that mIL-2 expressing rVACV have better anti-tumor effectiveness than the control groups. Moreover, we found that the immunogens expressed by VACV are able to elicit an appropriate immune response; meanwhile, the VACV expressing tumor-associated peptides greatly enhanced the therapeutic effects of mIL2, which can inhibit tumor growth in the 4T1 animal model and did improve the anti-tumor activity in vivo. Furthermore, we investigated the Mean Fluorescence Intensity (MFI) of PD-1 expression of CD4+ and CD8+ populations in all four animal groups and didn't find any significant difference among these groups. Finally, according to the research findings provided by Brittany A. Umer et al. [180], to further enhance the anti-tumor efficacy of the vaccine, some immunodominant epitopes of the VACV backbone should be deleted so that we can reduce the elimination of viruses by the immune system in vivo and improve the response in the non-immunogenic 4T1 tumor model.

Co-culture assay to assess specific anti-tumor CD8+ T cell cytotoxicity

Amelioration and potentiation of the tumor-specific killing ability of CD8+ T cells in vivo are some of the most critical points for successful immunotherapies. Several in vitro assay systems have been utilized to evaluate the ex vivo lytic activity of antigen-specific cytotoxic T cells and the antigen recognition capacity. The 51Cr-release assay is the gold standard method of measurement of in vitro lytic activity of T cell-mediated cytotoxicity due to its low effector cell number requirements and high sensitivity [188]. In this 4hour assay, the tumor cells are labeled ex vivo with chromium 51 (51Cr), then co-cultured with the effector cells, and cytolysis is monitored and measured by 51Cr release in the cell supernatants. However, this technique is limited because 51Cr is a radioactive metallic element having a half-life of 27.7 days and decaying with the emission of gamma rays. In this study, we developed a novel co-culture assay that can be easily applied by using a real-time imaging platform-IncuCyte®S3. We propose this assay to investigate ex vivo spleen CD8+ cytotoxic activity in the anti-tumor immune response induced by tumor-associate antigens. In this novel assay, to monitor and record the cell death by IncuCyte®S3, the target cells are fluorescence-labeled. Thus, the target cells must be evaluated the expression of MHC I molecules (H2-Kd and H2-Ld) through the FACS before the experiment is performed. At the beginning of the test, the target cells are seeded in the 96-well plate for overnight incubation. Then by adding the isolated CD8+ T cells with appropriate medium containing peptides, IL-2, and anti-CD28 antibody. Lastly, putting the plates into IncuCyte®S3 with set a schedule of programs to scan the plate once every few hours with fluorescence signal. Using this method, we tested the cytotoxic activity of CD8+ T cells against 4T1 and N2C cell lines under the stimulation of tumor antigens, which isolated from the spleen of vaccinated mice. Compared to the 51Cr-release assay for CD8+ T cell cytotoxicity assay, our method does not require a radiation-safe environment and can be easily carried out without the cell radioactive labeling step. Moreover, this system also can provide movies of different time points of images scanned by the IncuCyte®S3.

Taken together, using the modified plaque screen method developed by Mingyu Ye et al. [184], I additionally constructed several novel strains of recombinant Vaccinia viruses that express tumor-

associated peptides and mouse IL-2 proteins alone or simultaneously in combination. And using these novel strains as therapeutic cancer vectors, we investigated the combined effect of anti-tumor immune response with mouse Interleukin 2 (IL-2) and tumor-associated antigens in the 4T1 mouse syngeneic tumor model. As expected, the results confirmed our previous unpublished data that the mIL-2 expression driven by the synthetic early/late promoter from VACV Lister enhanced tumor regression in the 4T1 mouse model. Furthermore, the VACV expressed mIL-2 remarkably increased both CD4+ and CD8+ cell populations in vivo, and the virus-expressed tumor-associated peptides successfully elicited the antigen-specific T cell response to drastically inhibit the growth of the tumor. Moreover, the animal experiment results demonstrated that the mIL-2 plus tumor antigens expressing VACV vector showed a more elevated anti-cancer response than the mIL-2 expressing vector alone. The combination vector inhibited tumor growth former significantly more than the mIL-2 Vector alone.

6. Abbreviations

Breast cancer	BC
DMEM-2	DMEM containing 2% FBS
DMEM-5	DMEM containing 5% FBS
DMEM-10	DMEM containing 10% FBS
Oncolytic viruses	OVs
Vaccinia Virus	VACV
Recombinant Vaccinia Virus	rVACVs
Homologous recombination	HR
Enhanced green fluorescent protein	eGFP
L1c-Ig-Turbo-TK-Egfp	LVP-R-G
L1c-Ig-Turbo-SPARC/gp70 peptides-TK-Egfp	LVP-R-G-SPARC/gp70 peptides
L1c-Ig-Turbo-SPARC/gp70 peptides-TK-Egfp-mIL2	LVP-R-G-SPARC/gp70 peptides-mIL2
L1c-Ig-Turbo-TK-Egfp-mIL2	LVP-R-G-mIL2
Triple-negative breast cancer	TNBC

7. Supplementary Data

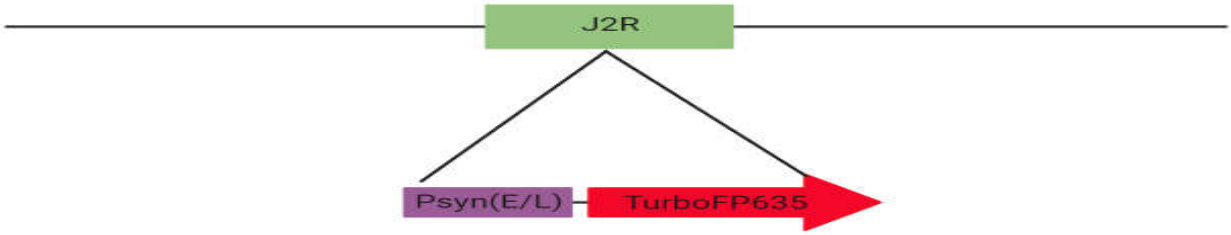

Figure S1. Schematic presentation of rVACV strain C1-opt1

Table S1. Primers for plasmid construction and DNA sequencing

Name of the primers	Sequence (5‘-3‘)
PSC65-eGFP-F	GGAAGTAGATCATAACTCGAGATGGTGAGCAAGGGCGAGGAGCTGT
PSC65-eGFP-R	GCGACCGGCGCTCAGCTGAATTCTTACTTGTACAGCTCGTCCATGCCGAGAGT
mIL2 Seq-F/TKR-F	CGGTTTCCTCACCCAATCGT
mIL2 Seq-R/TKR-R	CCTCGTCGCAATATCGCAT
PSG65-eGFP-IL2-F	AAGCTCGAAGTCGACAGATCTATGTACAGTATGCAGTTGGCGTCATGCGTAACTT
PSG65-eGFP-IL2-R	ACCCGGGTACCAGGCCTAGATCTTTATTGAGGTGAGGTAGAGATTATACTCT
Peptide sequencing F	GGCTTCTACTTCGTGGACAG
Peptide sequencing R	CGATGCCAAGTACATCGACG
rVACV SPARCgp70 peptides F	GCATACATTATACGAAGTTATGGATCCGC
rVACV SPARCgp70 peptides R	GCCGCATTTAAATGATATCGCATGCCTT
Peptide pool Forward Primer	CGAAGTTATGGATCCGCATG
PLV-PEL turbo F	GATCTCGACGGTATCGCTAGCAAAAATTGAAATTTTATTTTTTTTTTTTG
PLV-PEL turbo R	CCTTTTCTTTTAAAAGCTAGCTCAGCTGTGCCCCAGTTTGCTAGGCAGG
Peptide sequencing R	CGATGCCAAGTACATCGACG
EGFP-C-F-31	CAAAGACCCCAACGAGAAG
EGFP-N-rev	GCTTGCCGTAGGTGGCATC

8. Acknowledgements

It's my great pleasure to appreciate all the people who helped and supported me during my Ph.D. Studying period. Without the following people's help and instruction, I could not complete this thesis. First, I would like to thank Prof. Aladar A. Szalay and Prof. Utz Fischer for giving me the opportunity to complete my Ph.D. thesis research at the University of Würzburg and to the Hope Realized Medical Foundation and DFG for their financial support.

Secondly, I would like to thank Dr. Ivaylo Gentschev, who is always willing to talk with me and give me some important suggestions for my research projects. Thank Dr. Katalin Papai-Herczeg, who always helps us organize the office routine work and reagents ordering. Special thanks go to Ivan Petrov who helped me with the mouse treatments and shared with me his non-published results. Thank you to Dr. Ulla Gerling- Drießen, and Michael Renteln, for the critical reading and correction of my publications. Finally, I want to thank all my colleagues, including former colleagues at the University of Würzburg. Thank you for going along with me through every workday in my graduate student life, for supporting me in all the laboratory works, and for sharing all the scientific discussions.

Lastly, I would like to express my gratitude to my family and friends for their encouragement and support all through my studies.

9. Affidavit

Name, Vorname: Ye, Mingyu

Straße: Room B110, Department of Biochemistry, Biozentrum am Hubland, Universität Würzburg

PLZ und Ort: 97074 Würzburg

Tel.: +49015256840370

E-Mail: mingyu.ye@uni-wuerzburg.de

Eidesstattliche Erklärungen nach §7 Abs. 2 Satz 3, 4, 5

der Promotionsordnung der Fakultät für Biologie

Eidesstattliche Erklärung

Hiermit erkläre ich an Eides statt, die Dissertation: „**Immuntherapie von Brustkrebs in tumortragenden Mäusen mit genetisch modifizierten Vaccinia Viren, die simultan Interleukin-2 und tumorassoziierte Antigene exprimieren**“, eigenständig, d. h. insbesondere selbständig und ohne Hilfe eines kommerziellen Promotionsberaters, angefertigt und keine anderen, als die von mir angegebenen Quellen und Hilfsmittel verwendet zu haben.

Ich erkläre außerdem, dass die Dissertation weder in gleicher noch in ähnlicher Form bereits in einem anderen Prüfungsverfahren vorgelegen hat.

Weiterhin erkläre ich, dass bei allen Abbildungen und Texten bei denen die Verwertungsrechte (Copyright) nicht bei mir liegen, diese von den Rechtsinhabern eingeholt wurden und die Textstellen bzw. Abbildungen entsprechend den rechtlichen Vorgaben

gekennzeichnet sind sowie bei Abbbildungen, die dem Internet entnommen wurden, der entsprechende Hypertextlink angegeben wurde.

Affidavit

I hereby declare that my thesis entitled: "**Immunotherapy with Vaccinia virus co-expressing tumor-associated antigens and mouse IL-2 cytokine in mice with mammary cancer**" is the result of my own work. I did not receive any help or support from commercial consultants. All sources and / or materials applied are listed and specified in the thesis.

Furthermore, I verify that the thesis has not been submitted as part of another examination process neither in identical nor in similar form.

Besides I declare that if I do not hold the copyright for figures and paragraphs, I obtained it from the rights holder and that paragraphs and figures have been marked according to law or for figures taken from the internet the hyperlink has been added accordingly.

Würzburg, den____29.10.2021_____

Signature PhD-student

Eidesstattliche Erklärung für die Dissertation

10. Curriculum Vitae

Mingyu Ye

Gender: Male

Date of Birth: 02/27/1987 **Place of birth:** Zhejiang province, China

Add: Room B110, Department of Biochemistry, Biozentrum am Hubland, Universität Würzburg, 97074 Würzburg, Germany

---

Education

Hebei University of Science & Technology **September 2005- June 2009**

Bachelor of Science in Biology Shijiazhuang, China

Nankai University **September 2010- June 2013**

Master of Science in Physiology and Biology Tianjin, China

Universität Würzburg **November 2016-Present**

Ph.D. in Oncolytic immune therapy Würzburg, Germany

Working Experience

Abcam **July 2013-May 2015**

ACEA Biosciences | Agilent **May 2015- April 2016**

11. List of Publications

Ye M, Wilhelm M, Gentschev I, Szalay A. A Modified Limiting Dilution Method for Monoclonal Stable Cell Line Selection Using a Real-Time Fluorescence Imaging System: A Practical Workflow and Advanced Applications. Methods Protoc. 2021 Feb 20;4(1):16.

Ye, M.; Keicher, M.; Gentschev, I.; Szalay, A.A. Efficient Selection of Recombinant Fluorescent Vaccinia Virus Strains and Rapid Virus Titer Determination by Using a Multi-Well Plate Imaging System. Biomedicines 2021, 9, 1032.

12. Reference

1. Breast Cancer". NCI. January 1980. Archived from the original on 25 June 2014. Retrieved 29 June 2014.

2. Sung H, Ferlay J, Siegel RL, Laversanne M, Soerjomataram I, Jemal A, Bray F. Global Cancer Statistics 2020: GLOBOCAN Estimates of Incidence and Mortality Worldwide for 36 Cancers in 185 Countries. CA Cancer J Clin. 2021 May;71(3):209-249.

3. Anastasiadi Z, Lianos GD, Ignatiadou E, Harissis HV, Mitsis M. Breast cancer in young women: an overview. Updates Surg. 2017 Sep;69(3):313-317.

4. Elbachiri M, Fatima S, Bouchbika Z, Benchekroun N, Jouhadi H, Tawfiq N, Sahraoui S, Benider A. Cancer du sein chez l'homme: à propos de 40 cas et revue de la littérature [Breast cancer in men: about 40 cases and literature review]. Pan Afr Med J. 2017 Dec 4;28:287. French.

5. Dillon D, Guidi AJ, Schnitt SJ. Pathology of invasive breast cancer. In: Harris JR, Lippman ME, Morrow M, Osborne CK, eds. Diseases of the Breast.5th ed. Philadelphia, PA: Wolters Kluwer Health; 2014.

6. Boyle, P. Triple-negative breast cancer: Epidemiological considerations and recommendations. Ann. Oncol., 2012, 23. 7-12.

7. Choi, J.; Jung, W.H.; Koo, J.S. Clinicopathologic features of molecular subtypes of triple negative breast cancer based on immunohistochemical markers. Histol. Histopathol., 2012, 27,1481- 1493.

8. Waks AG, Winer EP. Breast Cancer Treatment: A Review. JAMA. 2019 Jan 22;321(3):288- 300.

9. Bergin ART, Loi S. Triple-negative breast cancer: recent treatment advances. F1000Res. 2019 Aug 2;8: F1000 Faculty Rev-1342.

10. Kumar P, Aggarwal R. An overview of triple-negative breast cancer. Arch Gynecol Obstet. 2016 Feb;293(2):247-69. doi: 10.1007/s00404-015-3859-y. Epub 2015 Sep 4.

11. Hamilton DH, Roselli M, Ferroni P, Costarelli L, Cavaliere F, Taffuri M, et al. Brachyury, a vaccine target, is overexpressed in triple-negative breast cancer. Endocr Relat Cancer (2016) 23(10):783–96.

12. Mansour M, Teo ZL, Luen SJ, Loi S. Advancing immunotherapy in metastatic breast cancer. Curr Treat Options Oncol (2017) 18(6):35.

13. Emens LA. Breast cancer immunobiology driving immunotherapy: vaccines and immune checkpoint blockade. Expert Rev Anticancer Ther 2012; 12:1597–611

14. Savas P, Salgado R, Denkert C, Sotiriou C, Darcy PK, Smyth MJ, et al. Clinical relevance of host immunity in breast cancer: from TILs to clinic. Nat Rev Clin Oncol 2016; 13:228–4.

15. Miko E, Meggyes M, Doba K, Barakonyi A, Szereday L. Immune Checkpoint Molecules in Reproductive Immunology. Front Immunol. 2019; 10:846. Published 2019 Apr 18.

16. Sharpe AH. Mechanisms of costimulation. Immunol Rev. 2009 May;229(1):5-11.

17. Chen L. Co-inhibitory molecules of the B7-CD28 family in the control of Tcell immunity. Nat Rev Immunol. 2004; 4:336–47.

18. Emens LA. Breast Cancer Immunotherapy: Facts and Hopes. Clin Cancer Res. 2018 Feb 1;24(3):511-520. doi: 10.1158/1078-0432.CCR-16-3001. Epub 2017 Aug 11.

19. Amedei A, Prisco D, D' Elios MM. The use of cytokines and chemokines in the cancer immunotherapy. Recent Pat Anticancer Drug Discov. 2013 May;8(2):126-42.

20. Miglietta F, Cona MS, Dieci MV, Guarneri V, La Verde N. An overview of immune checkpoint inhibitors in breast cancer. Explor Target Antitumor Ther. 2020;1:452-72.

21. Zhao, Bin et al. “Efficacy of PD-1/PD-L1 blockade monotherapy in clinical trials.” Therapeutic advances in medical oncology vol. 12 1758835920937612. 16 Jul. 2020.

22. Szostak B, Machaj F, Rosik J, Pawlik A. CTLA4 antagonists in phase I and phase II clinical trials, current status and future perspectives for cancer therapy. Expert Opin Investig Drugs. 2019 Feb;28(2):149-159.

23. Meggyes M, Szanto J, Lajko A, Farkas B, Varnagy A, Tamas P,et al. The possible role of CD8+/Vα7.2+/CD161++ T (MAIT) and CD8+/Vα7.2+/CD161 lo T (MAIT-like) cells in the pathogenesis of early-onset pre-eclampsia. Am J Reprod Immunol. (2018) 79:e12805

24. Keir ME, Butte MJ, Freeman GJ, Sharpe AH. PD-1 and its ligands in tolerance and immunity. Annu Rev Immunol. (2008) 26:677–704

25. Chikuma S. Basics of PD-1 in self-tolerance, infection, and cancer immunity.Int J Clin Oncol. (2016) 21:448–55. doi: 10.1007/s10147-016-0958-0

26. Pardoll DM. The blockade of immune checkpoints in cancer immunotherapy. Nat Rev Cancer 2012; 12:252–64.

27. Guo L, Wei R, Lin Y, Kwok HF. Clinical and Recent Patents Applications of PD-1/PD-L1 Targeting Immunotherapy in Cancer Treatment-Current Progress, Strategy, and Future Perspective. Front Immunol. 2020 Jul 7;11:1508.

28. Schreiber AR, Kagihara JA, Weiss JA, Nicklawsky A, Gao D, Borges VF, Kabos P, Diamond JR. Clinical Outcomes for Patients With Metastatic Breast Cancer Treated With Immunotherapy Agents in Phase I Clinical Trials. Front Oncol. 2021 Mar 17;11:640690.

29. Walker LSK. EFIS lecture: understanding the CTLA-4 checkpoint in the maintenance of immune homeostasis. Immunol Lett. (2017) 184:43–50.

30. Saito S, Sasaki Y, Sakai M. CD4+CD25high regulatory T cells in human pregnancy. J Reprod Immunol. (2005) 65:111–20.

31. Shiratori T, Miyatake S, Ohno H, et al. Tyrosine phosphorylation controls internalization of CTLA-4 by regulating its interaction with clathrin-associated adaptor complex AP-2. Immunity.1997; 6(5):583–589.

32. Sasaki Y. Decidual and peripheral blood CD4+CD25+ regulatory T cells in early pregnancy subjects and spontaneous abortion cases. Mol Hum Reprod. (2004) 10:347–53.

33. Liu Y, Zheng P. Preserving the CTLA-4 Checkpoint for Safer and More Effective Cancer Immunotherapy. Trends Pharmacol Sci. 2020 Jan;41(1):4-12.

34. Vonderheide RH, LoRusso PM, Khalli M, Gartner EM, Khaira D, Soulieres D, et al. Tremelimumab in combination with exemestane in patients with advanced breast cancer and treatment-associated modulation of inducible costimulatory expression on patient T cells. Clin Cancer Res 2010;16:3485–94.

35. McArthur HL, Diab A, Page DB, Yuan J, Solomon SB, Sacchini V, et al. A pilot study of preoperative single-dose ipilimumab and/or cryoablation in women with early-stage breast cancer with comprehensive immune profiling. Clin Cancer Res 2016; 22:5729–37.

36. Lacy, Paige. “Editorial: secretion of cytokines and chemokines by innate immune cells.” Frontiers in immunology vol. 6 190. 22 Apr. 2015, doi:10.3389/fimmu.2015.00190

37. Bridge JA, Lee JC, Daud A, Wells JW, Bluestone JA. Cytokines, Chemokines, and Other Biomarkers of Response for Checkpoint Inhibitor Therapy in Skin Cancer. Front Med (Lausanne). 2018 Dec 12; 5:351.

38. Zhang Y, Guan XY, Jiang P. Cytokine and Chemokine Signals of T-Cell Exclusion in Tumors. Front Immunol. 2020 Dec 14; 11:594609.

39. D'Elios MM, Del Prete G, Amedei A. New frontiers in cell-based immunotherapy of cancer. Expert Opin Ther Pat 2009; 19(5): 623-41

40. Mukaida, Naofumi et al. “Chemokines in cancer development and progression and their potential as targeting molecules for cancer treatment.” Mediators of inflammation vol. 2014 (2014): 170381.

41. Bhat, A.A., Nisar, S., Maacha, S. et al. Cytokine-chemokine network driven metastasis in esophageal cancer; promising avenue for targeted therapy. Mol Cancer 20, 2 (2021).

42. B. Moser, M. Wolf, A. Walz, and P. Loetscher, “Chemokines: multiple levels of leukocyte migration control,” Trends in Immunology, vol. 25, no. 2, pp. 75–84, 2004.

43. Baggiolini M, Dewald B, Moser B. Human chemokines: An update. Ann Rev Immunol 1997; 15: 675-705.

44. Lapteva N. CXCR4 knock down by small interfering RNA abrogates breast tumor growth in vivo. Cancer Gene Ther. 2015;12(1):84-89.

45. Behnam Azad B, Lisok A, Chatterjee S, et al. Targeted imaging of the atypical chemokine receptor 3(ACKR3/CXCR7) in human cancer xenografts. J Nucl Med. 2016; 257:981-988.

46. Boudot A, Kerdivel G, Habauzit D, et al. Differential estrogen-regulation of CXCL12 chemokine receptors, CXCR4 and CXCR7, contributes to the growth effect of estrogens in breast cancer cells. PLoS One. 2011;6(6): e20898.

47. Hinton CV, Avraham S, Avraham HK. Role of the CXCR4/CXCL12 signaling axis in breast cancer metastasis to the brain. Clin Exp Metastasis. 2012;27(2):97-105.

48. Liu H, Yang Z, Lu W, Chen Z, Chen L, Han S, Wu X, Cai T, Cai Y. Chemokines and chemokine receptors: A new strategy for breast cancer therapy. Cancer Med. 2020 Jun;9(11):3786- 3799.

49. Sharma P, Kumar P, Mahapatra T, An overview of cytokines; their current status & futuristic scope. Santosh Univ J Health Sci 2017;3(2):50-53

50. Turner MD, Nedjai B, Hurst T, Pennington DJ. Cytokines and chemokines: At the crossroads of cell signalling and inflammatory disease. Biochim Biophys Acta. 2014 Nov;1843(11):2563-2582.

51. Martínez Conesa C, Alvarez Sánchez N, Vicente Ortega V, García Reverte J, Pascual Carpe F, Campos Aranda M. In vitro and in vivo effect of IFNalpha on B16F10 melanoma in two models: subcutaneous (C57BL6J mice) and lung metastasis (Swiss mice). Biomed Pharmacother. 2009 May;63(4):305-12.

52. Isaacs, A. & Lindenmann, J. Virus interference. I. The interferon. Proc. R. Soc. Lond. Ser. B Biol. Sci. 147, 258–267 (1957).

53. Kirkwood, J. M. et al. Interferon alfa-2b adjuvant therapy of high-risk resected cutaneous melanoma: the Eastern Cooperative Oncology Group Trial EST 1684. J. Clin. Oncol. 14, 7–17 (1996).

54. Solal-Celigny, P. et al. Recombinant interferon alfa-2b combined with a regimen containing doxorubicin in patients with advanced follicular lymphoma. Groupe d'Etude des Lymphomes de l'Adulte. New Engl. J. Med. 329, 1608–1614 (1993).

55. Atkins, M. B. et al. High-dose recombinant interleukin 2 therapy for patients with metastatic melanoma: analysis of 270 patients treated between 1985 and 1993. J. Clin. Oncol. 17, 2105–2116 (1999).

56. Fyfe, G. et al. Results of treatment of 255 patients with metastatic renal cell carcinoma who received high-dose recombinant interleukin-2 therapy. J. Clin. Oncol. 13, 688–696 (1995).

57. Shi Z, Yang W-M, Chen L-P, Yang D-H, Zhou Q, Zhu J,Huang R-P. 2012. Enhanced chemosensitization in multidrug-resistant human breast cancer cells by inhibition of IL-6 and IL-8 production. Breast Cancer Res Treat 135(3): 737–747.

58. Korkaya H, Kim G-I, Davis A, Malik F, Henry NL, Ithimakin S,Wicha MS. 2012. Activation of an IL6 inflammatory loopmediates trastuzumab resistance in HER2 + breast cancer by expanding the cancer stem cell population. Mol Cell 47(4):570–584

59. Liu J, Liao S, Diop-frimpong B, Chen W, Goel S, Naxerova K, Xu L. 2012a. TGF-b blockade improves the distribution and efficacy of therapeutics in breast carcinoma by normalizing the tumor stroma. Proc Natl Acad Sci U S A 109(41):16618–16623.

60. Ehata S, Hanyu A, Fujime M, Katsuno Y, Fukunaga E, Goto K, Ishikawa Y, Nomura K, Yokoo H, Shimizu T et al (2007) Ki26894, a novel transforming growth factor-beta type I receptor kinase inhibitor, inhibits in vitro invasion and in vivo bone metastasis of a human breast cancer cell line. Cancer Sci 98:127–133

61. Hsu Y-H, Hsing C-H, Li C-F, Chan C-H, Chang M-C, Yan J-J,Chang M-S. 2012. Anti-IL-20 monoclonal antibody suppresses breast cancer progression and bone osteolysis in murine models. J Immunol 188(4):1981–1991.

62. Nicolini A, Carpi A. 2008. Immune manipulation of advanced breast cancer: an interpretative model of the relationship between immune system and tumor cell biology. Med Res Rev 29(3):436–471.

63. Klimka A, Yu N, Shami EY. Construction of proteolysis resistant human interleukin-2 by fusion to its protective single chain antibody. Cytokine. 2003 Jun 7;22(5):134-41.

64. Wang X, Rickert M, Garcia KC. Structure of the quaternary complex of interleukin-2 with its alpha, beta, and gammac receptors. Science. 2005 Nov 18;310(5751):1159-63.

65. N. A. Cacalano and J. A. Johnston, “Interleukin-2 signaling and inherited immunodeficiency,” American Journal of Human Genetics, vol. 65, no. 2, pp. 287–293, 1999.

66. Malek, T.R. & Castro, I. Interleukin-2 receptor signaling: at the interface between tolerance and immunity. Immunity 33, 153-165 (2010).

67. D. J. Stauber, E. W. Debler, P. A. Horton, K. A. Smith, and I.A. Wilson, “Crystal structure of the IL-2 signaling complex: Paradigm for a heterotrimeric cytokine receptor,” Proceedings of the National Acadamy of Sciences of the United States of America,vol. 103, no. 8, pp. 2788–2793, 2006.

68. R. J. Robb, A. Munck, and K. A. Smith, “T cell growth factor receptors: Quantitation,specificity, and biological relevance,”The Journal of Experimental Medicine, vol. 154, no. 5, pp. 1455–1474, 1981.

69. Amaria RN, Reuben A, Cooper ZA, Wargo JA. Update on use of aldesleukin for treatment of high-risk metastatic melanoma. Immunotargets Ther. 2015 Apr 7; 4:79-89.

70. Papa MZ, Vetto JT, Ettinghausen SE, Mulé JJ, Rosenberg SA. Effect of corticosteroid on the antitumor activity of lymphokine-activated killer cells and interleukin 2 in mice. Cancer Res. 1986 Nov;46(11):5618-23.

71. Rosenberg SA, Lotze MT, Muul LM, Leitman S, Chang AE, Ettinghausen SE, Matory YL, Skibber JM, Shiloni E, Vetto JT et al. Observations on the systemic administration of autologous lymphokine-activated killer cells and recombinant interleukin-2 to patients with metastatic cancer. N Engl J Med 1985; 313:1485-92.

72. Liao, W., Lin, J.X. & Leonard, W.J. Interleukin-2 at the crossroads of effector responses, tolerance, and immunotherapy. Immunity 38, 13-25 (2013).

73. Boyman, O. & Sprent, J. The role of interleukin-2 during homeostasis and activation of the immune system. Nat Rev Immunol 12, 180-190 (2012).

74. Sim GC, Radvanyi L. The IL-2 cytokine family in cancer immunotherapy. Cytokine Growth Factor Rev 2014; 25:377-90.

75. S. A. Long, M. Rieck, S. Sanda et al., “Rapamycin/IL-2 combination therapy in patients with type 1 diabetes augments Tregs yet transiently impairs p-cell function,” Diabetes, vol. 61, no. 9, pp. 2340–2348, 2012.

76. Mitra S, Leonard WJ. 2018. Biology of IL-2 and its therapeutic modulation: mechanisms and strategies. J. Leukoc. Biol. 103(4):643–55

77. Copsel S, Wolf D, Komanduri KV, Levy RB. The promise of CD4+FoxP3+ regulatory T-cell manipulation in vivo: applications for allogeneic hematopoietic stem cell transplantation. Haematologica. 2019 Jul;104(7):1309-1321.

78. Alva A, Daniels GA, Wong MK, et al. Contemporary experience with high-dose interleukin-2 therapy and impact on survival in patients with metastatic melanoma and metastatic renal cell carcinoma. Cancer Immunol Immunother. 2016;65(12):1533-1544. doi:10.1007/s00262-016-1910-x

79. Jiang T, Zhou C, Ren S. Role of IL-2 in cancer immunotherapy. Oncoimmunology. 2016;5(6): e1163462. Published 2016 Apr 25.

80. Overwijk WW, Theoret MR, Restifo NP. The future of interleukin 2: enhancing therapeutic anticancer vaccines. Cancer J Sci Am 2000; 6 (Suppl 1): S76-80.

81. Smith FO, Downey SG, Klapper JA, Yang JC, Sherry RM, Royal RE, Kammula US, Hughes MS, Restifo NP, Levy CL et al. Treatment of metastatic melanoma using interleukin-2 alone or in conjunction with vaccines. Clin Cancer Res 2008; 14:5610-8.

82. chwartzentruber DJ, Lawson DH, Richards JM, Conry RM, Miller DM, Treisman J, Gailani F, Riley L, Conlon K, Pockaj B et al. gp100 peptide vaccine and interleukin-2 in patients with advanced melanoma. N Engl J Med. 2011; 364:2119-27.

83. Sultan H, Kumai T, Fesenkova VI, Fan AE, Wu J, Cho HI, Kobayashi H, Harabuchi Y, Celis E. Sustained Persistence of IL2 Signaling Enhances the Antitumor Effect of Peptide Vaccines through T- cell Expansion and Preventing PD-1 Inhibition. Cancer Immunol Res. 2018 May;6(5):617-627.

84. Repka T, Chiorean EG, Gay J, Herwig KE, Kohl VK, Yee D, Miller JS. Trastuzumab and interleukin-2 in HER2-positive metastatic breast cancer: a pilot study. Clin Cancer Res. 2003 Jul;9(7):2440-6.

85. Mårlind J, Kaspar M, Trachsel E, Sommavilla R, Hindle S, Bacci C, Giovannoni L, Neri D. Antibody-mediated delivery of interleukin-2 to the stroma of breast cancer strongly enhances the potency of chemotherapy. Clin Cancer Res. 2008 Oct 15;14(20):6515-24.

86. Vlad AM, Finn OJ. Glycoprotein tumor antigens for immunotherapy of breast cancer. Breast Dis. 2004; 20:73-9.

87. V.Y. Phan, Mary L. Disis, Hailing LU,chapter 33 - Immune Recognition of Breast Cancer,Editor(s): Kirby I. Bland, Edward M. Copeland,The Breast (Fourth Edition),W.B. Saunders,2009,Pages 589-594,

88. De Smet C, Lurquin C, van der BP, De PE, BrasseurF, Boon T. Sequence and expression pattern of thehuman MAGE2 gene. Immunogenetics 1994; 39:121-129.

89. De Smet C, Lurquin C, Lethe B, Martelange V, Boon T. DNA methylation is the primary silencing mechanism for a set of germ line- and tumor-specific genes with a CpG-rich promoter. Mol Cell Biol 1999; 19:7327-7335.

90. Smith, C.C., Selitsky, S.R., Chai, S. et al. Alternative tumor-specific antigens. Nat Rev Cancer 19, 465–478 (2019).

91. Harao M, Mittendorf EA, Radvanyi LG. Peptide-based vaccination and induction of CD8+ T- cell responses against tumor antigens in breast cancer. BioDrugs. 2015 Feb;29(1):15-30.

92. Baral R. Tumor vaccine: current trends in antigen specific immunotherapy. Indian J Exp Biol. 2005 May;43(5):389-406.

93. Drijvers, Jefte M et al. “The effects of age and systemic metabolism on anti-tumor T cell responses.” eLife vol. 9 e62420. 10 Nov. 2020.

94. Richardson JR, Schöllhorn A, Gouttefangeas C, Schuhmacher J. CD4+ T Cells: Multitasking Cells in the Duty of Cancer Immunotherapy. Cancers (Basel). 2021 Feb 3;13(4):596.

95. Gatti-Mays ME, Balko JM, Gameiro SR, Bear HD, Prabhakaran S, Fukui J, et al. If we build it they will come: targeting the immune response to breast cancer. NPJ Breast Cancer. 2019 Oct 29; 5:37.

96. Beckers RK, Selinger CI, Vilain R, Madore J,Wilmott JS, Harvey K, et al. Programmed death ligand 1 expression in triple-negative breast cancer is associated with tumor-infiltrating lymphocytes and improved outcome.Histopathology. 2016 Jul;69(1):25–34.

97. Ali HR, Provenzano E, Dawson SJ et al. Association between CD8+ T-cell infiltration and breast cancer survival in 12 439 patients. Ann Oncol 2014; 25:1536–1543.

98. Ott PA, Bang YJ, Piha-Paul SA, Razak ARA, Bennouna J, Soria JC, et al. T-Cell-Inflamed gene-expression profile, programmed death ligand 1 expression, and tumor mutational burden predict efficacy in patients treated with pembrolizumab across 20 cancers: KEYNOTE-028. J Clin Oncol. 2019;37(4):318–27

99. M. Disis, Immunologic targets for breast cancer therapy, Breast Disease 15 (2003), 83–90

100. Radosa JC, Stotz L, Müller C, Kaya AC, Solomayer EF, Radosa MP. Clinical Data on Immunotherapy in Breast Cancer. Breast Care (Basel). 2020 Oct;15(5):450-469

101. Wei Q, Fang ZY, Zhang ZM, Zhang TF. Therapeutic tumor vaccines — a rising star to benefit cancer patients. Artif Intell Cancer 2021; 2(3): 25-41

102. Kalli KR, Block MS, Kasi PM, Erskine CL, Hobday TJ, Dietz A, Padley D, Gustafson MP, Shreeder B, Puglisi-Knutson D, Visscher DW, Mangskau TK, Wilson G, Knutson KL. Folate Receptor Alpha Peptide Vaccine Generates Immunity in Breast and Ovarian Cancer Patients. Clin Cancer Res. 2018 Jul 1;24(13):3014-3025.

103. Sears AK, Perez SA, Clifton GT, Benavides LC, Gates JD, Clive KS, Holmes JP, Shumway NM, Van Echo DC, Carmichael MG, Ponniah S, Baxevanis CN, Mittendorf EA, Papamichail M, Peoples GE. AE37: a novel T-cell-eliciting vaccine for breast cancer. Expert Opin Biol Ther. 2011 Nov;11(11):1543-50.

104. ClinicalTrials.gov [Internet]. NuGenerex Immuno-Oncology. May 3, 2019-. Identifier: NCT04024800, Establishing the Recommended Biological Dose for AE37 Peptide Vaccine in Combination With Pembrolizumab That Will Enhance the Tumor-specific Immune Response and Demonstrate Efficacy in Patients With Advanced Triple-negative Breast Cancer (NSABP FB-14). June 25, 2019.

105. L. Gross, “Development and serial cellfree passage of a highly potent strain of mouse leukemia virus,” Proceedings of the Society for Experimental Biology and Medicine, vol. 94, pp.767– 771, 1957.

106. J. B. Moloney, “Biological studies on a lymphoid-leukemia virus extracted from sarcoma 37. I. Origin and introductory investigations,” Journal of the National Cancer Institute, vol.24, pp. 933–951, 1960.

107. Huang AY, Gulden PH, Woods AS, Thomas MC, Tong CD, Wang W, Engelhard VH, Pasternack G, Cotter R, Hunt D, et al. The immunodominant major histocompatibility complex class I- restricted antigen of a murine colon tumor derives from an endogenous retroviral gene product. Proc Natl Acad Sci U S A 1996; 93:9730-5;

108. Scrimieri F, Askew D, Corn DJ, Eid S, Bobanga ID, Bjelac JA, Tsao ML, Allen F, Othman YS, Wang SC, Huang AY. Murine leukemia virus envelope gp70 is a shared biomarker for the high- sensitivity quantification of murine tumor burden. Oncoimmunology. 2013 Nov 1;2(11): e26889.

109. McWilliams JA, Sullivan RT, Jordan KR, McMahan RH, Kemmler CB, McDuffie M, Slansky JE. Age-dependent tolerance to an endogenous tumor-associated antigen. Vaccine. 2008 Mar 28;26(15):1863-1873.

110. Huang AYC, Gulden PH, Woods AS, et al. The immunodominant major histocompatibility complex class I–restricted antigen of a murine colon tumor derives from an endogenous retroviral gene product. Proc Natl Acad Sci USA. 1996; 93:9730–9735.

111. Slansky JE, Rattis FM, Boyd LF, Fahmy T, Jaffee EM, Schneck JP, Margulies DH, Pardoll DM. Enhanced antigen-specific antitumor immunity with altered peptide ligands that stabilize the MHCpeptide-TCR complex. Immunity. 2000; 13:529–538

112. McMahan RH, McWilliams JA, Jordan KR, Dow SW, Wilson DB, Slansky JE. Relating TCRpeptide-MHC affinity to immunogenicity for the design of tumor vaccines. J Clin Invest. 2006; 116:2543–2551.

113. Schirmbeck R, Riedl P, Kupferschmitt M, Wegenka U, Hauser H, Rice J, Kroger A, Reimann J.Priming protective CD8 T cell immunity by DNA vaccines encoding chimeric, stress proteincapturing tumor-associated antigen. J Immunol. 2006; 177:1534–1542.

114. Luznik L, Slansky JE, Jalla S, Borrello I, Levitsky HI, Pardoll DM, Fuchs EJ. Successful therapy of metastatic cancer using tumor vaccines in mixed allogeneic bone marrow chimeras. Blood. 2003 Feb 15;101(4):1645-52.

115. Jordan KR, McMahan RH, Kemmler CB, Kappler JW, Slansky JE. Peptide vaccines prevent tumor growth by activating T cells that respond to native tumor antigens. Proc Natl Acad Sci U S A. 2010 Mar 9;107(10):4652-7.

116. Slansky JE, Rattis FM, Boyd LF, Fahmy T, Jaffee EM, Schneck JP, Margulies DH, Pardoll DM. Enhanced antigen-specific antitumor immunity with altered peptide ligands that stabilize the MHC- peptide-TCR complex. Immunity. 2000 Oct;13(4):529-38.

117. Chen H, Huang XN, Stewart AFR, Sepulveda JL. Gene expression changes associated with fibronectin-induced cardiac myocyte hypertrophy. Physiol Genomics. 2004; 18: 273–283.

118. Harris BS, Zhang Y, Card L, Rivera LB, Brekken RA, Bradshaw AD. SPARC regulates collagen interaction with cardiac fibroblast cell surfaces. Am J Physiol Heart Circ Physiol. 2011; 301: H841–847.

119. Yan Q, Blake D, Clark JI, Sage EH. 2003. Expression of the matricellular protein SPARC in murine lens: SPARC is necessary for the structural integrity of the capsular basement membrane. J Histochem Cytochem 51:503–511.

120. Brekken RA, Sage EH: SPARC, a matricellular protein: at the crossroads of cell-matrix communication. Matrix Biol 2001, 19:816e827

121. Yan Q, Weaver M, Perdue N, Sage EH. Matricellular protein SPARC is translocated to the nuclei of immortalized murine lens epithelial cells. J Cell Physiol. 2005 Apr;203(1):286-94.

122. Shi, Q., Bao, S., Song, L. et al. Targeting SPARC expression decreases glioma cellular survival and invasion associated with reduced activities of FAK and ILK kinases. Oncogene 26, 4084– 4094 (2007).

123. Fenouille N, Puissant A, Tichet M, Zimniak G, Abbe P, Mallavialle A, Rocchi S, Ortonne JP, Deckert M, Ballotti R, Tartare-Deckert S. SPARC functions as an anti-stress factor by inactivating p53 through Akt-

mediated MDM2 phosphorylation to promote melanoma cell survival. Oncogene. 2011 Dec 8;30(49):4887-900.

124. Tai IT, Tang MJ. SPARC in cancer biology: its role in cancer progression and potential for therapy. Drug Resist Updat. 2008 Dec;11(6):231-46.

125. Bellahcene, A., Castronovo, V., 1995. Increased expression of osteonectin and osteopontin, two bone matrix proteins, in human breast cancer. Am.J. Pathol. 146, 95–100.

126. Jones, C., Mackay, A., Grigoriadis, A., Cossu, A., Reis-Filho, J.S., Fulford, L., et al., 2004. Expression profiling of purified normal human luminal and myoepithelial breast cells: identification of novel prognostic markers for breast cancer. Cancer Res. 64, 3037–3045.

127. Wong S, Crowley D, Bronson RT, Hynes RO. Analyses of the role of endogenous SPARC in mouse models of prostate and breast cancer. Clinical & Experimental Metastasis. 2008; 25: 109-118.

128. Koblinski JE, Kaplan-Singer BR, VanOsdol SJ, Wu M, Engbring JA, Wang S, et al. Endogenous osteonectin/SPARC/BM-40 expression inhibits MDAMB-231 breast cancer cell metastasis. Cancer Res. 2005; 65: 7370-7377.

129. Chiodoni C, Colombo MP, Sangaletti S. Matricellular proteins: from homeostasis to inflammation, cancer, and metastasis. Cancer Metastasis Rev. 2010; 29: 295-307.

130. Ikuta Y, Hayashida Y, Hirata S, Irie A, Senju S, Kubo T, Nakatsura T, Monji M, Sasaki Y, Baba H, Nishimura Y. Identification of the H2-Kd-restricted cytotoxic T lymphocyte epitopes of a tumor- associated antigen, SPARC, which can stimulate antitumor immunity without causing autoimmune disease in mice. Cancer Sci. 2009 Jan;100(1):132-7.

131. Inoue M, Senju S, Hirata S, Ikuta Y, Hayashida Y, Irie A, Harao M, Imai K, Tomita Y, Tsunoda T, Furukawa Y, Ito T, Nakamura Y, Baba H, Nishimura Y. Identification of SPARC as a candidate target antigen for immunotherapy of various cancers. Int J Cancer. 2010 Sep 1;127(6):1393-403.

132. Hoster, H, Zanes R and vonHaam E (1949). The association of “viral” hepatitis and Hodgkin’s disease. Cancer Res 9: 473–480.

133. SOUTHAM CM, MOORE AE. Clinical studies of viruses as antineoplastic agents with particular reference to Egypt 101 virus. Cancer. 1952 Sep;5(5):1025-34.

134. Cerullo V, Koski A, Vaha-Koskela M, Hemminki A. Chapter eight–Oncolytic adenoviruses for cancer immunotherapy: data from mice,hamsters, and humans. Adv Cancer Res. 2012; 115:265–318.

135. Liang M. Clinical development of oncolytic viruses in China. Curr Pharm Biotechnol. 2012; 13:1852–57

136. Raty JK, Pikkarainen JT, Wirth T, Yla-Herttuala S. Gene therapy: the first approved gene- based medicines, molecular mechanisms and clinical indications. Curr Mol Pharmacol. 2008; 1:13–23.

137. Andtbacka RH, Kaufman HL, Collichio F, Amatruda T, Senzer N, Chesney J, Delman KA, Spitler LE, Puzanov I, Agarwala SS, et al. Talimogene laherparepvec improves durable response rate in patients with advanced melanoma. J Clin Oncol. 2015; 33:2780–88.

138. Lundstrom K. New frontiers in oncolytic viruses: optimizing and selecting for virus strains with improved efficacy. Biologics. 2018 Feb 9; 12:43-60.

139. ClinicalTrials.gov Identifier: NCT02759588. Available online: https://clinicaltrials.gov/ct2/show/study/NCT02759588 (accessed on 21 July 2021).

140. Silva NIO, de Oliveira JS, Kroon EG, Trindade GS, Drumond BP. Here, There, and Everywhere: The Wide Host Range and Geographic Distribution of Zoonotic Orthopoxviruses. Viruses. 2020 Dec 30;13(1):43.

141. Baldick Jr., C.J., Moss, B., 1993. Characterization and temporal regulation of mRNAs encoded by vaccinia virus intermediate stage genes. J. Virol. 67, 3515–3527.

142. Walsh, S. R., & Dolin, R. (2011). Vaccinia viruses: vaccines against smallpox and vectors against infectious diseases and tumors. Expert review of vaccines, 10(8), 1221–1240.

143. Smith GL, Vanderplasschen A, Law M. The formation and function of extracellular enveloped vaccinia virus. J Gen Virol. 2002 Dec;83(Pt 12):2915-2931.

144. Kieser Q, Noyce RS, Shenouda M, Lin YJ, Evans DH. Cytoplasmic factories, virus assembly, and DNA replication kinetics collectively constrain the formation of poxvirus recombinants. PLoS One. 2020 Jan 16;15(1): e0228028.

145. Guo, Z.S., Lu, B., Guo, Z. et al. (2019). Vaccinia virus-mediated cancer immunotherapy: cancer vaccines and oncolytics. j. immunotherapy cancer 7,6.

146. Thorne SH, Bartlett DL, Kirn DH. The use of oncolytic vaccinia viruses in the treatment of cancer: a new role for an old ally? Curr Gene Ther. 2005 Aug;5(4):429-43.

147. Jenne L, Schuler G, Steinkasserer A. (2001). Viral vectors for dendritic cell-based immunotherapy. Trends Immunol; 22:102–7.

148. Aghi, M., Martuza, R. (2005). Oncolytic viral therapies – the clinical experience. Oncogene 24, 7802–7816.

149. Thorne SH, Kirn DH. (2004) Future directions for the field of oncolytic virotherapy: a perspective on the use of vaccinia virus. Exp Opin Biol Ther; 4:1307–21.

150. Sachin R Jhawar, Aditya Thandoni, Praveen K Bommareddy, Suemair Hassan, Frederick J Kohlhapp, Sharad Goyal, Jason M Schenkel, Ann W Silk, Andrew Zloza. (2017). Oncolytic Viruses- Natural and Genetically Engineered Cancer Immunotherapies. Front Oncol; 7: 202.

151. Ye M, Wilhelm M, Gentschev I, Szalay A. A Modified Limiting Dilution Method for Monoclonal Stable Cell Line Selection Using a Real-Time Fluorescence Imaging System: A Practical Workflow and Advanced Applications. Methods Protoc. 2021 Feb 20;4(1):16.

152. Frentzen A, Yu YA, Chen N, Zhang Q, Weibel S, Raab V, Szalay AA. Anti-VEGF single-chain antibody GLAF-1 encoded by oncolytic vaccinia virus significantly enhances antitumor therapy. Proc Natl Acad Sci U S A. 2009 Aug 4;106(31):12915-20.

153. Cotter CA, Earl PL, Wyatt LS, Moss B. Preparation of Cell Cultures and Vaccinia Virus Stocks. Curr Protoc Protein Sci. 2017 Aug 1; 89:5.12.1-5.12.18.

154. Moynahan ME, Jasin M. Mitotic homologous recombination maintains genomic stability and suppresses tumorigenesis. Nat Rev Mol Cell Biol.2010; 11:196–207.

155. Panicali D, Paoletti E. Construction of poxviruses as cloning vectors: insertion of the thymidine kinase gene from herpes simplex virus into the DNA of infectious vaccinia virus. Proceedings of the National Academy of Sciences of the United States of America. 1982; 79(16):4927–31.

156. Mackett M, Smith GL, Moss B. Vaccinia virus: a selectable eukaryotic cloning and expression vector.Proceedings of the National Academy of Sciences of the United States of America. 1982; 79(23):7415–9.

157. SMITH, G. L. GODSON, G. N., NUSSENZWEIG, V., NUSSENZWEIG, R. S., BARNWELL, J. & MOSS, B. (1984). Plasmodium knowlesi sporozoite antigen: expression by infectious recombinant vaccinia virus. Science224, 397-399

158. MACKETT, M., SMITH,G. L. & MOSS,B. (1984). General method for production and selection of infectious vaccinia virus recombinants expressing foreign genes. Journalof Virology49, 857-864.

159. MACKETT,M., SMITH,G. L. &MOSS,B. (1985 b). The construction and characterization of vaccinia virus recombinants expressing foreign genes. In DNA Cloning: A PracticalApproach, pp. t91-211. Edited by D. M. Glover,Oxford: IRL Press

160. Haider SR, Reid HJ, Sharp BL. Tricine-SDS-PAGE. Methods Mol Biol. 2019;1855:151-160.

161. Lau CP, Poon RT, Cheung ST, Yu WC, Fan ST. SPARC and Hevin expression correlate with tumor angiogenesis in hepatocellular carcinoma. J Pathol. 2006 Dec;210(4):459-68.

162. Paciotti GF, Tamarkin L. Interleukin-2 differentially affects the proliferation of a hormone- dependent and a hormone-independent human breast cancer cell line in vitro and in vivo. Anticancer Res. 1988 Nov-Dec;8(6):1233-9.

163. Artyomov MN, Lis M, Devadas S, Davis MM, Chakraborty AK. CD4 and CD8 binding to MHC molecules primarily acts to enhance Lck delivery. Proc Natl Acad Sci U S A. 2010 Sep 28;107(39):16916-21.

164. Chatzileontiadou DSM, Sloane H, Nguyen AT, Gras S, Grant EJ. The Many Faces of CD4+ T Cells: Immunological and Structural Characteristics. Int J Mol Sci. 2020 Dec 23;22(1):73.

165. St Paul M, Ohashi PS. The Roles of CD8+ T Cell Subsets in Antitumor Immunity. Trends Cell Biol. 2020 Sep;30(9):695-704.

166. Waldman AD, Fritz JM, Lenardo MJ. A guide to cancer immunotherapy: from T cell basic science to clinical practice. Nat Rev Immunol. 2020 Nov;20(11):651-668.

167. Kalia V, Sarkar S. Regulation of Effector and Memory CD8 T Cell Differentiation by IL-2-A Balancing Act. Front Immunol. 2018 Dec 20; 9:2987.

168. Plebanski M, Katsara M, Sheng KC, Xiang SD, Apostolopoulos V. Methods to measure T-cell responses. Expert Rev Vaccines. 2010 Jun;9(6):595-600.

169. Olivo Pimentel V, Yaromina A, Marcus D, Dubois LJ, Lambin P. A novel co-culture assay to assess anti-tumor CD8+ T cell cytotoxicity via luminescence and multicolor flow cytometry. J Immunol Methods. 2020 Dec; 487:112899.

170. La Gruta NL, Gras S, Daley SR, Thomas PG, Rossjohn J. Understanding the drivers of MHC restriction of T cell receptors. Nat Rev Immunol. 2018 Jul;18(7):467-478.

171. Liu Y, Xin T, Huang DY, Shen WX, Li L, Lv YJ, Jin YH, Song XW, Teng C, Jiang QY. Prognosis in very young women with triple-negative breast cancer: retrospective study of 216 cases. Med Oncol. 2014 Dec;31(12):222.

172. Bergin ART and Loi S. Triple-negative breast cancer: recent treatment advances [version 1; peer review: 2 approved]. F1000Research 2019, 8(F1000 Faculty Rev):1342

173. Bonotto M, Gerratana L, Poletto E, Driol P, Giangreco M, Russo S, Minisini AM, Andreetta C, Mansutti M, Pisa FE, et al: Measures of outcome in metastatic breast cancer: Insights from a real-world scenario. Oncologist 19: 608-615, 2014.

174. Mittendorf EA, Philips AV, Meric-Bernstam F, et al. PD-L1 expression in triple-negative breast cancer. Cancer Immunol Res 2014; 2:361–370.

175. Gatalica Z, Snyder C, Maney T, et al. Programmed cell death 1 (PD-1) and its ligand (PD-L1) in common cancers and their correlation with molecular cancer type. Cancer Epidemiol Biomarkers Prev 2014; 23:2965–2970.

176. Won KA, Spruck C. Triple-negative breast cancer therapy: Current and future perspectives (Review). Int J Oncol. 2020 Dec;57(6):1245-1261. doi: 10.3892/ijo.2020.5135. Epub 2020 Oct 16.

177. Denkert C, von Minckwitz G, Darb-Esfahani S, et al. Tumor-infiltrating lymphocytes and prognosis in different subtypes of breast cancer: a pooled analysis of 3771 patients treated with neoadjuvant therapy. Lancet Oncol 2018; 19:40–50.

178. Fehrenbacher L, Spira A, Ballinger M, et al. Atezolizumab versus docetaxel for patients with previously treated non-small-cell lung cancer (POPLAR): a multicentre, open-label, phase 2 randomised controlled trial. Lancet 2016; 387:1837–1846

179. Isakoff SJ, Tolaney SM, Tung NM, et al. A phase 1b study of safety and immune response to PVX-410 vaccine alone and in combination with durvalumab (MEDI4736) in HLA-A21 patients following adjuvant therapy for stage 2/3 triple negative breast cancer [abstract]. J Clin Oncol 2017; 35(Suppl): Abstract TPS1126

180. Norton, N., Youssef, B., Hillman, D.W. et al. Folate receptor alpha expression associates with improved disease-free survival in triple negative breast cancer patients. npj Breast Cancer 6, 4 (2020).

181. Gholami S, Marano A, Chen NG, Aguilar RJ, Frentzen A, Chen CH, Lou E, Fujisawa S, Eveno C, Belin L, Zanzonico P, Szalay A, Fong Y. A novel vaccinia virus with dual oncolytic and anti- angiogenic therapeutic effects against triple-negative breast cancer. Breast Cancer Res Treat. 2014 Dec;148(3):489-99. doi: 10.1007/s10549-014-3180-7. Epub 2014 Nov 13. Erratum in: Breast Cancer Res Treat. 2016 Apr;156(3):607-8.

182. Limacher JM, Quoix E. TG4010: A therapeutic vaccine against MUC1 expressing tumors. Oncoimmunology. 2012 Aug 1;1(5):791-792.

183. Quoix E, Lena H, Losonczy G, Forget F, Chouaid C, Papai Z, Gervais R, Ottensmeier C, Szczesna A, Kazarnowicz A, Beck JT, Westeel V, Felip E, Debieuvre D, Madroszyk A, Adam J, Lacoste G, Tavernaro A, Bastien B, Halluard C, Palanché T, Limacher JM. TG4010 immunotherapy and first-line chemotherapy for advanced non-small-cell lung cancer (TIME): results from the phase 2b part of a randomised, double-blind, placebo-controlled, phase 2b/3 trial. Lancet Oncol. 2016 Feb;17(2):212-223.

184. Ye, Mingyu, Markus Keicher, Ivaylo Gentschev, and Aladar A. Szalay 2021. "Efficient Selection of Recombinant Fluorescent Vaccinia Virus Strains and Rapid Virus Titer Determination by Using a Multi-Well Plate Imaging System" Biomedicines 9, no. 8: 1032.

185. Zhang Q, Yu YA, Wang E, Chen N, Danner RL, Munson PJ, Marincola FM, Szalay AA. Eradication of solid human breast tumors in nude mice with an intravenously injected light-emitting oncolytic vaccinia virus. Cancer Res. 2007 Oct 15;67(20):10038-46.

186. Guo ZS, Lu B, Guo Z, Giehl E, Feist M, Dai E, et al. Vaccinia virus-mediated cancer immunotherapy: cancer vaccines and oncolytics. J Immunother Cancer 2019; 7:6

187. Umer BA, Noyce RS, Franczak BC, Shenouda MM, Kelly RG, Favis NA, Desaulniers M, Baldwin TA, Hitt MM, Evans DH. Deciphering the Immunomodulatory Capacity of Oncolytic Vaccinia Virus to Enhance the Immune Response to Breast Cancer. Cancer Immunol Res. 2020 May;8(5):618- 631.

188. Brunner, K. T., Mauel, J., Cerottini, J. C. and Chapuis, B. (1968). Quantitative assay of the lytic action of immune lymphoid cells on 51-Cr-labelled allogeneic target cells in vitro; inhibition by isoantibody and by drugs. Immunology 14(2): 181-196.